Critical Reviews and Perspectives

Chemistry, structure and function of approved oligonucleotide therapeutics

Martin Egli [iD][1],[*] **and Muthiah Manoharan** [iD][2],[*]

[1]Department of Biochemistry, Center for Structural Biology, and Vanderbilt Ingram Cancer Center, Vanderbilt University, School of Medicine, Nashville, TN 37232-0146, USA and [2]Alnylam Pharmaceuticals, 300 Third Street, Cambridge, MA 02142, USA

ABSTRACT

Eighteen nucleic acid therapeutics have been approved for treatment of various diseases in the last 25 years. Their modes of action include antisense oligonucleotides (ASOs), splice-switching oligonucleotides (SSOs), RNA interference (RNAi) and an RNA aptamer against a protein. Among the diseases targeted by this new class of drugs are homozygous familial hypercholesterolemia, spinal muscular atrophy, Duchenne muscular dystrophy, hereditary transthyretin-mediated amyloidosis, familial chylomicronemia syndrome, acute hepatic porphyria, and primary hyperoxaluria. Chemical modification of DNA and RNA was central to making drugs out of oligonucleotides. Oligonucleotide therapeutics brought to market thus far contain just a handful of first- and second-generation modifications, among them 2′-fluoro-RNA, 2′-O-methyl RNA and the phosphorothioates that were introduced over 50 years ago. Two other privileged chemistries are 2′-O-(2-methoxyethyl)-RNA (MOE) and the phosphorodiamidate morpholinos (PMO). Given their importance in imparting oligonucleotides with high target affinity, metabolic stability and favorable pharmacokinetic and -dynamic properties, this article provides a review of these chemistries and their use in nucleic acid therapeutics. Breakthroughs in lipid formulation and GalNAc conjugation of modified oligonucleotides have paved the way to efficient delivery and robust, long-lasting silencing of genes. This review provides an account of the state-of-the-art of targeted oligo delivery to hepatocytes.

INTRODUCTION

Half a century may seem like an eternity but occasionally it feels like the years just flew by. Consider what has been achieved in roughly that time frame as we went from: the Wright brothers' first flight (1903) ([1]) to manned space flight (Gagarin/Sheppard, 1961) ([2]), Turing's paper on computable numbers and the decision problem (Turing machine, 1936) ([3],[4]) to the release of the Cray-2 supercomputer (1985) ([5]), and Sanger's sequencing of bovine insulin (1953) ([6],[7]) to the completion of the human genome project (2003) ([8]). These amazing feats have in common that they happened within some short 50 years! Viewed from such a perspective, chemically modified oligonucleotide drugs getting US FDA approval, VITRAVENE® (fomivirsen)—1998 ([9–11]), MACUGEN® (pegaptanib sodium)—2004 ([12–14]), and KYNAMRO® (mipomersen)—2013 ([15],[16]), just half a century after the publication of the structure of DNA (1953) ([17]), is no small achievement.

A look back at the beginnings of molecular biology makes clear how little was known about concepts we now take for granted, concepts that foreshadowed a watershed of techniques and discoveries that can be traced back to early insights. The model of the DNA double helix sparked intense interest in the structural properties of RNA. It was unclear at the time how the ribose 2′-hydroxyl group would affect the conformation of RNA ([17]) and whether RNA could form a duplex at all. In a landmark publication in 1956, Rich and Davies demonstrated the existence of an RNA duplex by mixing poly-A and poly-U ([18]). Remarkably, the same paper also put forth the concept of nucleic acid hybridization, i.e. the spontaneous pairing using specific interactions between two long nucleic acid strands ([19]). In 1960, Rich presented evidence that DNA and RNA can hybridize such that the resulting duplex is held together by hydrogen bonds (H-bonds) between purine and pyrimidine

*To whom correspondence should be addressed. Tel: +1 615 343 8070; Email: martin.egli@vanderbilt.edu
Correspondence may also be addressed to Muthiah Manoharan. Tel: +1 617 551 8319; Email: mmanoharan@alnylam.com
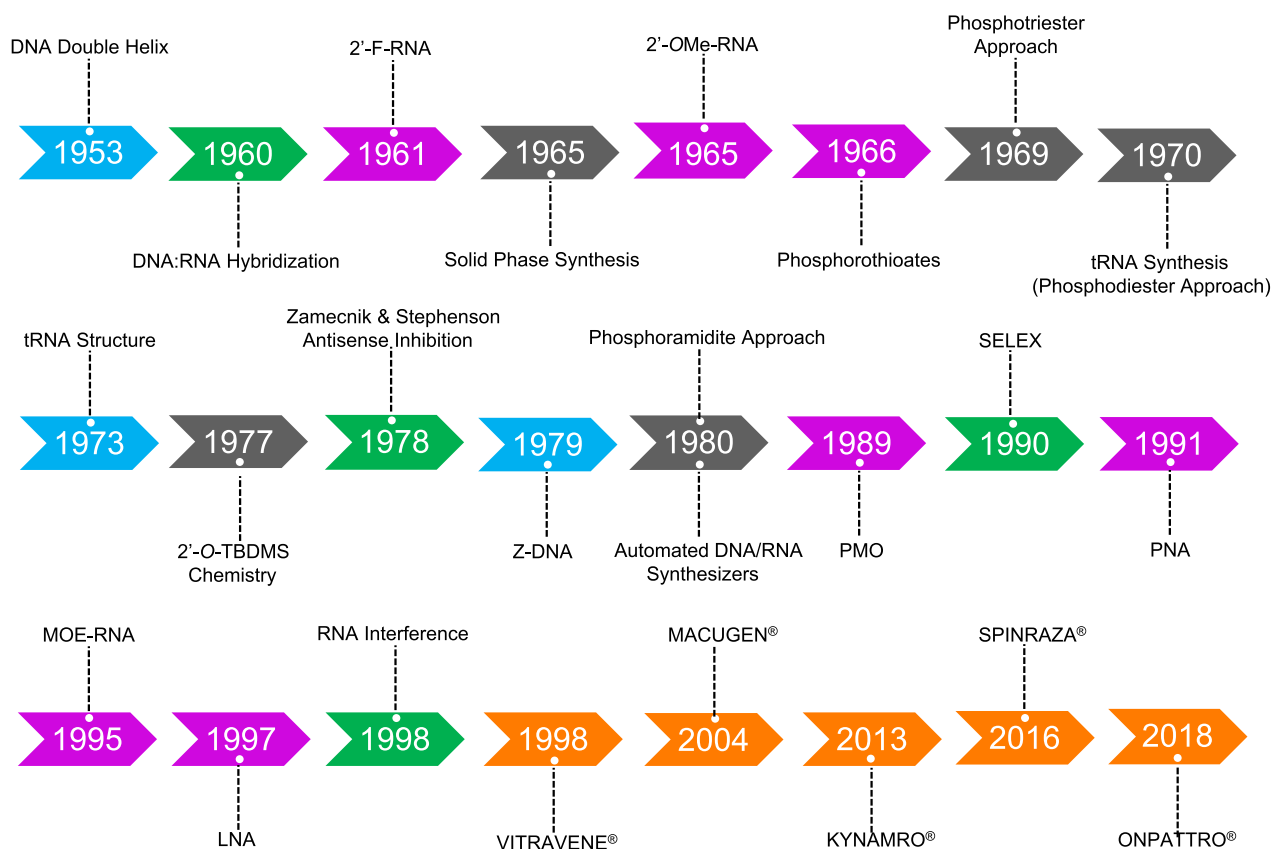
Figure 1. Timeline of the development of chemical modifications (magenta), oligonucleotide synthetic approaches (black), interference in biological information transfer (green), structures of DNA and RNA (blue), and FDA-approved oligo therapeutics (orange).

residues (20). This finding provided a mechanism for information transfer between DNA and RNA.

Hybridization reactions are the backbone of modern molecular biology; approaches from the Southern blot to microarrays and the polymerase chain reaction (PCR), as well as genome sequencing and the forensic sciences, all depend at their core on nucleic acid hybridization. The same applies to the inhibition of biological information transfer, first successfully demonstrated by Zamecnik and Stephenson using the antisense and antigene approaches (21,22). In just a few years in the late 1950s and early 1960s, discoveries were made that laid the foundation for therapeutic intervention targeting RNA (e.g. hybridization via antisense, alternative splicing or RNA interference) and identified the RNA duplex as a key component of RNA structure (and, we now know, as an important actor in therapeutic intervention in the form of siRNA duplexes). Indeed, the earliest suggestion that RNA might have both a phenotype and a genotype, hinting at the existence of an RNA world, also dates back to the early 1960s (23,24).

Beginning in 1955, nucleotide and oligonucleotide syntheses started in the laboratories of Todd, Khorana, Letsinger and Eckstein (25–40). Following these initial discoveries, DNA and RNA oligonucleotide syntheses and methods for the same were developed in the laboratories of Caruthers (41,42) and Ogilvie (43,44), respectively. Phosphorothioate oligonucleotide synthesis was developed by Stec (45). These synthetic revolutions led to the discovery

of the genetic code, and paved the way to molecular biology, chemical biology, and nucleic acid-based medicine (see also https://www.trilinkbiotech.com/a-short-history-of-oligonucleotide-synthesis).

Figure 1 depicts a brief history of key discoveries, nucleic acid structure analysis, and breakthroughs in DNA and RNA synthesis as well as modification strategies on the way to FDA-approved oligonucleotide therapeutics. Chemical modification efforts at the levels of nucleosides and nucleotides got underway >50 years ago and the syntheses of $2'$-fluorothymidine, $2'$-fluoro-$2'$-deoxyuridine ($2'$-F-U) (46), nucleoside phosphorothioates (PSOs) (33), and $2'$-O-methylated ($2'$-O-Me) polyadenylic acid (47) were all reported in the 1960s (Figure 2A).

The $2'$-F and $2'$-O-Me modifications figure prominently in MACUGEN, an anti-VEGF aptamer for the treatment of wet age-related macular degeneration, and GIVLAARI® (givosiran), an siRNA for the treatment of acute hepatic porphyria (48) (Figure 3). The $2'$-O-Me modification is also present in ONPATTRO® (patisiran), the first FDA-approved RNAi therapeutic (2018), indicated for the treatment of the polyneuropathy of hereditary transthyretin-mediated amyloidosis (hATTR) (49). The delivery system for ONPATTRO is a lipid nanoparticle (LNP, Figure 2B). VITRAVENE, an antisense drug indicated for cytomegalovirus retinitis and the very first oligonucleotide therapeutic to receive clinical approval was a fully PS-modified 21mer oligo-$2'$-deoxynucleotide. These first-generation chemistries are still commonly encountered

Figure 2. (**A**) Native DNA, RNA and chemical modifications that are approved in therapeutics so far. (**B**) Different delivery systems; LNP = lipid nanoparticle.

Figure 3. Currently approved oligonucleotide drugs and mRNA vaccines, year of approval (between 1998 and 2022), and indication. From top left to bottom right: VITRAVENE®, MACUGEN®, KYNAMRO®, EXONDYS 51®, VYONDYS 53®, SPINRAZA®, HEPLISAV-B®, ONPATTRO®, TEGSEDI®, WAYLIVRA®, GIVLAARI®, OXLUMO®, VILTEPSO®, AMONDYS 45®, LEQVIO®, AMVUTTRA®, COMIRNATY® and SPIKEVAX®. The mechanisms of action are: antisense oligonucleotide (ASO), aptamer, splice-switching oligonucleotide (SSO), small interfering RNA (siRNA) and mRNA (vaccine).

in the backbones of oligonucleotide therapeutic candidates that are currently in phase I to III clinical trials in the US (50,51). This is especially true for the phosphorothioates (PS-DNA/-RNA) but $2'$-O-Me/$2'$-F modified oligonucleotides are also represented and include LEQVIO® (inclisiran, Figure 3, Table 1), an siRNA against hypercholesterolemia that was approved by regulators in the European Union in 2021 (52) and the US FDA in 2022 (53).

Among second-generation antisense modifications (54,55), $2'$-O-(2-methoxyethyl)-RNA (MOE-RNA) has emerged as the most successful chemistry (Figure 2A). The synthesis of MOE-modified building blocks and oligonucleotides was first reported in 1995 (56) and MOE chemistry subsequently moved from bench to bedside within about 20 years (Figure 1). The first of three MOE-based therapeutics approved by the FDA was KYNAMRO for the treatment of homozygous familial hypercholesterolemia (Figure 3, Table 1). The 20mer antisense oligonucleotide is an all-PS modified gapmer with a central DNA decamer gap and pentameric MOE flanks (57). The gapmer approach is needed to elicit RNase H, the endonuclease that cleaves the RNA target opposite the DNA window (58,59).

SPINRAZA® (nusinersen) that was approved three years later acts via an entirely different mechanism (Fig-

ures 1 and 3). The all-PS/MOE-modified RNA 18mer is used in the treatment of spinal muscular atrophy and modulates alternate splicing of the survival motor neuron 2 (*SMN2*) gene (60). The third therapeutic is TEGSEDI® (inotersen) that resembles KYNAMRO in that it is also a PS-modified 5-10-5 gapmer with MOE flanks and a central DNA gap. The drug was approved in 2018 for the treatment of the polyneuropathy in hereditary transthyretin-mediated amyloidosis (61,62). Lastly, another MOE based 5-10-5 gapmer, WAYLIVRA® (volanesorsen), was approved by the European Commission as an adjunct therapy to diet for treatment of a rare lipid disorder, familial chylomicronemia syndrome (63).

An antisense-like approach similar to the one exemplified by SPINRAZA and using a splice-switching oligonucleotide that targets exon 51 of the dystrophin mRNA was pursued for treatment of certain forms of Duchenne muscular dystrophy (DMD). EXONDYS 51® (eteplirsen), a phosphorodiamidate morpholino (PMO) (64) 30mer with an uncharged backbone was approved in 2016 (65) (Figures 1, 2A and 3). Another PMO oligonucleotide, VYONDYS 53 (golodirsen), that targets exon 53 of the dystrophin transcript (about 8% of the DMD community) was approved by the FDA in 2019 (66).

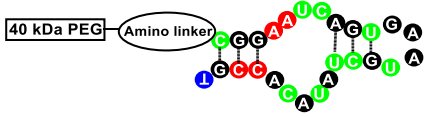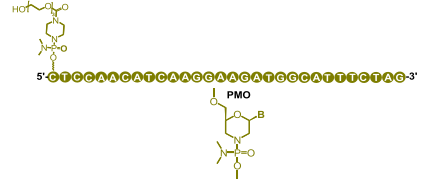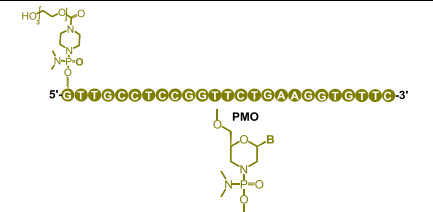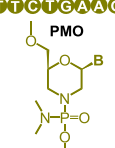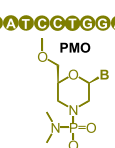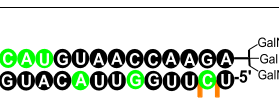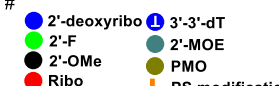**Table 1.** Summary of approved oligonucleotide-based therapeutics

No.	Drug name, year of approval, indication	Molecular target, tissue	Details of chemical mechanism	Chemistry, sequence[#]	Dose, route, delivery mechanism
1	VITRAVENE® (fomivirsen), 1998, CMV retinitis	CMV IE-2, eye	21-mer ASO, PS DNA, RNase H1 and TLR9	5'-GCGTTTGCTCTTCTTCTTGCG-3'	300 μg every 4 weeks, IVT
2	MACUGEN® (pegaptanib), 2004, neovascular AMD	VEGF165, eye	27-mer anti-VEGF aptamer, 2'-OH/2'-F/2'-OMe/2'-H inverted DNA, 5'-PEG, aptamer binds to VEGF165	40 kDa PEG — Amino linker — (aptamer structure)	0.3 mg every 6 weeks, IVT
3	KYNAMRO® (mipomersen), 2013, homozygous familial hypercholesterolemia (HoFH)	ApoB-100, liver	20-mer gapmer ASO, PS, 2'-O-MOE/2'-H, activates RNase H1	5'-GCCTCAGTCTGCTTCGCACC-3' C: 5-Methyl-C	200 mg once weekly, SC
4	EXONDYS 51® (eteplirsen), 2016, Duchenne muscular dystrophy (DMD)	Dystrophin (exon 51), muscle	30-mer SSO, morpholino (PMO), splicing modification (exon skipping)	5'-CTCCAACATCAAGGAAGATGGCATTTCTAG-3' PMO	30 mg/kg once weekly, IV
5	SPINRAZA® (nusinersen), 2016, spinal muscular atrophy (SMA)	SMN2, CNS	18-mer SSO, PS, 2'-O-MOE, splicing modification (exon inclusion)	5'-TCACTTTCATAATGCTGG-3' C: 5-Methyl-C	12.5 mg once every 4 months, IT
6	ONPATTRO® (patisiran), 2018, hereditary ATTR (hATTR)	TTR, liver	21-mer/21-mer siRNA, 2'-OH/2'-OMe/2'-H, RISC Ago2	Passenger 5'-GUAACCAAGAGUAUUCCAUTT-3' 3'-TTCAUUGGUUCUCAUAAGGUA-5' Guide	0.3 mg/kg once every 3 weeks, IV, LNP (DLin-MC3-DMA, PEG-DMG lipid, cholesterol, DSPC)
7	TEGSEDI® (inotersen), 2018, hereditary ATTR (hATTR)	TTR, liver	20-mer gapmer ASO, PS, 2'-O-MOE/2'-H, RNase H1	5'-TCTTGGTTACATGAAATCCC-3' C: 5-Methyl-C	300 mg once weekly, SC
8	GIVLAARI® (givosiran), 2019, acute hepatic porphyria	ALAS1, liver	21-mer/23-mer siRNA, enhanced stabilization chemistry (ESC), PS, 2'-OMe/2'-F, RISC Ago2	Passenger 5'-CAGAAAGAGUGUCUCAUCUUA—GalNAc-GalNAc-GalNAc 3'-UGGUCUUUCUCACAGAGUAGAAU-5' Guide	2.5 mg/kg once a month, SC, GalNAc conjugate
9	VYONDYS 53® (golodirsen), 2019, Duchenne muscular dystrophy (DMD)	Dystrophin (exon 53), muscle	25-mer SSO, PMO, splicing modification (exon skipping)	5'-GTTGCCTCCGGTTCTGAAGGTGTTC-3' PMO	30 mg/kg once weekly, IV
10	WAYLIVRA® (volanesorsen), 2019, familial chylomicronemia syndrome (FCS)	Apolipoprotein CIII (apoCIII), liver	20-mer gapmer ASO, PS, 2'-O-MOE/2'-H, RNase H1	5'-TATTTCGACCTGTTCTTCGA-3' C: 5-Methyl-C	285 mg once weekly, SC
11	OXLUMO® (lumasiran), 2020, primary hyperoxaluria type 1 (PH1)	Hydroxyacid oxidase 1 (HAO1), liver	21-mer/23-mer siRNA, ESC, PS, 2'-OMe/2'-F, RISC Ago2	Passenger 5'-GACUUUCAUCCUGGAAAUAUA—GalNAc-GalNAc-GalNAc 3'-ACCUGAAAGUAGGACCUUUAUAU-5' Guide	3 mg/kg or 6 mg/kg and dosing frequency varies by body weight and age, SC, GalNAc conjugate
12	LEQVIO® (inclisiran), 2020 (EMA), 2021 (FDA), heterozygous familial hypercholesterolemia (HeFH) or clinical atherosclerotic cardiovascular disease (ASCVD)	PCSK9, liver	21-mer/23-mer siRNA, ESC, PS, 2'-OMe/2'-F/2'-H, RISC Ago2	Passenger 5'-CUAGACCUGUUUUGCUUUUGU—GalNAc-GalNAc-GalNAc 3'-AAGAUCUGGACAAAACGAAACA-5' Guide	284 mg/kg administered initially, 3 months after the same dose, and then every 6 months, SC, GalNAc conjugate

Table 1. Continued

No.	Drug name, year of approval, indication	Molecular target, tissue	Details of chemical mechanism	Chemistry, sequence[#]	Dose, route, delivery mechanism
13	VILTEPSO® (viltolarsen), 2020, Duchenne muscular dystrophy (DMD)	Dystrophin (exon 53), muscle	21-mer SSO, PMO, splicing modification (exon skipping)	5'-CCTCCGGTTCTGAAGGTGTTC-3'	80 mg/kg once weekly, IV
14	AMONDYS 45® (casimersen), 2021, Duchenne muscular dystrophy (DMD)	Dystrophin (exon 45), muscle	22-mer SSO, PMO, splicing modification (exon skipping)	5'-CAATGCCATCCTGGAGTTCCTG-3'	30 mg/kg once weekly, IV
15	HEPLISAV-B® 2017, hepatitis B vaccine (recombinant, adjuvanted)	Hepatitis B	22-mer PS DNA, B-class CpG-containing oligonucleotide as adjuvant	5'-TGACTGTGAACGTTCGAGATGA-3'	2-dose vaccine, 0.5 mL each
16	COMIRNATY® BNT162b2 (tozinameran), 2021, vaccine	SARS-CoV-2	mRNA, 1N-Me pseudouridine, 2'-OMe in 5'-cap	4284 nucleotides, mRNA encodes SARS-CoV-2 spike protein	30 µg, intramuscular, LNP (ALC-0315, ALC-0159, PEG2000-DMG analogue, cholesterol, DSPC)
17	SPIKEVAX® (elasomeran), 2022, vaccine	SARS-CoV-2	mRNA, 1N-Me pseudouridine, 2'-OMe in 5'-cap	mRNA encodes the full-length SARS-CoV-2 spike protein	100 µg, intramuscular, LNP (SM-102, PEG-2000 DMG lipid, cholesterol, DSPC)
18	AMVUTTRA® (vutrisiran), 2022, hereditary ATTR (hATTR)	TTR, liver	21-mer/23-mer siRNA, ESC, PS, 2'-OMe/2'-F RISC Ago2	Passenger 5'-UGGGAUUUCAUGUAACCAAGA-3' (GalNAc) 3'-CUACCCUAAAGUACAUUGGUUCU-5' Guide	25 mg total dose, once every three months, SC GalNAc conjugate

[#]
- ● 2'-deoxyribo
- ● 2'-F
- ● 2'-OMe
- ● Ribo
- ◑ 3'-3'-dT
- ● 2'-MOE
- ● PMO
- ❚ PS modification

Over the course of the last 25 years, countless new nucleic acid modifications were introduced besides the first- and second-generation chemistries discussed above, and their activities have been evaluated at least in vitro (50,51,67–75). From the outset, it was clear that chemical modification of DNA and RNA was key to the successful therapeutic deployment of the antisense strategy, whereby increasing the binding affinity of the antisense oligonucleotide (ASO) was a particular concern (76). But there was an early recognition in the field that, besides affinity, multiple other hurdles needed to be overcome on the path to successful oligonucleotide drugs. These include chemical stability, resistance to degradation by a host of cellular exo- and endonucleases, i.e. metabolic stability, target site accessibility, delivery and biodistribution, i.e. binding to proteins and receptors, pharmacokinetics and pharmacodynamics as well as toxicity and complement activation (54,57,58,77).

Looking back, it is quite extraordinary that the breakthroughs achieved in bringing 18 oligonucleotide (nucleic acids) drugs to market (Figure 3, Table 1) are chiefly based on just a handful of sugar and backbone modifications, namely the very early 2'-F, 2'-O-Me, and PS chemistries as well as the 2'-O-MOE RNA and neutral PMO backbone analogs (Figure 2A). We included two mRNA vaccines in Figure 3 although these are technically not oligonucleotides. However, these mRNAs also feature chemical modification (N-Me-pseudouridine, and 2'-O-Me in the cap, Figure 2A), and, like ONPATTRO, their delivery entails LNPs (Figure 2B).

In this critical review and perspective article, we review the chemistries of FDA-approved antisense (ASO), splice-switching (SSO), small interfering RNAs (siRNAs) and aptamer oligonucleotides, and discuss properties of the 2'-F, 2'-O-Me, 2'-O-MOE, PS and PMO analogs that cemented

their status as privileged modifications in oligonucleotide therapeutics. Particularly as far as the phosphorothioates are concerned, recent research has uncovered the origins of altered protein binding affinities and interaction modes as a consequence of replacing non-bridging phosphate oxygens by sulfur (78,79) and cast a light on the benefits of stereopure PS modification (80,81). Another focus of this review concerns GalNAc conjugation chemistry for optimized delivery of oligonucleotides to liver (82–88) (Figure 2B). GIVLAARI (28), LEQVIO, OXLUMO (89), and AMVUTTRA all employ GalNAc conjugation chemistry. For other summary articles, specifically regarding advances and challenges in the delivery of nucleic acid therapeutics, please see excellent recent reviews (90,91). Throughout this article we will refer to approved nucleic acid therapeutics with their US trade names.

OLIGONUCLEOTIDE THERAPEUTICS: TARGETS AND CHALLENGES

Physicochemical properties of oligonucleotides

DNA and RNA are polyanions and form duplexes that are held together by H-bonding and stacking interactions between nucleobases. Stacking is ultimately more important for pairing stability than H-bonds; the latter of course provide specificity (92,93). The core of a nucleic acid duplex is essentially hydrophobic as water molecules are squeezed out upon base pairs collapsing on each other (hydrophobic effect) (94). The negative charges of phosphates are dotting the outside and the grooves created by the two strands winding around each other represent regions of varying negative electrostatic potential (95). Metal ions such as Mg^{2+}, Ca^{2+}, Na^+ and K^+ provide neutralizing charges, whereby both a diffuse counterion atmosphere (e.g. around DNA) and specific metal ion binding sites (e.g. Mg^{2+} in RNA) affect folding and stability (96,97).

Cellular DNA is typically double-stranded and the pairing rules follow the Watson-Crick conventions, i.e. A:T and G:C. Conversely, RNA is single-stranded (tRNA, mRNA, rRNA), but folded RNAs exhibit extensive double-stranded regions (98–103). RNA duplexes are of the A-form with 11 base pairs per turn, a helical rise of <3 Å, and strongly inclined bases relative to the helical axis. RNA also displays tighter spacings between adjacent intra-strand phosphate groups compared to the physiological duplex type adopted by DNA, the so-called B-form (104). Base pairs in B-DNA are more or less normal to the direction of the helical axis, with an average rise of 3.4 Å and 10 base pairs per turn. DNA can also adopt the A-form (104) and flip to left-handed Z-DNA (105,106) as a result of torsional stress and dependent on sequence (CG-rich), ionic strength (107) and hydration level (108).

The most significant difference between the backbones of DNA and RNA is the presence of the 2′-hydroxyl group in the ribose sugar of the latter. The 2′-hydroxyl group prefers an axial orientation and steric and stereoelectronic effects (109) result in the preferred C3′-*endo* sugar conformation or pucker. In contrast, 2′-deoxyriboses in B-form DNA adopt a C2′-*endo* pucker (110,111). The 2′-OH group affects not just conformation but also stability and the water structure around the duplex (112). RNA duplexes are more stable

than DNA duplexes of the same sequence and the gain is enthalpy-driven (112,113).

Both DNA and RNA can also form three- and four-stranded structures (triplexes and quadruplexes, respectively) (114,115). Although DNA is capable of forming complex 3D structures in principle (116,117), as exemplified by a catalytic motif (118) and nanostructures (119), it is clearly outdone by RNA as far as complex folds are concerned. As with sugar conformation and thermodynamic stability, RNA's folding repertoire is aided by a multitude of interactions that involve the 2′-hydroxyl group, e.g. ribose zippers (120). Moreover, RNA base pairing is more versatile than the strict pairings in DNA, and G:U, A:C and pyrimidine:pyrimidine and purine:purine pairs (121) as well as base triples and quadruples are commonplace (122). The 2′-hydroxyl group also plays a key role in RNA function and phenotype; thus, is acts as the nucleophile in self-cleaving reactions (123).

More than 150 natural chemical modifications of RNA have been identified, among them 2′-*O*-methylation and complex decorations of nucleobases ((124) and cited refs.). It is now also recognized that DNA nucleobases are not limited to A, T, G and C, and that it is more appropriate to think of an expanded set of bases in the context of epigenetics (125). PS modifications have been established in the DNA of bacteria and archaea and they are exclusively of the *R*p configuration (126–130). However, the PS modification does not appear to exist naturally in RNA (131). DNA PS modification is regulated by the *Dnd* gene cluster (126,130,131).

In line with the above-described differences in structure, stability and function between DNA and RNA, the physicochemical properties of antisense oligonucleotides (ASOs) and small interfering RNAs (siRNAs) are quite distinct (Figure 4). A single-stranded DNA ASO has a molecular weight of typically 7 kDa and a 20mer would carry 19 negative charges. The single strand has a width of ca. 1 nM and is relatively flexible with the hydrophobic faces of bases partly stacked but otherwise accessible for protein interactions. In contrast, a typical siRNA duplex has a molecular weight of ca. 13 kDa and carries 40 negative charges. The duplex is more rigid than an ASO single strand and has a diameter of ca. 2 nM, whereby bases are tucked away in the core with virtually no hydrophobic faces exposed except for the 2-residue overhangs at the 3′-ends. These different physical/chemical properties result in marked differences in pharmacokinetic profiles. They also lead to very different chemical modification strategies, although phosphorothioates and 2′-functionality (132,133) are of general importance for modification.

Antisense modes of action

Rational or structure-based drug design requires knowledge of the 3D-structure of the target, typically an enzyme or a receptor. Screening of a compound library is used to identify initial leads and provides the starting point of an optimization via structure-activity relationships (SARs) that ideally results in a tightly binding candidate molecule for further *in vitro* and *in vivo* tests. But the path to a small-molecule drug is arduous, time-consuming and costly, and
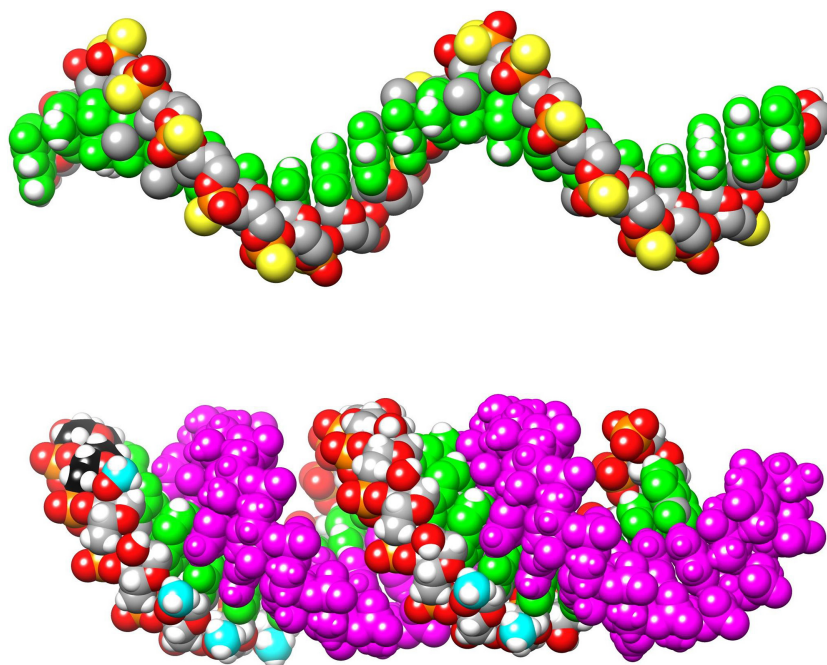
Figure 4. Structures and physicochemical properties of single-stranded DNA (top; 21mer PS-DNA based on the VITRAVENE sequence with random phosphorothioate stereochemistry) and double-stranded siRNA (bottom; 21mer based on the ONPATTRO sequence and modification chemistry). Nucleobase C, O and N atoms are highlighted in green and backbone carbon, oxygen, hydrogen, phosphorus and sulfur atoms are colored in gray, red, white, orange, and yellow, respectively. In the RNA duplex, residues of the sense strand are colored in magenta. In the antisense strand, carbon atoms of the 3′-terminal dTdT overhang and 2′-O-methyl modifications are highlighted in black and cyan, respectively. In the single stranded ASO bases are exposed. In contrast, bases are paired and buried inside the duplex in the double-stranded siRNA.

more often than not fails during the preclinical phase of the evaluation or later during the various phases of a clinical trial. The major attraction of the antisense strategy is that inhibition at the level of gene expression only requires knowledge of the targeted DNA or mRNA sequence. A 17mer oligonucleotide sequence is expected to occur only once in the human genome and the antisense approach therefore promises to be more efficient than the search for an enzyme inhibitor (134). Thus, therapeutic intervention at the nucleic acid level offers a rational path to drug discovery, whereby high specificity is afforded by Watson–Crick H-bonding interactions between ASO and target RNA.

Although knowledge of the target sequence readily enables the design of an ASO, it is important to bear in mind that RNA molecules don't exist as random coils. Because RNAs adopt intricate folds and are commonly decorated by proteins, many regions along the target sequence may be inaccessible to an ASO. Although efforts were made to predict sites on an RNA that allow ASO binding (135–137), an oligonucleotide screen—basically covering a large portion of the entire transcript with individual ASOs, e.g. 5′-UTR and 3′-UTR (Figure 5)—to identify the most active oligo in cell culture offers a more viable approach (138). In a very recent example of an oligo screen, Alnylam researchers synthesized 350 siRNAs against all available RNA genomes of SARS-CoV and SARS-CoV-2 (139)

For the further discussion of oligonucleotide therapeutics, it is helpful to properly define an ASO. It is a single stranded oligonucleotide that pairs with a complementary region on an RNA via Watson–Crick H-bonds and then acts, for example, via a steric block, splice site shifting or RNase-H mediated RNA degradation mechanism (Figure 5). On one hand, this contrasts with the antigene approach that targets DNA and functions via triplex formation, single-stranded decoys (140), and aptamers (141–143) directed at DNA, RNA or proteins. On the other hand, double-stranded RNA molecules (siRNAs (67–69), ribozymes (123,144,145), and synthetic oligo metallonucleases (146–148) all function via the antisense mechanism as well, although they are not typically referred to as ASOs.

Perhaps categorizing antisense mechanisms is more useful than focusing on definitions that concern the oligonucleotides themselves. Thus, one can distinguish between mechanisms that involve binding and modulation of function without resulting in degradation of the target and others that promote cleavage of the targeted sequence ((149) and cited refs.). The former includes translation arrest, inhibition of translation initiation, inhibition of exon inclusion, promotion of exon inclusion, RNA antagonists (antagomirs), RNA agonists and disruption of RNA structure. Mechanisms that result in degradation of the targeted RNA can involve RNase H (elicited by an ASO), Argonaute2 (Ago2; RNAi), microRNA (miRNA; P-body and Ago proteins), U1 RNA adaptors and various catalytic motifs as well as chemically facilitated nucleases. Both RNase H and Ago2 are endogenous factors that play roles in natural pathways. A key difference between the actions of the two nucleases is that an ASO is bound to its RNA target prior to RNase H docking and cleavage. Conversely, the guide or
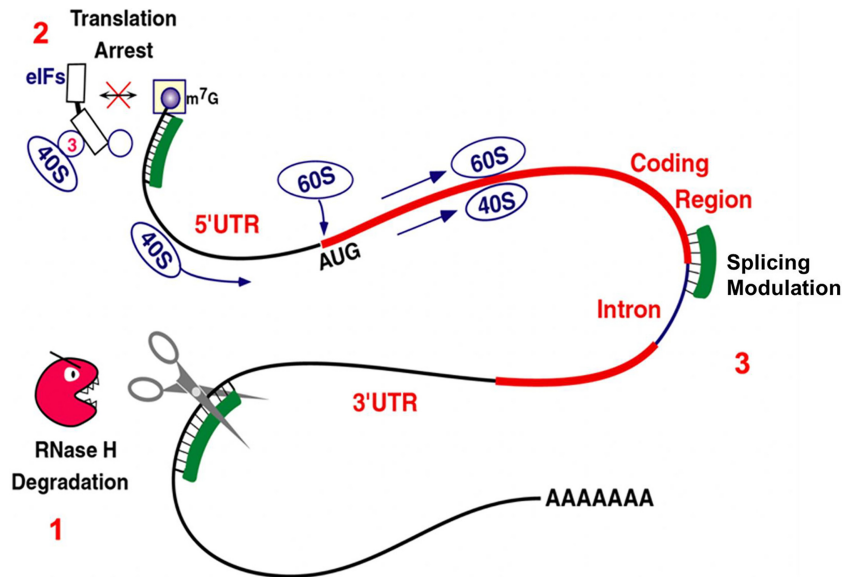
Figure 5. Cartoon of combined ASO mechanisms of action vis-à-vis an mRNA target, either in the nucleus or cytoplasm of the cell: (1) Eliciting RNase H with subsequent degradation of the target, (2) translation arrest, i.e. steric blockage and (3) modulation of splicing. mRNA regions include 5′-cap and 5′-untranslated region (5′-UTR), coding region, 3′-UTR and poly-A tail.

antisense siRNA forms a complex with Ago2 before the enzyme interacts with the target.

In this context, it is interesting to consider the evolution of our understanding of nucleic acid hybridization. As recounted by Alexander Rich (150), when he and David Davies demonstrated the spontaneous formation of a duplex by poly-A and poly-U (18), the observation was widely greeted with skepticism as many believed that a double helix could only be 'made' by an enzyme. The question therefore arises whether there are cellular factors that promote the hybridization of an ASO to its target? Indeed, it was reported that RNA binding proteins such as hnRNP A1 and YB1 significantly facilitate the hybridization of an oligonucleotide to RNA (151,152).

Finally, in terms of a classification of antisense mechanisms and ASOs, it is important to distinguish cellular localizations, i.e. nucleus vs. cytoplasm (153,154). Thus, ASOs that modulate splicing, for example, by exon inclusion (SPINRAZA) or exon skipping (EXONDYS 51) act in the nucleus, whereas ASOs eliciting RNase H can operate either in the nucleus or in the cytoplasm. Subcellular localization of an ASO can affect its potency and the particular chemical makeup of an ASO impinges on its intracellular distribution.

The last point about an ASO's chemistry having an effect on biodistribution is really an understatement as the chemical composition of an oligo affects pairing stability, metabolic stability, protein binding and toxicities caused by binding to Toll-like receptors (155,156), altered coagulation (157), immune cell (158,159) and/or complement activation (160), off-target effects, pharmacokinetics and pharmacodynamics. Native DNA and RNA oligonucleotides are degraded rapidly in cells as they are unable to dodge attack by a host of exo- and endonucleases. RNA and RNA-like analogs exhibit higher pairing stability opposite RNA targets than DNA or DNA-like analogs (76). However, despite

RNase H binding to both DNA and RNA duplexes (161), neither elicits enzyme action as the endonuclease recognizes a hybrid duplex in which the RNA is in the A-form and the DNA is in a B-like conformation (162,163).

Uniform locked nucleic acids (LNAs) exhibit very high binding affinity for both DNA and RNA (164), but they also produce increased liver toxicity (165,166). Perhaps unexpectedly, uncharged peptide nucleic acids (PNAs) do not easily cross cell membranes, although the solubility can be increased with amino acids carrying charges in the PNA backbone (167). And, unlike PS-DNAs, PNA, PMO and regular phosphodiester-backbone oligonucleotides exhibit limited binding to plasma proteins, causing them to be rapidly excreted in the urine (57,168,169). Interestingly, the stabilin class of scavenger receptors has been shown to bind to PS-ASOs and aid in their cellular internalization (170). All these tidbits aim to illustrate that making drugs out of oligonucleotides is not easy and that modification chemistry was and remains crucial for overcoming numerous challenges on the way to nucleic acid therapeutics.

SIMPLE BEGINNINGS: PHOSPHOROTHIOATES AND VITRAVENE

VITRAVENE (fomivirsen) was the first antisense therapeutic approved by the FDA, and the only antiviral oligonucleotide-based drug brought to market to date (9,10,171). Several ongoing clinical trials in various phases are assessing the efficacy of oligonucleotides against HBV and HCV targets (50,51) and there is continued interest in the antimicrobial antisense therapeutic platform (172). VITRAVENE was a 21mer phosphorothioate oligo-2′-deoxynucleotide (PS-DNA; Figures 4, 6) that binds to the complementary mRNA sequence of major immediate-early region (IE2) proteins of human cytomegalovirus (CMV), thereby inhibiting replication of the virus ((173–175) and
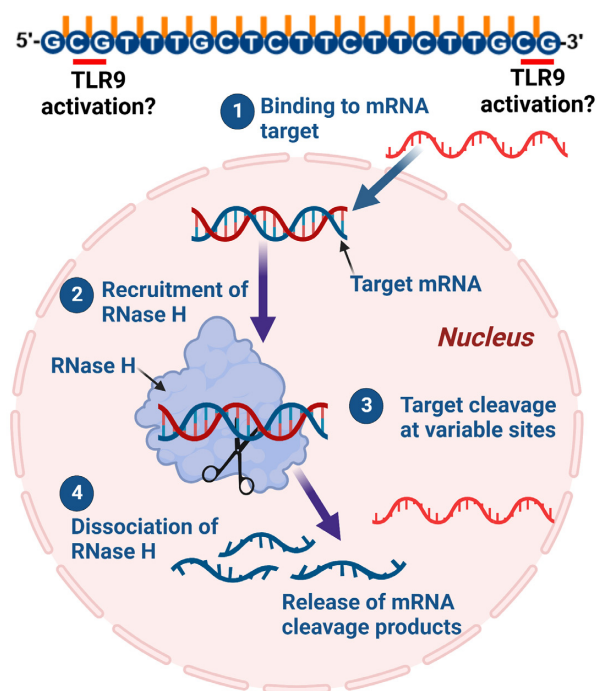
Figure 6. VITRAVENE chemistry and mode(s) of action. Top: ASO sequence and chemical modification; yellow bars indicate phosphorothioate moieties and CpG steps are marked with a red bar. Bottom: individual steps in the ASO's mechanism of action from cellular uptake to target degradation.

cited refs.). The drug was administered intravitreally to delay progression of CMV retinitis in AIDS patients. In immunocompromised individuals this disease leads to loss of retinal cells and eventually vision. In cell culture, the ASO was demonstrated to reduce immediate-early protein synthesis in CMV-infected dermal fibroblasts in a dose-dependent fashion. Fomivirsen also showed activity against drug-resistant mutants of the virus in vitro and combinations of fomivirsen with the antiviral drugs ganciclovir or foscarnet resulted in additive anti-CMV activity. Studies of the pharmacokinetic parameters of fomivirsen in non-human primates established half-lives of its elimination from the vitreous and retina of 22 and 78 h, respectively. This clearance occurred because of the distribution of the drug to other ocular tissues and some chain shortening was most consistent with exonuclease degradation. Fomivirsen was not detected in the plasma of either animals or patients, indicating that there was no appreciable systemic exposure to the oligonucleotide (173).

At the time VITRAVENE was approved, antisense drug discovery and the utility of ASOs as pharmaceutical agents were viewed with skepticism by many (176). The 21mer PS-DNA shares none of the features of a typical small-molecule drug (177); it carries 20 negative charges and is actually a mixture of 2^{20} Rp- and Sp-PS diastereoisomers (Figures 6 and 7A). The main mechanism of action is by RNase H-mediated degradation (Figure 6); at higher concentration of the oligo binding to viral coat proteins was suggested, although this non-antisense mode of action did not con-

tribute to its activity (176). Similarly, there is no evidence that VITRAVENE is cleared by oxidative metabolic pathways (i.e. P450 enzymes) (173). Oligo PS-DNAs bind to plasma proteins (mainly albumin and α2-macroglobulin) (178), and are cleared from plasma by dose-dependent distribution to various tissues and nuclease metabolism with only minor excretion in urine or feces (179–183).

One of the attractive features of the PS modification compared to the parent phosphodiester-based oligonucleotides is the enhanced nuclease resistance. The susceptibility to attack by nucleases differs for the two stereoisomers. Thus, snake venom phosphodiesterase (SVPD, 3′-exonuclease) degrades the Rp PS isomer more rapidly than the Sp isomer ((184) and cited refs.). Crystal structures of DNA polymerase I Klenow fragment exonuclease in complex with short PS-modified oligos demonstrated that the Sp-PS modification affords better protection. Accordingly, the sulfur atom of that isomer intrudes into the coordination sphere of one of the two metal ions bound at the active site (185). By comparison, the endonucleases DNase I, S1 and P1 all prefer the Sp- over the Rp-PS isomer.

Unfortunately, in light of the fact that Sp PS-DNA is more resistant to attack by 3′-exonuclease (186), this isomer forms thermodynamically less stable duplexes with complementary RNA than the Rp isomer (187). Incorporation of PS modifications with mixed stereochemistry into a DNA reduces the melting temperature T_m of the duplex with RNA by about 1°C per modification relative to the parent hybrid (76). Since the reduction in stability is greater for PS-modified A:T pairs than G:C pairs, a high GC content of PS-DNA oligos may be desirable for biological applications. However, the demonstration that RNase H activity with PS-DNA:RNA hybrids exceeds considerably that vis-à-vis all-phosphodiester hybrid duplexes is perhaps more important in this regard (184).

PS oligonucleotide-associated toxicities and immune-stimulation have been analyzed in detail (188). In the case of the VITRAVENE 21mer PS-ASO it is clear that the antiviral activity did not arise as result of immune stimulation by the two CpG motifs (Figure 6) in the sequence (189). Thus, methylation of the cytosines in the CpG dimers did not lead to a reduction in the antiviral activity and an ASO mechanism remains the most plausible mode of action by VITRAVENE (188). Ultimately, the drug was taken off the US market in 2006 as the development of highly active antiretroviral therapies led to a reduced number of CMV cases (190).

SECOND-GENERATION MODIFICATIONS

Conformational preorganization and gamper approach

The RNA 2′-hydroxyl group shifts the conformational equilibrium of the sugar ring to the so-called *North* or C3′-*endo* conformation (191,192). There is a linear correlation between the electronegativity of the 2′-substituent and the ratio between the *North/South* sugar conformations (193–195). Although C3′-*endo* is the pucker mode preferred by ribonucleotides, the sugar is by no means frozen and RNA nucleotides (e.g. in tRNA) adopt a *Southern* conformation on occasion (111). In 2′-*O*Me-RNA and 2′-F-RNA (Figure 7B) the gauche effect between 2′-substituent and O4′ is
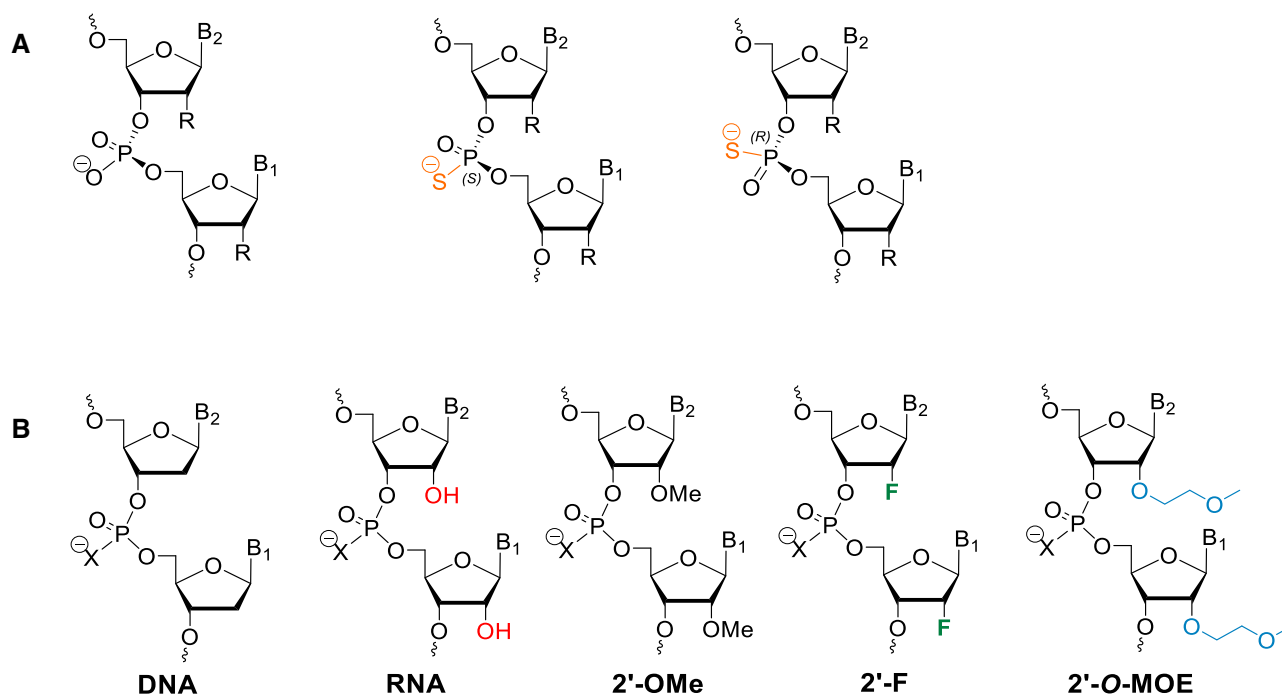
Figure 7. (**A**) Phosphorothioates are first-generation ASO modifications. Structures of the phosphate (left), *S*p-phosphorothioate (*S*p-PS, center) and *R*p-phosphorothioate (*R*p-PS, right) backbones. R = H (DNA), R = OH (RNA), R = F (2′-F RNA), and R = OMe (2′-*O*-Me RNA). (**B**) First- and second-generation RNA modifications. PS (X = S) is important both for ASOs and SSOs and can be combined with 2′-modifications. PS, 2′-*O*-Me and 2′-F are initial RNAi modifications, and 2′-*O*-MOE is prominently represented in ASOs and SSOs. Advantages of RNA 2′-modifications are affinity, nuclease resistance and chemical and metabolic stability, and modulation of hydration and protein binding.

maintained and both exhibit a preference for the C3′-*endo* sugar conformation. These analogs paired opposite RNA increase the thermodynamic stability of the resulting duplex compared with native RNA (196,197). The methyl moiety in 2′-*O*Me-RNA points into the minor groove and the C3′–C2′–O2′–Me torsion angle is always in the antiperiplanar range (198). DNA sugars favor the *South* or C2′-*endo* conformation, but the conformational equilibrium can be shifted to the C3′-*endo* pucker by altering the gauche effect between O3′ and O4′. Thus, the 3′-methylene and N3′→P5′ phosphoramidate DNA analogs mimic RNA and prefer the C3′-*endo* sugar pucker (199,200).

In chimeric RNA-DNA oligonucleotides, ribonucleotides can conformationally dominate the DNA portion to various degrees. We and others found in crystal structures that a single or a few ribonucleotides can flip a 10mer DNA duplex into the A-form (201–204). It is possible that this effect is influenced by lattice forces and dehydration as well as sequence, as the degree of conformational dominance appears to be different in solution (205). Also, in the crystal structure of the duplex [d(CGCGAA)-U*U*-d(CGCG)]₂ with 2′-*S*Me-U (U*), only underlined nucleotides adopt a C3′-*endo* sugar pucker. Neighboring 2′-deoxyadenosines retain a C2′-*endo* pucker and the RNA-like modified uridines in the center force just the 3′-adjacent cytidine into a *North* conformation (206). As a result of the sugar pucker switch from *South* to *North* and back to *South* due to the presence of the 2′-*S*Me substituents, the minor groove in the center of the duplex widens significantly relative to the parent DNA duplex. The EcoRI restriction endonuclease

cleaves the all-DNA strand between G and A (bold font) in the recognition sequence 5′-**GA**ATTC-3′/3′-CTTA**AG**-5′. However, when either one of the Ts or both are replaced by 2′-*S*eMe-U endonuclease activity is completely abolished, thus demonstrating that nucleic acid-binding and/or processing proteins are sensitive to local changes in backbone geometry and duplex conformation.

The nucleotide sugar pucker is also a key determinant of the catalytic efficiency with which DNA polymerases (pols) incorporate dNTPs into the growing chain, whereby preferences vary widely among different pols. DNA primer insertion and extension assays using dATP analogs with methanocarba bicyclo[3.1.0]hexane sugar scaffolds that lock the pucker either in the North C2′-*exo* or South C3′-*exo* forms (N-MC-dATP and S-MC-dATP, respectively) identified distinct behaviors by so-called Y-family error bypass pols (207). Interestingly, given that they are DNA pols, human pol η, κ and ι all preferably or exclusively incorporate N-MC-dATP. In the steady-state kinetic analysis, the efficiency (k_{cat}/K_m) relative to incorporation of dATP was decreased 4-fold (pols η and κ) and increased 5-fold (pol ι). Neither pol κ nor pol ι were able to incorporate S-MC-dATP, but the former could at least extend from the N-MC-dA nucleotide. Conversely, pol η was able to also incorporate S-MC-dATP, albeit with an 80-fold decreased efficiency relative to dATP, and to extend from both the N- and S-MC-dA nucleotides. As expected, HIV reverse transcriptase preferred N-MC-dATP and the efficiency of incorporation was unchanged relative to that of dATP.

The distinct behaviors of the DNA pols vis-à-vis nucleotides of opposite puckers were also seen with the B-family Dpo1 and Y-family Dpo4 pols from the archaeal hyperthermophile *Sulfolobus solfataricus*. Thus, the former inserts both the N- and S-MC-dATPs with relatively minor reductions in efficiency, whereas the latter only inserts N-MC-dATP (208). Dpo4 was then unable to extend; extensions by Dpo1 from the MC-dA nucleotides were inhibited in both cases relative to dA, whereby incorporation following S-MC-dA was slightly favored. The tolerance toward both fixed conformation nucleotide analogs exhibited by human pol η foreshadowed the enzyme's ability to incorporate ribonucleotide triphosphates relatively efficiently (209), act as a reverse transcriptase (210), accommodate RNA for strand extension, and bind to DNA–DNA, DNA–RNA and RNA–RNA duplexes with similar affinities (211).

RNase H also displays affinity for all three duplex types as well as for single strands, but it binds DNA–RNA hybrid and RNA duplexes ca. 60-fold more tightly than DNA duplexes and ca. 300-fold more tightly than single stranded nucleic acids (161). However, as indicated before the enzyme only processes the RNA strand opposite DNA, although it is noteworthy that RNase HI from the thermoacidophilic archaeon *Sulfolobus tokodaii* was reported to cleave RNA strands opposite either DNA or RNA (212). RNase H and Ago2—the former targeting RNA opposite antisense DNA, the latter RNA opposite antisense (guide) RNA—catalyze the same reaction, namely phosphodiester hydrolysis via a dual metal ion mechanism that results in formation of two strands, one with a free 3′-hydroxyl group and the other with a 5′-phosphate group ((213) and cited refs.) (Figure 8A). The PIWI domain that harbors the RNA endonuclease activity in Ago2 also adopts an RNase H-type fold (214–216) (Figure 8B).

In the crystal structure of a bacterial RNase H bound to an RNA–DNA hybrid, the RNA strand is properly oriented at the active site with two Mg^{2+} ions coordinated by Asp and Glu residues and the scissile phosphate lined up to be attacked by the water nucleophile (162). Conversely, the complex of Ago2 with an siRNA duplex is not trapped in an active conformation, Mg^{2+} ions are absent, and the sense strand does not reach the active site (seed region complex (217)). An overlay of the Ago2 Piwi domain and RNase H from the two complex structures demonstrates that the respective RNA strands exhibit different curvatures (Figure 8B) and exposes Ago2 loop regions that need to recoil for the scissile phosphate to move into the active site.

RNase H probes the width of the minor groove of the duplex it docks onto, whereby that groove in an RNA-DNA substrate is narrower and wider than the corresponding grooves in RNA and DNA duplexes, respectively. An overlay of crystal structures of *Bacillus halodurans* RNase H bound to an RNA-DNA substrate duplex (162) and a DNA–DNA inhibitor duplex of the same length (218) shows that the groove widths and strand curvatures in the two duplexes differ distinctly (Figure 8C). RNase H interacts directly with several 2′-hydroxyl groups of the RNA strand and the lack of these contacts in the complex with a DNA duplex precludes proper recognition and of course processing, even if the 2′-OH groups are not directly involved in cleavage. The importance of the 2′-OH interactions for substrate recognition and action by RNase H is further demonstrated by the observation that the enzyme does not cleave a 2′-F-RNA strand opposite DNA (219). The absence of metal ions at the RNase H active site in the structure of the complex with the 2′-F-RNA–DNA duplex further highlights the key role played by 2′-hydroxyls in the proper functioning of the enzyme.

Importantly, 2′-F-RNA as antisense oligo paired to a complementary RNA abrogates cleavage of the latter by RNase H, as do all ASOs that adopt an A-form geometry (220,221). Thus, a uniform 2′-O-modification strategy cannot be applied with ASOs that are intended to elicit RNase H and act via degradation of the RNA target. It also sheds light on the origins of the inability of RNase H to cleave RNA opposite a DNA containing 4′-thio-2′-deoxynucleotides (222). The gapmer ASO design provides a solution to this conundrum: the central PS-DNA window promotes cleavage by RNase H and 2′-O-modified wings afford stability (59,223). The central region is typically between six and ten nucleotides long and the PS modification ensures metabolic stability and favorable biodistribution compared to native DNA. Evidence has been presented that RNase H enzymes prefer particular sequences (224), and it turns out that RNase H is exquisitely sensitive to conformational changes induced by chemical modifications in the strand opposite RNA. Two of only a handful of ASO modifications that are tolerated by RNase H are arabinonucleic acid (ANA) and 2′-deoxy-2′-fluoro-arabinonucleic acid (FANA) (225). FANA nucleotides in a DNA duplex background were found early on to adopt an *Eastern* O4′-*endo* pucker (226) and both ANA and FANA appear capable of mimicking the DNA strand geometry in a hybrid duplex with RNA that is recognized and processed by RNase H (227–229).

2′-Modifications and MOE

Nucleic acids bearing modifications at the 2′-O-position are among the best studied analogs in the antisense, siRNA and aptamer contexts, starting of course with the 2′-O-methyl modification. One of the reasons the 2′-position has proved so fertile for antisense applications is that modification at that site maintains and potentially enhances preorganization of the sugar for an A-type backbone conformation (132). Modification also affords chemical stability in that it precludes 2′-OH-mediated strand cleavage. Moreover, it should result in better protection against nuclease attack owing to the vicinity of the 2′-position to the adjacent phosphate.

Conformational preorganization produces entropy-based gains in pairing stability and recent work has shed light on the origins of the ca. 1°C increase in T_m per modification seen with 2′-O-Me modified strands opposite RNA (230). Accordingly, orientations of the 2′-OH group that have the hydrogen directed toward the phosphate group are at the root of the rich tertiary structure of RNA in that this induces non-canonical backbone conformations. Conversely, the 2′-OH hydrogen directed toward the base prevents it from scanning the backbone, thereby stabilizing a canonical (A-form) strand conformation. 2′-O-Me modification mimics the latter situation as it replaces the
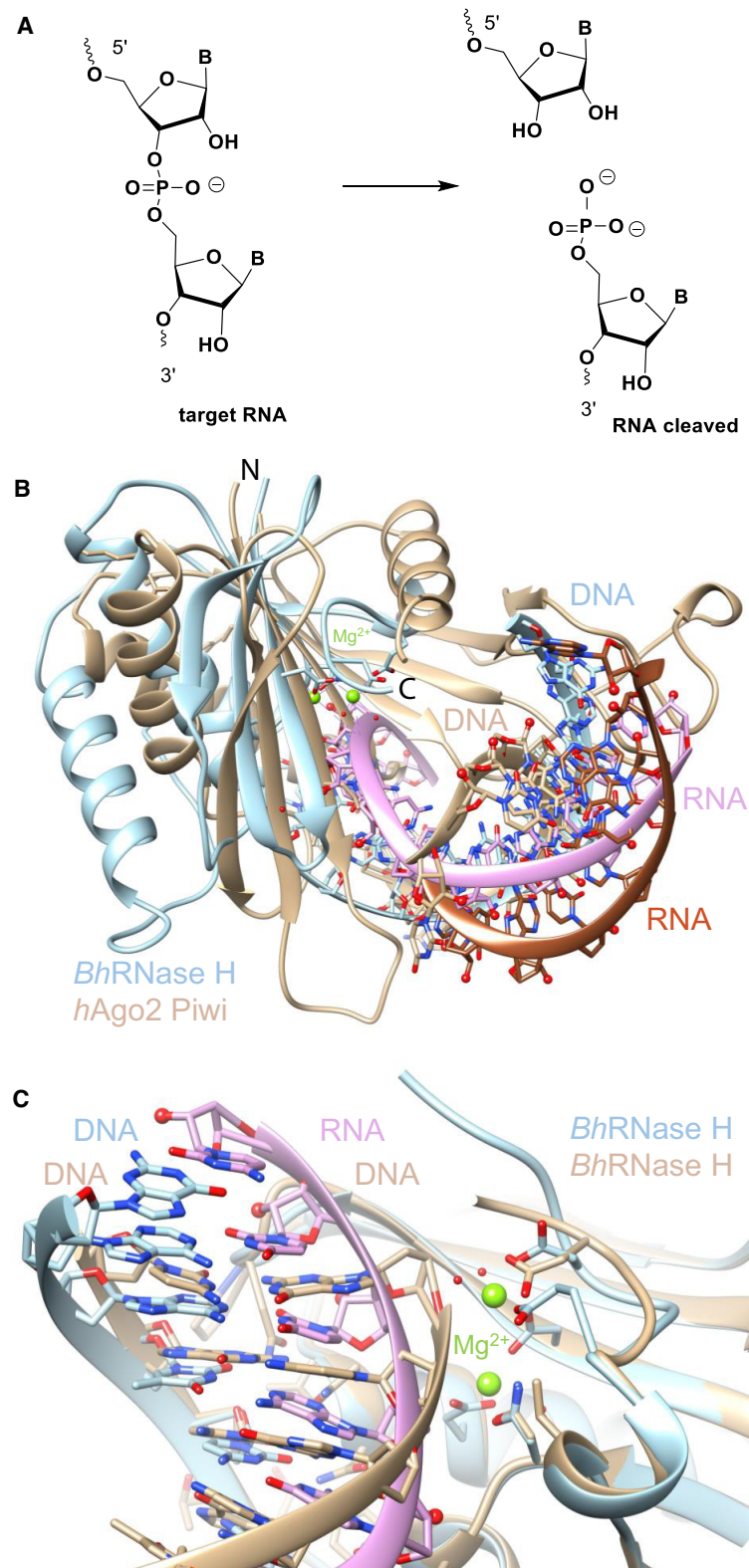
Figure 8. (**A**) Phosphodiester cleavage reaction catalyzed by RNase H and Ago2. (**B**) Overlay of the crystal structures of *B. halodurans* (*Bh*) RNase H (light-blue ribbon cartoon) bound to a DNA (light-blue carbon atoms)-RNA (pink carbon atoms) hybrid (PDB ID 1zbi), and human Ago2 (Piwi domain; tan ribbon cartoon) bound to a passenger strand (tan carbon atoms)-guide strand (brown carbon atoms) duplex (PDB ID 4w5t). Mg^{2+} ions seen in RNase H complex are green spheres and 2′-OH oxygens are red spheres. Only protein atoms were used to superimpose the two complexes: RNase H E66–G194; Piwi Q589–Y790. (**C**) Overlay of the crystal structures of *Bh*RNase H (light-blue ribbon cartoon) bound to a DNA (light-blue carbon atoms)–RNA (pink carbon atoms) hybrid (PDB ID 1zbi) and *Bh*RNase H bound to DNA dodecamer duplex (tan ribbon cartoon; PDB ID 3d0p). Mg^{2+} ions seen in the complex with the hybrid duplex are green spheres. Only protein atoms were used to superimpose the two complexes.

hydrogen with a methyl group that points away from the backbone and towards the minor groove.

We examined the pairing stability and nuclease resistance of ten 2′-*O*-modifications, including smaller substituents such as propyl, butyl, allyl, 2-fluoroethyl (FET) and 2-(methoxy)ethyl (MOE), as well as bulky, e.g. 2-(benzyloxy)ethyl (BOE), and positively charged moieties, e.g. 2-(imidazol-1-yl)ethyl (IME) and 2-[(*N*,*N*-dimethylamino)oxy]ethyl (DMAOE). The nucleobase in most cases was thymine and the tested DNA ASOs contained between three and ten modified nucleotides (133). The FET, IME and DMAOE modifications stabilized the duplex with RNA most, up to ca. 1.5°C ΔT_m per modified nucleotide. By comparison, the MOE modification (Figure 7B) resulted in a ca. 1°C/residue average gain in T_m for the three sequences tested. Interestingly, the ASO with four and ten consecutive BOE modifications still afforded T_m increases of 0.8°C/residue and 0.7°C/residue, respectively.

However, perhaps somewhat unexpectedly given its bulky nature, BOE only provided very little protection against degradation by the 3′-exonuclease snake venom phosphodiesterase (SVPD). In fact, among the investigated modifications, only the 2′-*O*-propargyl modification was worse. The crystal structure of a 2′-*O*-BOE-modified duplex revealed that the phenyl rings were positioned relatively far away from the phosphate group. IME, DMAOE and MOE incorporated at the 3′-end were ranked 1–3 in terms of protection against SVPD attack. The higher resistance to nuclease degradation seen with the IME and DMAOE modifications is consistent with the zwitterionic nature of these analogs that may position a positive charge near the 3′-phosphate group. This is consistent with the observation in crystal structures that virtually all 2′-*O*-substituents were directed toward the 3′-termini of strands.

The MOE-modified nucleoside features extra conformational preorganization as a gauche effect not only dictates the C3′-*endo* sugar ring pucker but also governs the conformation of the ethylene glycol moiety in the 2′-substituent (Figure 9). A crystal structure of a DNA A-form duplex with a single 2′-*O*-MOE residue per strand confirmed that the substituents assume a *synclinal* (*sc*) conformation (231). In the crystal structure both MOE-modified nucleosides cradle a water molecule that is coordinated to O3′, O2′ and the outer oxygen atom of the substituent (Figure 9). The structure of a duplex that contained modified residues with a 2′-*O*-methyl[(tri(oxyethyl)]-substituent (TOE) demonstrated that TOE moieties snake along the backbone, are well ordered and that torsion angles around C-C bonds in the substituent are all in the *sc* range. In addition to the water molecule associated with MOE substituents, TOE substituents stabilize a second water that coordinates to the two outermost oxygen atoms. Without the gauche effect, conformational preorganization is diminished as seen in the crystal structure of a duplex with incorporated 2′-*O*-ethoxymethylene (EOM)-modified residues. Unlike MOE- or TOE-modified residues that enhance the thermodynamic stability of a duplex, the EOM modification is destabilizing and the crystal structure showed local unstacking caused by EOM moieties (231).

A subsequently determined crystal structure of a fully modified MOE–RNA duplex attested further to the impor-

tance of conformational preorganization as the underlying cause of the increased stability and nuclease resistance of this analogue (232). Of the 24 MOE substituents in the duplex 22 adopted the sc^+ or sc^- conformations and most of them trapped a water in a chelate-like fashion between substituent, sugar and phosphate. Thus, MOE modification can stabilize up to three first-shell water molecules per residue, resulting in extensive hydration networks in the minor groove and around backbones in MOE–RNA.

Oligonucleotides with zwitterionic 2′-*O*-(3-aminopropyl)-modified (AP, Figure 10) ribonucleotides at the 3′-end displayed extraordinary resistance against degradation by SVPD (233). To gain insight into the origins of this protective effect, we determined the crystal structure of an AP-modified oligo in complex with *E. coli* DNA polymerase I 3′-exonuclease Klenow fragment. Rather than just altering the orientation of the substrate strand relative to active site residues, the AP substituent knocked out a catalytic metal ion and engaged in a salt bridge to an aspartic acid side chain (234). MOE can deliver enhanced pairing stability and nuclease resistance but is no match for the aminopropyl modification in terms of warding off an attack by an exonuclease.

To combine the conformational preorganization of MOE with the record nuclease resistance delivered by the AP substituent, we created the 2′-*O*-2-[2-(*N*,*N*-dimethylamino)ethoxy]ethyl] (180) (DMAEOE) modification (235) (Figure 10). Indeed, DMAEOE affords gains in T_m per modified residue of up to 1.2°C even with stretches of 10 consecutive modified nucleotides in the strand opposite RNA. Consecutive placement of analogues with positively charged 2′-*O*-substituents, e.g. AP, typically creates Coulombic repulsion in the minor groove with adverse effects on stability. The DMAEOE modification constitutes an exception in this regard as conformational preorganization by the MOE portion prevents entanglement by protonated dimethylamino moieties. Indeed, the crystal structure of a DMAEOE-modified duplex confirmed the hydration motif previously seen with MOE and TOE substituents. Finally, the 2′-*O*-[2-(guanidinium)ethyl] (GE, Figure 10) modification boosted the stability of ASO-RNA duplexes by 2°C (ΔT_m) per modification and the stability of triplexes with duplex DNA by between 2.5 and 4.1°C per modification (236). This analogue also showed exceptional nuclease resistance but, unlike the findings with DMAEOE, consecutive placement of GE-substituted residues was not tolerated and resulted in a slight loss in T_m of –0.1°C per modified residue.

KYNAMRO, TEGSEDI and WAYLIVRA

Since the original synthesis and characterization in 1995 (56), MOE–RNA has been the focus of numerous investigations regarding its clinical efficacy, culminating in the approval of three MOE–RNA/PS–DNA ASO gapmers, KYNAMRO (mipomersen) (15,16,237), TEGSEDI (inotersen) (61,62) and WAYLIVRA (volanesorsen) (63) (Figure 11). The plasma pharmacokinetics (PK) following intravenous (i.v.) administration of an all-PS 5–10–5 ASO with MOE wings targeting human tumor necrosis factor α were characterized in mouse, rat, dog, monkey and human and found
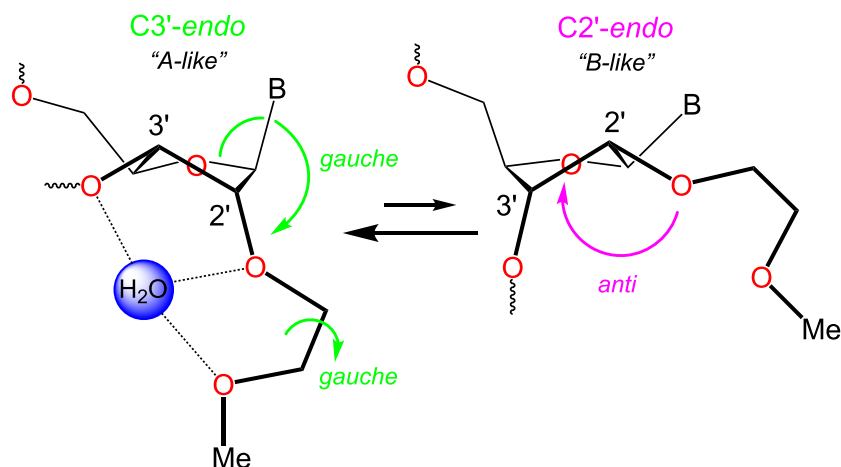
Figure 9. Conformational preorganization by additive *gauche* effects in 2′-*O*-[(2-methoxy)ethyl]-RNA (MOE RNA).
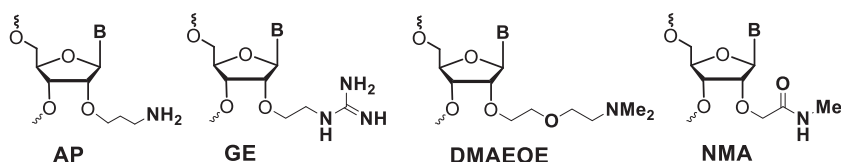

Figure 10. 2′-*O*-modifications with zwitterionic substituents, 2′-*O*-(3-aminopropyl) (AP), 2′-*O*-[2-(guanidinium)ethyl] (GE) and 2′-*O*-2-[2-(*N*,*N*-dimethylamino)ethoxy]ethyl] (DMAEOE). 2′-*O*-[2-(methylamino)-2-oxyethyl] (NMA).
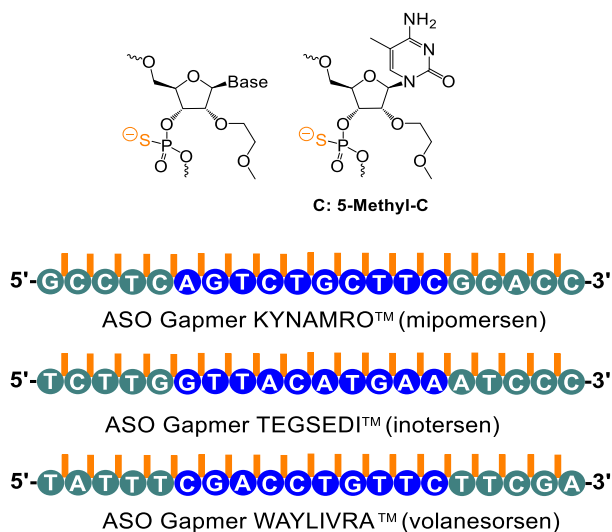

Figure 11. Sequences of three approved gapmer ASO therapeutics, KYNAMRO, TEGSEDI and WAYLIVRA. All elicit RNase H and encompass a 5–10–5 motif with PS/MOE–RNA wings (green) and a central PS–DNA window (blue).

to exhibit quite rapid distribution with a half-life of between 15 and 45 min in all species. Subcutaneous injection of the ASO resulted in absorptions of 80–100%, and when the oligo was administered intrajejunally, bioavailability reached 10% compared to i.v. administration (238). In monkeys less than 1% of the ASO administered by i.v. at up to 5 mg/kg was excreted in urine, the high levels of plasma protein-bound oligo presumably preventing renal filtration. In all species elimination of the ASO from tissue was very slow (several days) and dependent on tissue and organ, whereby the highest concentrations were seen in kidney, liver, lymph nodes, spleen and bone marrow. In a further plasma PK study, tissue distribution and metabolism of three ASOs with a phosphodiester (PO) backbone, all-PS and MOE at both 5′- and 3′-end, or all-PS but with MOE only at the 3′-end were compared after i.v. infusion of a 10 mg/kg dose in monkeys. Plasma clearance was significantly higher for the PO oligos compared to the two PS ones and was attributed to reduced plasma protein binding and nuclease resistance.

The ASO with MOE modification at both ends exhibited greatly enhanced nuclease resistance in plasma and tissues, whereas the one with MOE modification only at the 3′-end resisted degradation in plasma to a certain degree but displayed only moderate resistance in tissues. Urinary excretion was a major elimination pathway for the PO oligo, but accounted for only a minor role in the elimination of the two PS/MOE-modified ASOs (239). The in vitro metabolic stabilities of PO and all-PS ASOs with MOE wings were also studied in a whole liver homogenate from rat or human and the outcomes including the metabolites compared to in vivo half-lives (240). The metabolites identified in vitro were consistent with those from in vivo observations and the relative stabilities of PO and PS/MOE oligos were similar in vitro and in vivo. However, the in vitro assay had limited predictive value in terms of the differences in metabolic stability exhibited by individual MOE/PS oligos. The metabolic pathway inferred from analysis of the metabolites in the preincubated liver homogenates was consistent with an initial endonucleolytic attack in the middle of the central PS–DNA window, followed by 5′- and

3′-exonuclease action. Among all investigated analogues, MOE–RNA constitutes the most thoroughly investigated modification with extensive clinical trial data available (241–243).

KYNAMRO targeted the mRNA of ApoB protein, reduced cholesterol and was approved for treatment of familial hypercholesterolemia. It was the first systemically delivered ASO that obtained market approval (2013). KYNAMRO was given by injection once a week and lowered LDL-C levels in patients, but adverse effects included hepatotoxicity and injection site reactions. JUXTAPID® (lomitapide), a small molecule drug that, like KYNAMRO, comes with a risk of hepatotoxicity, ultimately proved more successful commercially, perhaps, in part, due to its oral administration (50,51,244,245).

TEGSEDI is an ASO that targets the transthyretin (TTR) 3′-UTR and thereby inhibits production of wild-type and mutant TTR proteins. TTR acts as the primary transporter of retinol-binding protein and is also a redundant transport protein for thyroxine. The protein forms a homo-tetramer but mutations in the TTR monomer – there are some 150 reported mutations – destabilize the tetrameric structure (62). Dissociation of the tetramer releases misfolded monomers that can associate to form toxic oligomers and amyloid fibrils. Deposition of these TTR amyloid fibrils is referred to as TTR amyloidosis (ATTR) and the hereditary form of the autosomal dominant disorder is called hATTR. The predominant manifestations of the disease are either polyneuropathy or cardiomyopathy.

Therapeutic intervention for hATTR in the US prior to 2018 included liver transplantation, stabilizing the TTR tetramer (diflunisal), or reducing TTR deposition with a combination of doxycycline and tauroursodeoxycholic acid. The first siRNA for hATTR treatment, ONPATTRO was approved in 2018 for the treatment of the polyneuropathy of hATTR mediated amyloidosis in adults (49). The antisense oligonucleotide TEGSEDI was approved later in the same year for the same indication. The two drugs have different routes of administration, and different safety profiles. TEGSEDI is administered subcutaneously, whereas ONPATTRO is administered intravenously as an LNP formulation (51,246).

WAYLIVRA is an ASO that targets the 3′-untranslated region (3′-UTR) of apolipoprotein CIII (apoCIII) mRNA and was approved by the European Union to treat familial chylomicronemia syndrome (FCS) in 2019. FCS is a metabolic disorder, causes hypertriglyceridaemia that involves a functionally impaired lipoprotein lipase (LPL) and is associated with potentially fatal consequences such as pancreatitis (63). The disorder is characterized by chylomicronemia and hypertriglyceridemia resulting from LPL action. ApoCIII inhibits LDL and increases the concentration of plasma triglyceride by lowering the hepatic uptake of triglyceride-rich lipoproteins while also raising hepatic secretion of triglycerides. The drug is administered by subcutaneous injection; adverse effects include mild injection site reactions, a decreased platelet count and thrombocytopenia. In further clinical trials the utility of WAYLIVRA was assessed for the treatments of hypertriglyceridemia, familial partial lipodystrophy and partial lipodystrophy (63).

However, it doesn't appear in the current pipeline and was replaced by the corresponding GalNAc conjugate (https://www.ionispharma.com/ionis-innovation/pipeline/).

SPLICE SITE SWITCHING OLIGONUCLEOTIDES

SPINRAZA, MOE and spinal muscular atrophy

The ability to modulate alternative splicing is clearly of therapeutic value, given that this process is a major contributor to proteome diversity. Thus, some 70% of human genes are thought to undergo alternative splicing and up to half of all human genetic diseases may arise as a result of mutations that affect splicing (247). Unlike ASOs that are designed to elicit RNase H action, splice-switching oligonucleotides (SSOs) need to bind the target sequence with high affinity and sterically block and redirect the spliceosome (Figure 5). SSOs enable highly specific targeting of essential sequence elements such as splicing enhancers and silencers in pre-mRNA. The splicing of a pre-mRNA transcript can be redirected by various means that include exon exclusion, intron retention, exon shuffling, selection of alternative 5′- and 3′-splice sites, shifting of promoter and polyadenylation sites, and so forth (247). Using an oligo to do so would seem more achievable that identifying small molecules to orchestrate the splicing machinery. However, there are numerous ongoing efforts directed at the discovery of small molecule modulators of alternative splicing (248–254).

All-PS, all-PS/MOE-wing and all-MOE oligonucleotides against human h-ras or rat PKCα were delivered to rats by intrathecal injection (IT) in order to reach the cerebrospinal fluid (CSF) (255). The MOE–ASO remained intact both in spinal cord tissue and in the CSF for up to a day after injection. The ASO was taken up by neurons and glia alike and found to downregulate PKCα in the spinal cord. By comparison, the PS–ASO was considerably less stable and metabolites were detected only 30 minutes after IT administration. Data resulting from this study also indicated that IT injection using increased dosages might successfully deliver ASOs to dorsal root ganglia cells and thus enable downregulation of sensory neuron targets (255). The findings were also exciting because they indicated that the MOE chemistry might open the door to a pharmacological approach for treating neurodegenerative disorders.

Indeed, in 2016 SPINRAZA (nusinersen), a fully modified 18mer PS/MOE–ASO (Figure 12) was approved by the US FDA for treatment of spinal muscular atrophy (SMA) (60,256). SMA is a major genetic disorder associated with degeneration of alpha motor neurons and leading to progressive muscular weakness and atrophy. Infantile-onset SMA robs the individual of the ability to move, eat or breathe and was reported as the leading genetic cause of death for infants (257). The vast majority of SMA cases are due to mutations or deletions in the survival motor neuron 1 (*SMN1*) gene that result in reduced levels of SMN, a multifunctional protein that is required for survival of all animal cells (258). Humans possess two nearly identical copies of the *SMN* gene, *SMN1* and *SMN2*. However, unlike in *SMN1*, exon 7 of *SMN2* is predominantly skipped during splicing in most tissues, thereby resulting in an unstable and only partially functioning protein. SPINRAZA promotes inclusion of exon 7 in
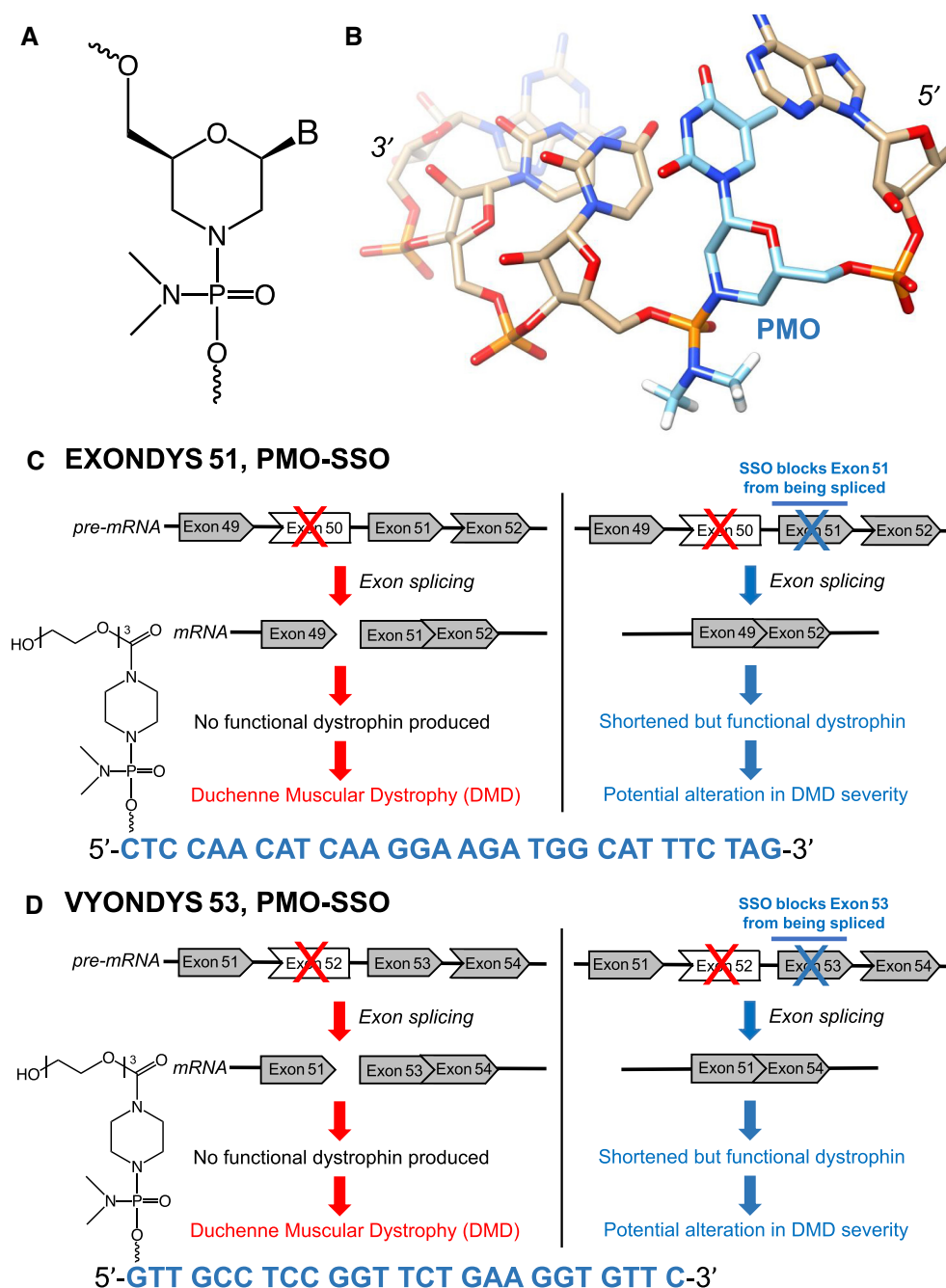
Figure 12. Schematic representation of the *SMN2* exon 7 (capital font)/intron 7 (small font) junction. SPINRAZA blocks the intronic splicing silencer N1 (ISS-N1) located within intron 7 of *SMN2* pre-mRNA (purple arrow), thereby preventing the skipping of exon 7 and promoting production of stable SMN2 protein. *SMN2* intron 7 contains several U-rich clusters that are contacted by glutamine-rich RNA binding protein TIA1 to stimulate exon inclusion. The 3′-terminal end of exon 7, ISS-N1 and TIA1 binding site are highlighted with boxes and intron GU dinucleotides are colored in red. The SPINRAZA SSO contains 5-methyl-C (C*) and is fully PS and 2′-*O*-MOE modified.

SMN2 by blocking an intronic splicing silencer and thus increases the total amount of SMN protein produced (259) (Figure 12).

There is no doubt that SPINRAZA has had a fundamental impact on the treatment of SMA and the lives of infants and adolescents inflicted by this genetic disorder. Not only has treatment resulted in prolonged survival but it has led to dramatic improvements in motor development in children with early and late onset of the disease, such as the abilities to sit up or walk without support. Two additional drugs have been developed for the treatment of SMA. One is ZOLGENSMA® (onasemnogene abeparvovec-xioi), a gene therapy that replaces the defect *SMN1* gene that was approved by the US FDA in 2019 for use with all types of SMA in newborns and toddlers up to age 2 via a single i.v. administration (260). The other is an orally administered small molecule drug, EVRYSDI® (risdiplam), that acts like SPINRAZA at the level of splicing by modulating the *SMN2* pre-mRNA splicing pattern and increasing the amount of full-length functional SMN protein (249). The breakthrough with respect to treatment of a neurodegenerative disorder by an SSO has raised the prospect of successfully expanding oligonucleotide-based therapies to combatting neurological disorders. Examples are Huntington's disease and multiple sclerosis for which MOE-based oligonucleotides are currently being evaluated in various phase clinical trials (50,51).

EXONDYS 51/VYONDYS 53, PMOs and Duchenne muscular dystrophy

Additional SSOs that received market approval are EXONDYS 51 (eteplirsen, 2016 (65)) and VYONDYS 53 (golodirsen, 2019 (66)) (Figure 3, Table 1), both used in the treatment of Duchenne muscular dystrophy (DMD) and targeting exon 51 and exon 53, respectively, of dystrophin pre-mRNA (Figure 13). The two exon-skipping therapies aim to produce shortened but functional dystrophin to increase the levels of the protein in muscle. Dystrophin is expressed in skeletal and cardiac muscle as well as in the brain and is key for strengthening and connecting muscle fibers (261). Unlike SMA, DMD is not a CNS disease but a fatal X-linked disorder that is caused by any of >2000 mutations that affect the *DMD* gene and result in the loss of functional dystrophin protein. Some 70% of patients exhibit single- or multi-exon deletions that result in aberrant expression of dystrophin or duplications, thus leading to progressive skeletal weakness, muscle wasting and cardiomyopathy. DMD patients show levels of dystrophin that are less than 3% of normal. Symptoms of DMD are not limited to motor difficulties such as getting up or climbing stairs, but also include developmental delay and behavioral issues in children as well as impaired growth, delayed puberty and gastrointestinal problems. Life-threatening respiratory and cardiac complications are common in the second or third decade of life. Delays in disease progression and improved life expectancy have been achieved with corticosteroid treatment, surgical intervention and preventive measures in regard to heart failure related to cardiomyopathy.

EXONDYS 51 and VYONDYS 53 are phosphorodiamidate morpholino oligonucleotides (PMOs), often referred to as morpholinos (64). Morpholinos possess a neutral backbone that is completely resistant to nucleases. However, like the phosphorothioates or the neutral methylphosphonates, the PMO modification generates a mixture of *R*p- and *S*p-diastereoisomers (Figure 13A). PMOs are water soluble and display good cell permeability without assistance from cellular factors, but hybridized to RNA they do not elicit RNase H. Although there is a large body of data regarding cell-based assays and in vivo applications of morpholinos (262), and protocols for solid-phase synthesis of PMO oligomers, e.g. (263), detailed biophysical data (264) and in particular experimental structural information are missing.

We modeled a morpholino nucleotide into an RNA A-form oligonucleotide and achieved a virtually seamless fit. Specifically, inserting a morpholino residue maintains the puckers of 5′- and 3′-adjacent riboses and no signifi-

Figure 13. Phosphorodiamidate morpholino (PMO) SSOs that mediate skipping of additional exons for treatment of two types of Duchenne muscular dystrophy (DMD). (**A**) PMO structure. (**B**) Model of PMO conformation in a stretch of A-form RNA. Nucleotide sequence, 5′-modification and mode of action of PMO-SSOs (**C**) EXONDYS 51 and (**D**) VYONDYS 53.

cant alterations of backbone angles were necessary apart from a flip from *sc⁻* to *sc⁺* for ζ in the 5′-ribonucleotide (Figure 13B). All three substituents of the morpholine chair (base, C5′, and 3′-phosphate) adopt an equatorial orientation and stacking is maintained. The model was built with the program UCSF Chimera (265) and energy-minimized with the Amber14 force field (266) (https://ambermd.org/), using steepest descent and conjugate gradient methods until convergence. A PMO nucleotide can just as easily be slipped into a DNA B-form backbone and

accommodated without significant structural perturbation (not shown).

Considering that 5 out of the 16 oligonucleotide therapeutics approved to date are splice-shifting oligos (Figure 3) and that they have paved the road to treatments of devastating diseases for which there are no cures, certainly the development of SSOs should be seen as a success, despite the somewhat controversial FDA approval of EXONDYS 51 (65). Several other targets, however, are being pursued in future treatments of DMD patients, among them therapies to

counter muscle degeneration and fibrosis, reduce inflammation, bypass aberrant stop codons and modulate utrophin, a protein that is similar to dystrophin and may replicate some of its functions (261). Thus, other splice site-targeting drugs are currently undergoing clinical evaluation, and the exon 53 PMO-SSO therapeutic VILTEPSO® (viltolarsen) received FDA approval in 2020 (267). The exon 45 PMO–SSO therapeutic AMONDYS 45® (casimersen) received FDA approval in 2021 (268). In addition, CRISPR/Cas9-based gene replacement approaches may be pursued in the case of DMD treatment as with SMA before (269), and small-molecule drug discovery might result in the identification of new orally available therapeutics that effectively modulate *DMD* pre-mRNA splicing to boost dystrophin expression.

THIRD-GENERATION SUGAR MODIFICATION CHEMISTRIES

We reviewed the concept of conformational preorganization in one of the above sections and discussed various effects on the equilibrium between the C2′-*endo* (DNA-like) and C3′-*endo* (RNA-like) pucker modes of the sugars in the backbones of DNA and RNA. Particularly modifications targeting the 2′-position such as 2′-F, 2′-*O*-Me, 2′-*O*-MOE and 2′-*O*-substitution in general favor the A-form backbone geometry (132,133,232). The sugar ring flips between the North and South regions of the pseudorotation phase cycle (191,192) and the Eastern region is only sparsely populated, FANA being the prime example of a modification that prefers the East O4′-*endo* pucker (226–229). However, without further constraints the pentose retains its ability to fluctuate conformationally, which typically results in an entropically unfavorable contribution to pairing stability opposite an RNA target.

Chemical modifications that could freeze or lock the sugar moiety in the nucleic acid backbone would offer the ultimate control of conformational preorganization. Bicyclic frameworks achieve just that, and so-called locked nucleic acid (LNA) has arguably become the most well-known representative of this class of analogues since its inception in 1997/1998 (Figure 14) (270,271). Bridging ribose O2′ and C4′ with a methylene group effectively locks the sugar moiety in the C3′-*endo* conformation. The concept to bridge various atoms of 2′-deoxyribose, ribose and other sugar stereoisomers and using various linker chemistries has given rise to a wealth of bridged nucleic acids (BNAs, see Figure 14 for a small selection) (272). As expected, pairing between an oligonucleotide containing LNA and either complementary DNA or RNA results in a strongly stabilized duplex - up to 10°C per modified nucleotide compared to the parent duplex (164). In principle, this renders LNA a promising modification for antisense applications, although the analogue could only be used in the wings of ASOs so as not to abolish RNase H activity (73). Indeed, LNA oligos show 5- to 10-fold increased potencies relative to MOE-ASOs in animal studies. However, in rodents, non-human primates and humans, LNA-ASO were found to cause renal and hepatic toxicities and adverse injection site reactions (reviewed in (50)). Clinical trials with a number of LNA-ASOs against various targets as well as with an LNA anti-miRNA oligo (antagomir) are continuing.

The LNA O2′-C4′ bridge allows for further chemical modification. The cEt BNA isomers feature methyl substituents at C4′ and the cMOE BNA isomers are the result of stitching together C4′ and the inner carbon of the ethyl moiety in the 2′-*O*-MOE substituent (Figure 14). Not only do these BNAs maintain the ability to stabilize duplexes relative to MOE-modified strands, but both cyclic analogs exhibit better resistance to 3′-exonuclease degradation than the parent MOE modification (273). Surprisingly, cEt BNA affords better protection than cMOE and crystal structures of modified duplexes and models of 3′-terminally modified strands bound to exonuclease point to a steric origin of the favorable resistance. Several clinical trials with cEt-modified oligonucleotides are underway (50). A carbocyclic analog of LNA (cLNA) with an exocyclic methylene group in place of the 2′-oxygen (methylene-cLNA) afforded similar pairing stability gains and mismatch discriminations as the parent LNA. The corresponding ASOs showed similar affinities but reduced toxicity relative to LNA (274). The methylene-cLNA modification was superior to Me-cLNA isomers, both in terms of affinity and ASO activity.

Bicyclic frameworks do not just allow one to freeze the sugar conformation in the C3′-*endo* mode, but judicious use of isomers and types of bridges has resulted in analogs that are limited to a DNA-like sugar pucker. Thus, α-*L*-LNA adopts solely the South-type C3′-*exo* pucker (Figure 14) (275), but nonetheless does not elicit RNase H when paired with RNA (276). The synthesis of bicyclo-DNA (bcDNA) represents a very early attempt to rigidify the DNA sugar-phosphate backbone. The analogue formed entropically favored duplexes and displayed a propensity for triplex formation, whereby the preferred sugar pucker was either C2′-*endo* or C1′-*exo* (277). Tricyclo-DNA (tcDNA) contains an additional cyclopropyl ring compared with bcDNA, but its sugar adopts a C3′-*endo* pucker instead. In the crystal structure of a DNA duplex with tcDNA residues, the cyclopropyl ring was positioned at the edge of the major groove (278). This observation helped rationalize the considerably increased nuclease resistance seen with tcDNA-modified oligos. Tricyclo-DNA was also extensively tested inside PS-modified ASO gapmers and found to exhibit robust antisense activity in the absence of hepatotoxicity (279).

Finally, the aforementioned methanocarbacyclic N-MC and S-MC sugar modifications also feature a cyclopropyl moiety, between C4′ and C7′ (replaces O4′) and C7′ and C1′, respectively (Figure 14). This rather simple measure locks the pucker in the North C2′-*exo* (N-MC) or South C3′-*exo* (S-MC) mode (280). The N-MC analogue was combined with the 2′-fluoro modification (2′-F-NMC), initially only at the level of thymidine (281). More recently all four nucleoside phosphoramidites have been prepared and incorporated into siRNAs to evaluate the activity of this modification in the context of RNAi (282,283).

RNAi THERAPEUTICS: DOUBLE-STRANDED MECHANISM OF ACTION

A natural defense and regulatory system

The most obvious difference between ASOs and small interfering RNAs (siRNAs) as embodied by current oligonucleotide therapeutics is that the former are single-stranded and the latter double-stranded (Figure 4). The origin of the
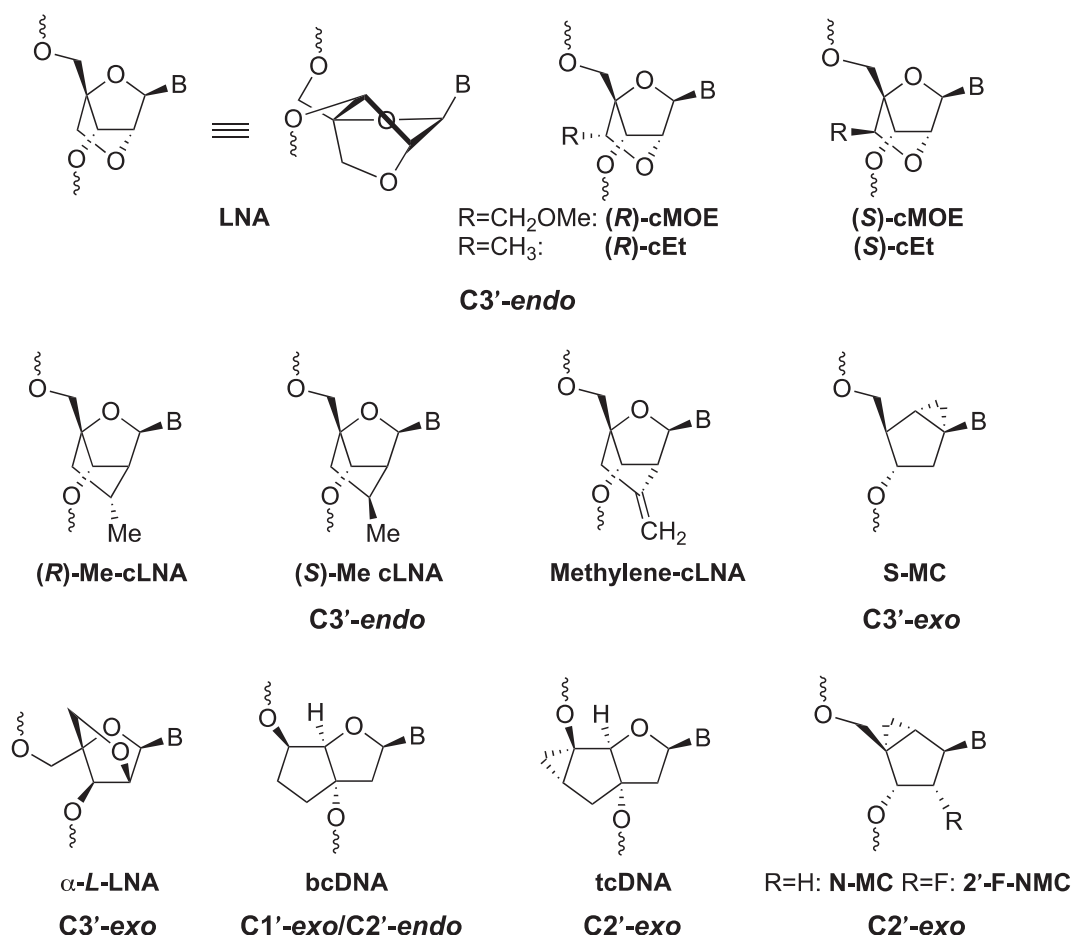
Figure 14. Structures of locked nucleic acid (LNA), bridged nucleic acids (BNAs), bicyclo-DNA (bcDNA), tricylco-DNA (tc-DNA) and North and South methanocarba nucleic acids (N-MC and S-MC, respectively). The preferred sugar puckers of the RNA and DNA analogs are given below the structural formulas.

double-stranded nature of siRNA is not entirely clear. It may be rooted in the archaeal ancestry of the eukaryotic Argonaute (eAgo) proteins or a consequence of a subsequently acquired mode of action during the assembly of the eukaryotic RNA interference (RNAi) machinery from prokaryotic sources. Thus, all cell-based life forms rely on defense systems that provide protection against viruses or transposable elements (284,285). The actual mechanism involves a DNA- or RNA-based guide that directs a nuclease (slicer) to destroy the target, whereby specificity is conferred by base complementarity between guide and target (286).

A ribozyme would represent the primordial version of this defense mechanism in that the catalytic RNA combines guide and nuclease. Because host and parasite have co-evolved since the earliest stages of cellular life (287), defense mechanisms must have emerged simultaneously as part of the diversification of host cells and given rise to the host-parasite arms race that is a central element in the evolution of life. The prokaryotic Ago system (pAgo) is the direct predecessor of eAgo and constitutes the core of proteins and domains that underlie DNA- or RNA-guided innate immunity. Proteins containing MID, PIWI and/or PAZ domains (Figures 8 and 15A) and potentially associated with other nucleases, helicases and nucleic acid-binding proteins

served RNA guide processing, maturation and amplification and the subsequent recognition and destruction of targets (288).

The eAgo system features additional components such as Dicer (Figure 15B) with a helicase domain of archaeal origin and RNase III domains of bacterial origin as well as RNA-dependent RNA polymerase (RdRp) of phage origin that emerged from a predecessor DdRp and is concerned with siRNA amplification in eukaryotes. Dicer is the endoribonuclease that processes double-stranded RNA (dsRNA) into siRNA (287,289,290) (hence the double-stranded nature of fragments), and pre-microRNA into miRNA (291). In eukaryotic cells, the RNAi machinery sets up the innate immunity response and the piwiRNA branch constitutes the distinct type of adaptive immunity (284). In the evolution of the eukaryotic RNAi machinery, the prokaryotic CRISPR/Cas system that represents adaptive immunity in the lower organisms was thus discarded. Not only is the eAgo system inherently more complex than its pAgo predecessor, but it exclusively uses RNA guides and chiefly targets RNA, a change that was presumably triggered by the transition from the prokaryotic world of viruses mainly governed by DNA to a eukaryotic virosphere that is dominated by RNA viruses (292).
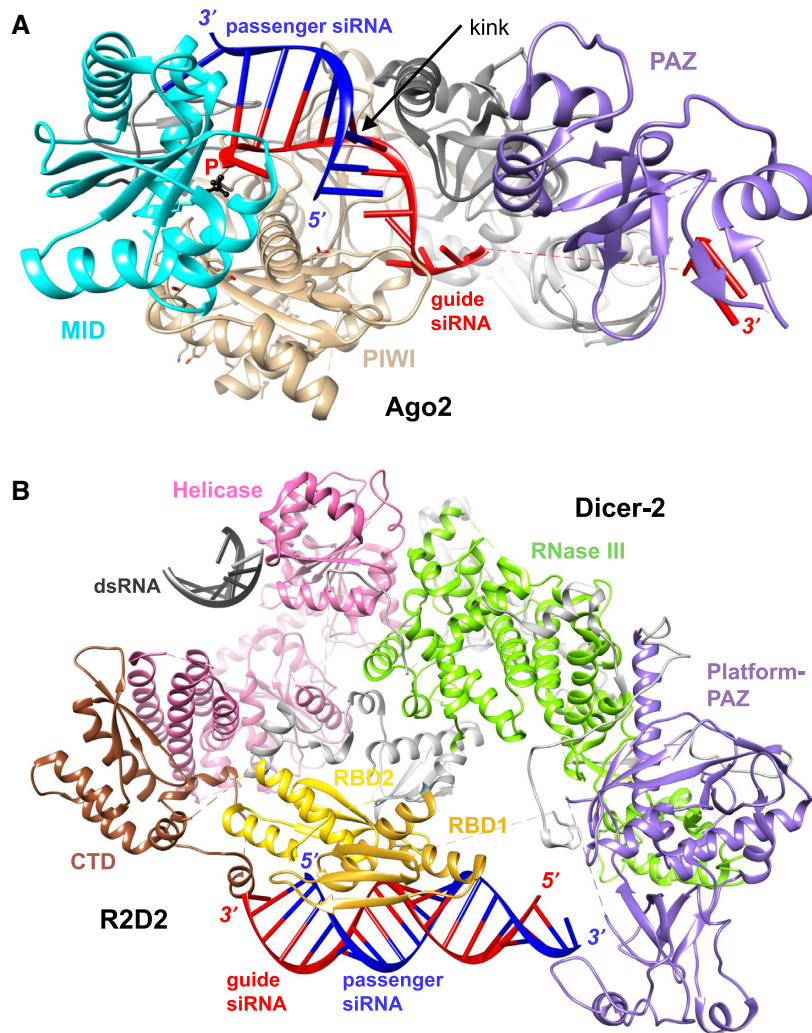
Figure 15. (**A**) Crystal structure at 2.5 Å resolution of human Ago2 in complex with a guide (red)-passenger (blue) strand siRNA duplex (PDB ID 4w5t) (217). Individual enzyme domains are colored differently and are labeled; N-terminal and linker domains are colored in different shades of gray. The MID domain harbors the binding site for the 5′-phosphate group of the guide strand that is colored in black, highlighted in ball-and-stick mode and marked with a red P. The PIWI RNA endonuclease domain ('slicer') cleaves the targeted mRNA opposite guide siRNA. The PAZ domain binds to the 3′-terminal overhang of the guide strand. Dashed lines indicate missing portions of either protein or RNA, e.g. nucleotides 15 to 19 of the guide strand. The arrow points to the sharp kink between base pairs arising from AS6 and AS7. (**B**) Cryo EM structure at 3.3 Å resolution of Drosophila Dicer-2:R2D2 heterodimer in complex with a guide (red)-passenger (blue) strand siRNA duplex and a piece of double-stranded RNA, dsRNA (PDB ID 7v6c) (290). Individual Dicer-2 and R2D2 domains are colored differently and are labeled (R2D2 RBD, RNA binding domain and CTD, C-terminal domain). Regions in Dicer-2 outside the helicase, RNase III and platform-PAZ domains are colored in light gray, and dashed lines indicate missing portions in the protein chains.

The discovery of RNAi as the agent of gene silencing in *C. elegans* (293) and later the demonstration that short dsRNA fragments could be used to silence genes in mammalian cells without triggering an immune response (294,295) was greeted with excitement, as it offered a path to a new therapeutic approach by hitchhiking on a natural defense and regulatory machine. Andrew Z. Fire and Craig C. Mellow were jointly awarded the 2006 Nobel Prize in Physiology or Medicine for their discovery of RNA interference - gene silencing by double-stranded RNA. However, the challenges encountered with early clinical trials echoed those with ASOs a decade before and included toxicity related to immune stimulation, problems with delivery and insufficient therapeutic efficacy (296).

However, RNAi established itself very quickly as a powerful tool in cell-based assays, using either transfection or vector-based delivery in combination with high-throughput screens to knockdown gene expression to ferret out their function and for target validation (297). As well, existing ASO modification chemistries could be applied immediately to siRNAs and tested. Although effective for downregulating genes in vitro, unmodified siRNAs are quickly degraded in vivo and protective steps need to be taken to prevent degradation by nucleases. Unlike natural noncoding RNAs that are composed mostly of native ribonucleotides and sparsely modified, RNAi therapeutics require extensive chemical modification (50,51,67–71,298,299).

Shared features between ASOs and siRNAs contrast with clear differences. As pointed out above, siRNAs are 21mer duplexes that consist of the paired guide (antisense, AS) and passenger (sense, S) strands (Figure 4). Although activity based on the guide strand alone (ss-siRNA) has been demonstrated (300–302), the use of duplex constructs remains much more common. The nuclease in RNAi-mediated cleavage of target mRNA is Ago2, whereby the PIWI domain that adopts an RNase H-like fold harbors the endonuclease (Figure 8). Deviating architectures of RNase H and Ago2 create fundamentally different protein inter-actions with ASO and guide RNA that direct degradation of their respective targets (75,217,303–305). Among the Ago family of proteins, Ago2 is the only one that pos-sesses endonuclease activity (306,307). Other family mem-bers are involved in miRNA-mediated pathways of post-transcriptional regulation (217,284,308).

The various steps of RNA interference using an exogenous siRNA are depicted in Figure 16. Following delivery and cellular uptake, (i) the siRNA duplex is loaded into RISC Ago2, (ii) the passenger strand is peeled off the guide strand and discarded, (iii) after which the target mRNA is accommodated opposite the guide siRNA, (iv) prompting cleavage of the former by Ago2 and (v) removal of the sliced target and initiation of the next round of endo-nucleolytic cleavage. The illustration in Figure 16 highlights another difference between guide siRNA and ASO, namely a 5′-phosphate group in the former that is important for recognition and stable binding of the guide as well as discriminating between guide and passenger strands (Figure 15A).

The presence of two strands and the lack of proper discrimination between them can trigger an off-target effect (OTE) (296,297,299). An OTE can arise from a passenger strand directing cleavage of a complementary target, i.e. sense-mediated silencing. Alternatively, downregulation of an mRNA target is based on partial complementarity between siRNA and mRNA target, also referred to as seed-mediated silencing (the seed region entails nucleotides 2–8 of the guide strand). Other OTEs are the induction of type I interferons and inflammatory cytokines (immune stimulation) and upregulation of miRNA-controlled genes as a result of a saturation of the RNAi machinery (309). Shortened passenger strands as well as blunt-end siRNA designs were introduced to counter the likelihood of OTEs (310–313).

Compared to ASOs, the double-stranded nature of siR-NAs also creates unique challenges for delivery that need to be addressed with tailored approaches for formulation and new modification/conjugation chemistries. Not unexpectedly, single-stranded ASO and siRNA duplexes exhibit divergent pharmacokinetic and pharmacodynamic profiles (296). To make siRNAs into drugs, chemical modification strategies need to consider both the guide and the passenger strand, thus precluding a uniform modification design seen, for example, with SSO therapeutics such as SPINRAZA or EXONDYS 51 (75).

Initial RNA modifications: PS, 2′-*O*-Me and 2′-F

We discussed in detail the benefits of the phosphorothioate and 2′-*O*-modifications for ASOs and SSOs. They include nuclease protection, conformational preorganization and enhanced pairing strength (2′-*O*-mods.), low toxicity and favorable pharmacokinetic and pharmacodynamic behavior (PS, MOE). In a study dating back almost a decade, we compared the in vitro and in vivo efficacies of various 2′-modifications in siRNA against Factor VII, an established endogenous target system. In both the guide (AS) and passenger (S) strands every pyrimidine ribonucleotide was replaced with the 2′-F, 2′-*O*-Me, 2′-*O*-MOE or LNA analogues (314). Relative levels of Factor VII protein were measured in mice on day 2 and up to three weeks after administering 2, 3 or 5 mg/kg of F/F, OMe/OMe, MOE/MOE, LNA/LNA, OMe/F, MOE/F or LNA/F (S/AS strands) siRNA in a lipid formulation. Factor VII amounts resulting from treatment with the F/F combination were >3-fold lower than those seen with the second ranked siRNA, LNA/F and ca. 10-fold reduced relative to the levels measured for OMe/OMe, MOE/MOE and LNA/LNA.

The overall ranking was as follows: F/F < LNA/F < OMe/F < MOE/F ≈ MOE/MOE ≈ OMe/OMe ≈ LNA/LNA. The F/F siRNA also outperformed the parent duplex (OH/OH) in terms of silencing and was non-immunostimulatory, unlike OH/OH that stimulated IFN-α and TNF-α. The melting temperature (T_m) of the F/F duplex was about 20°C above that of the parent duplex, but LNA/LNA and MOE/MOE as well as LNA/F and MOE/F duplexes were all more stable than F/F. The increased stability of the F/F duplex is chiefly enthalpy-based which points to improved stacking and/or H-bonding interactions because of fluorine modification. Indeed, we subsequently demonstrated using solution NMR and thermodynamic assays with RNA hairpins that featured 2′-F-modified overhangs at the 3′-end that the fluorine modification strengthens both Watson-Crick H-bonds and base stacking (315).

Fluorine is smaller than the 2′-hydroxyl group, hydrophobic and typically lacks the ability to participate in H-bonds (316). This is definitely the case in the RNA minor groove as we showed using crystallographic data and osmotic stressing assays (317) (Figure 17). However, organic fluorine leads somewhat of a double life and there have been observations where it does act as an H-bond acceptor (e.g. (318,319)). The poor hydration in the minor groove precludes the need for de-solvation of 2′-F-modified siRNA upon transport and uptake and may have an impact on cellular trafficking and endosomal release. One limitation of the 2′-F modification is the limited protection against nuclease degradation it affords compared to other 2′-modifications such as 2′-*O*-Me and 2′-*O*-MOE. Moreover, at high concentrations 2′-F nucleotides are recognized, although somewhat poorly, by human RNA polymerases (320,321).

A design principle that emerged as a solution to these shortcomings is to combine 2′-F and 2′-*O*-Me modified nucleotides in fully modified siRNAs (322). An example of the successful application of this approach is GIVLAARI (givosiran), an siRNA approved by the US FDA in 2019 for treatment of acute hepatic porphyria (Figures 1 and 18). GIVLAARI also contains pairs of PS modifications at the 5′- and 3′-ends of the guide siRNA as well as PS modifications on the first and second phosphates in the passenger siRNA as well as the tri-
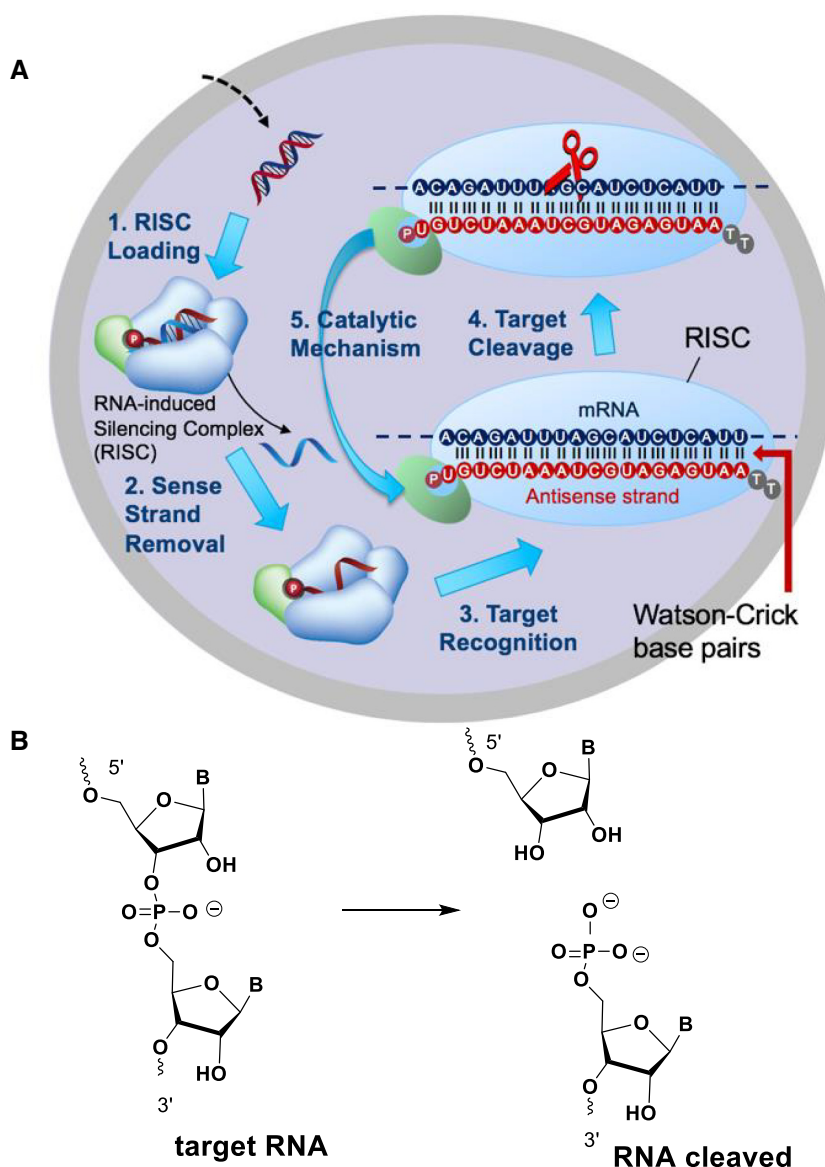
Figure 16. (**A**) Individual steps of RNA interference directed by exogenously delivered siRNA: (1) RISC loading, (2) passenger strand removal, (3) binding of mRNA target, (4) target cleavage, and (5) release of cleavage products and pairing with the next target to begin a new round of cleavage. Guide siRNA, passenger siRNA, and mRNA target are colored in red, blue and black, respectively. The Ago2 MID domain is highlighted in green and red and gray dots mark the 5′-terminal phosphate and 3′-terminal TT overhang, respectively. (**B**) The phosphodiester cleavage reaction catalyzed by Ago2.

antennary GalNAc linker at its 3′-end to facilitate uptake (vide infra).

As mentioned above, MOE modification of siRNA strands did not result in favorable in vitro or in vivo efficacies against the Factor VII target (314). The modification is sterically quite demanding in the minor groove and a model of a modified RNA duplex bound to Piwi protein revealed clashes between protein side chains and MOE substituents at the protein-siRNA interface (314). Conversely the small fluorine substituent is well tolerated and mimics 2′-hydroxyl groups in the complex with the parent duplex. Thus, it is the only 2′-modification that is tolerated at the second position of the guide strand (AS2), where Ago2 forces the RNA to make a tight turn (75). We also used the crystal struc-

ture of human Ago2 in complex with miR-20a to build a model with 2′-*O*-MOE substituents attached to all residues of the guide strand seed region (AS2–AS8) (75). The model exposed clashes between all MOE moieties and Ago2 side chains, indicating that the MOE modification is likely too bulky to be accommodated at many sites in the siRNA guide and passenger strands. An MOE-modified residue was introduced at the first position of the guide strand (AS1), but the crystal structure of the complex with Ago2 did not reveal an interaction between the 2′-*O*-substituent and MID domain residues (75,323).

Another modification at that site, 2′-*O*-[2-(methylamino)-2-oxoethyl] (2′-*O*-NMA), in combination with a 5′-(*E*)-vinylphosphonate ((*E*)-VP) moiety, a metabolically stable
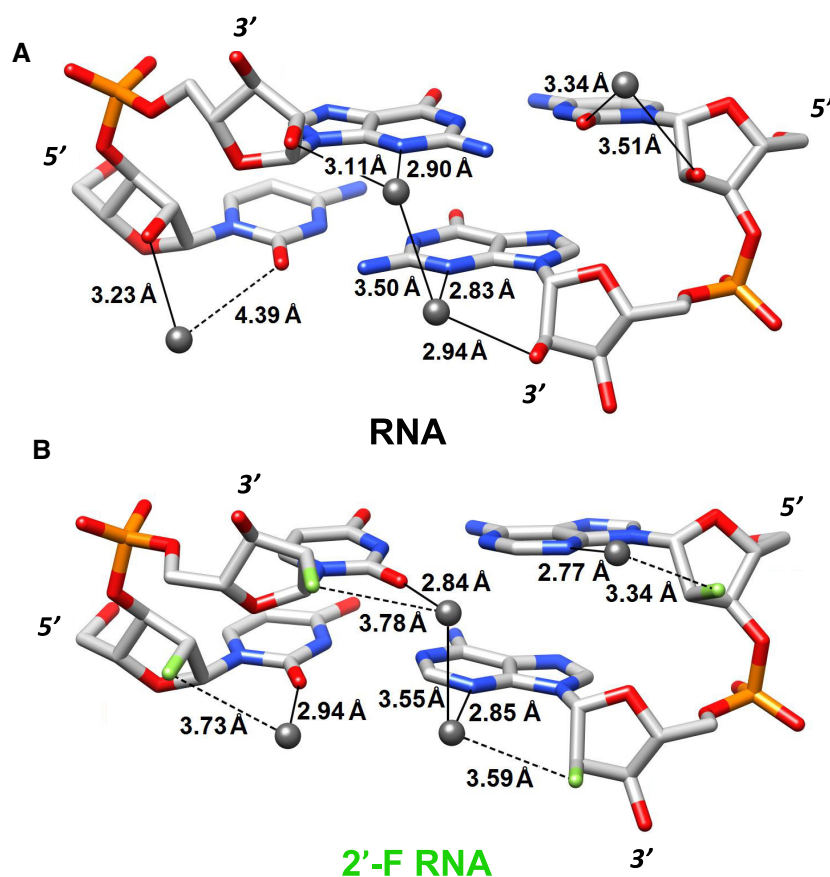
Figure 17. Effects of chemical modification on the water structure around RNA. Minor groove hydration in (**A**) RNA and (**B**) 2′-F-RNA. RNA 2′-hydroxyl groups serve as bridge heads for tandem water bridges across the minor groove (89). Introduction of fluorine (highlighted in green) abolishes H-bonds between 2′-substituent and water, as apparent by altered distances and shifted water molecules. (291,294). Water molecules are gray spheres, H-bonds are thin solid lines and selected distances are indicated by dashed lines.

phosphate mimic (Figure 19), improved RISC loading and showed robust siRNA-mediated gene silencing (324). A structural model of 5′-terminal guide strand residues with 5′-(*E*)-VP/2′-*O*-NMA-U at AS1 bound to Ago2 was consistent with an H-bond between the NMA substituent and the side chain of Gln-548 that together with Asn-551 stabilizes the tight turn in the guide strand at that site.

Conformational flexibility and reduced off-target effects: GNA

We touched upon off-target effects (OTEs) in the siRNA introductory section and discussed the various origins and types of OTEs, including silencing of genes due to passenger strand activity and RNAi-mediated silencing caused by matching sequences between guide-strand seed region and non-targeted RNAs. Careful selection of target sequence and region (325), avoidance of non-Ago2 mediated silencing involving guide-strand seed pairing opposite non-targeted sequences (activation of miRNA pathway of silencing (326,327)) and reduced dosage combined with chemical modification to modulate seed pairing (88) can all reduce OTEs. The latter idea was inspired by a kink between nucleotides AS6 and AS7 in the siRNA seed region in the structures of Ago2 complexes bound either to miRNA

(303) or guide/passenger strand seed duplexes (217) (Figure 15A). The wrinkle in the RNA chain causes local unstacking and appears to be promoted by an isoleucine side chain that inserts itself between AS6 and AS7 nucleobases. Moreover, the RNA backbone at the site of the kink is characterized by closely spaced phosphate groups, whereby potential Coulombic repulsion is relieved by adjacent arginine residues.

Incorporation of an (*S*)-glycol nucleic acid (GNA, Figure 19) residue or GNA base pair at the site of the kink resulted in favorable in vitro and in vivo silencing activity of the modified siRNA relative to the parent duplex (ca. 2-fold gain in potency) (328). GNA is the simplest phosphate-based nucleic acid, lacks a cyclic sugar moiety and its backbone is shortened by a bond compared to DNA and RNA. GNA is chiral and the pairing behavior is quite unusual. GNA self-pairing is of the Watson-Crick type, but base pairs are inverted—like in left-handed Z-DNA—inside the (*S*)-GNA right-handed duplex with a backbone geometry that resembles the A-form (329). Paired opposite RNA—only (*S*)-GNA pairs with RNA but not (*R*)-GNA—GNA does not alter its inverted base orientation. Thanks to its shorter backbone (*S*)-GNA mimics the kinked RNA conformation between AS6 and AS7, thereby mitigating OTEs. First, GNA conformationally preorga-
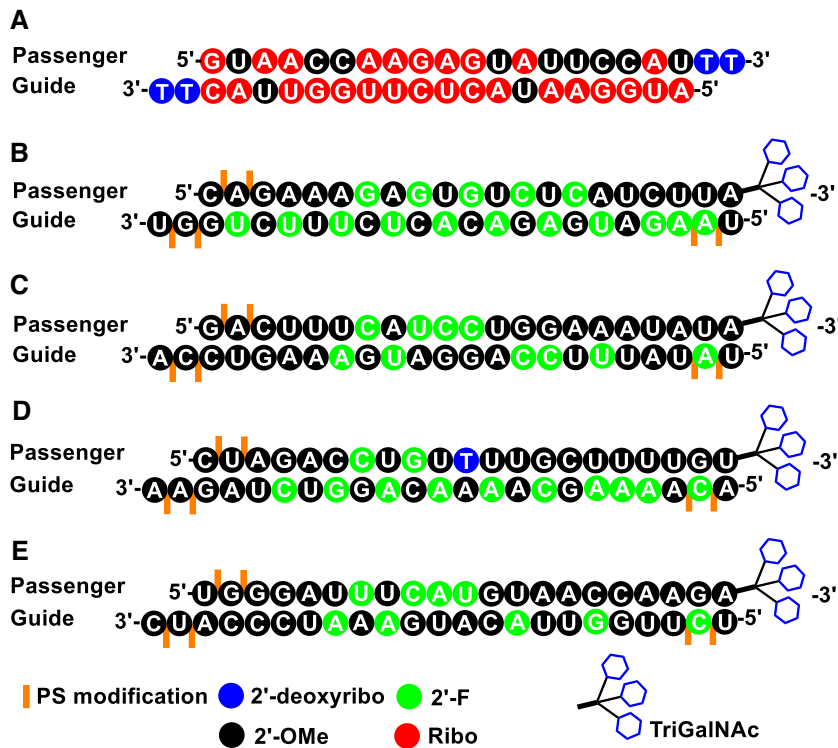
Figure 18. Guide and passenger strand sequences and modifications in the five RNAi therapeutics that have received market approval to date. (**A**) ONPAT-TRO, (**B**) GIVLAARI, (**C**) OXLUMO, (**D**) LEQVIO and (**E**) AMVUTTRA. Ribo-, 2′-deoxyribo-, 2′-*O*-Me- and 2′-F-nucleotides are depicted as circles colored in red, blue, black and green, respectively. GIVLAARI, OXLUMO, LEQVIO and AMVUTTRA feature PS modifications (orange bars) and a triantennary GalNAc conjugate at the 3′-terminal end of the passenger strand.
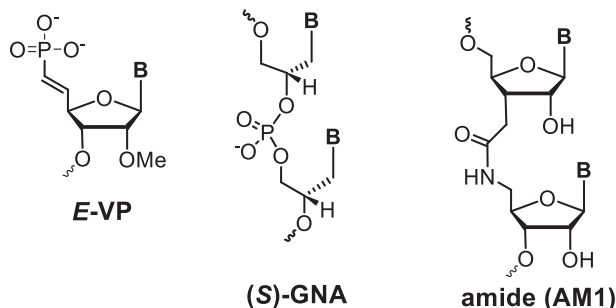
Figure 19. Structures of the phosphate analog *E*-vinylphosphonate (*E*-VP, left), (*S*)-GNA (center), and the amide backbone linkage (AM1, right).

nizes the RNA backbone for the kinked conformation that is sculpted by Ago2 after loading. Second, the conformationally flexible GNA residue incorporated into RNA lowers the thermodynamic stability of modified duplexes and depresses the affinity of pairing between guide siRNA seed region and matching sequences of non-targeted RNAs (330). This work demonstrated the benefits of structure-based and regiospecific chemical modification of siRNAs (75).

There are many other design strategies to combat RNAi OTEs and improve siRNA potency. A recent example is the blockage of 5′-phosphorylation of the passenger strand by a 5′-morpholino modification (331). This modification results in improved antisense strand selection and RNAi

activity. When the morpholino moiety is placed at the 5′-end of the guide strand it triggers complete loss of activity. Morpholino modification makes the sense strand siRNA a more effective passenger and can be combined with the (*E*)-VP moiety instead of phosphate at the 5′-end of the guide strand (Figure 19). The interaction between the 5′-phosphate and a strongly positively polarized binding pocket on the MID domain (332) is probably key to loading and discrimination between guide and passenger strand. The (*E*)-VP but not the (*Z*)-VP modification mimics the 5′-phosphate bound to MID (75,333) and affords enhanced potency by precluding dephosphorylation and repeated phosphorylation in cellular environments (324,334). The enhanced stability and activity afforded by the (*E*)-VP phosphate analog is particularly important for ss-siRNA efficacy (334).

Finally, yet another way for reducing potential OTEs was demonstrated with a neutral amide modification (Figure 19) that replaces the RNA phosphate group. Amides are well tolerated at many sites in the backbone of guide and passenger strands and were found to emulate interactions between the negatively charged phosphate group and protein side and main chain atoms (335). However, the amide moiety is not a suitable mimic of the phosphate at the site of a sharp turn between the AS1 and AS2 residues of guide siRNA bound to Ago2. Thus, an amide linkage incorporated at the corresponding site in passenger siRNA, between S1 and S2, can prevent off-target activity by the sense strand (336).

The first RNAi therapeutic: ONPATTRO

In 2018, ONPATTRO® (patisiran) received approval in the US and Europe for the treatment of the hereditary disease transthyretin-mediated amyloidosis in adults. (hATTR (337)) (Figures 1 and 3, Table 1). As pointed out above, the PS/MOE-modified ASO gapmer TEGSEDI (inotersen) was granted approval by the EC and subsequently by the FDA in the same year. Both therapeutics target the 3′-UTR of *TTR* mRNA but are administered via different routes, namely intravenously and subcutaneously, respectively (50,51,338).

ONPATTRO features 21mer guide and passenger strands with deviating modification patterns (Figure 18A). They share the use of 2′-deoxythymidines at the 3′-ends and 2′-*O*-Me modification of selected pyrimidine nucleotides. However, in the guide only two uridines are 2′-modified as compared to five uridines and four cytidines in the passenger strand. 2′-*O*-Me modification affords increased nuclease resistance at sites that were found to be prone to strand cleavage. TEGSEDI and ONPATTRO exhibited somewhat different safety profiles in phase 3 clinical trials, whereby thrombocytopenia, renal dysfunction or elevated levels of liver enzymes were not observed with administration of ONPATTRO (51,339). ONPATTRO is delivered in a lipid nanoparticle (LNP) formulation and in order to minimize potential proinflammatory effects, patients are pretreated with H1 and H2 antihistamines, an analgesic and a glucocorticoid (338). LNP formulation is not unique to ONPATTRO, as 10 other LNP drugs have been given the green light by regulatory agencies over the last 30 years (49). However, ONPATTRO is the only oligonucleotide therapeutic so far that employs LNPs for delivery (Figures 2B and 20).

The success with LNP formulation built on the initial breakthroughs with systemic delivery of modified siRNA by i.v. in mice (340) and systemic delivery in a liposomal formulation to non-human primates (341). Although LNP formulation had been developed for delivery of small molecule drugs, those concepts did not yield viable formulations for clinical use of the much larger and negatively charged siRNAs. Ultimately, it took several breakthroughs to optimize LNPs with the ability to encapsulate the siRNA duplex and deliver it to the cytoplasm of hepatocytes in vivo (49). One of these was the identification of ionizable cationic lipids that are positively charged at acidic pH but neutral at physiological pH to prevent toxic effects due to immune stimulation triggered by positively charged systems. Another was the use of PEG lipids with C_{14} acyl chains for incorporation into the surface of LNPs to generate diameters in the 20–100 nm range and minimize interactions between PEG and target cells that could hamper delivery. Lastly, a large number of ionizable lipids was screened and evaluated initially in rodents and subsequently in non-human primates in the search for a chemistry that would afford optimal potency (Figure 21A). And so ONPATTRO became the first RNAi therapeutic to be brought to market, 20 years after the discovery of RNA interference.

GIVLAARI and acute hepatic porphyria

GIVLAARI® (givosiran) is used in the treatment of acute hepatic porphyria (AHP) in adults and was the second RNAi therapeutic to receive approval by the FDA. AHP are rare inherited, metabolic disorders of heme biosynthesis that lead to build-up of porphyrins which negatively affects skin or the nervous system, with some patients experiencing serious and potentially life-threatening attacks. Symptoms of an attack include chest and abdominal pain, vomiting, constipation, and high blood pressure and heart rate (342). Treatment options depend on the type of porphyria and a patient's symptoms. Avoiding sunlight helps with porphyria of the skin and the treatment of an attack may involve intravenous application of heme or glucose solution. The disease can be inherited from one parent or both and be of the autosomal dominant, autosomal recessive or X-linked dominant types.

AHP arises from an autosomal dominant loss-of-function of one of three enzymes in the heme biosynthesis pathways, namely the third (leading to acute intermittent porphyria), sixth (leading to hereditary coproporphyria) or seventh enzyme (leading to variegate porphyria). A fourth rarer type stems from an autosomal recessive inheritance (48). As a consequence of these disorders, precursors such as δ-aminolevulinic acid and porphobilinogen are being accumulated, eventually triggering AHP attacks. Notable individuals who were speculated to have suffered from porphyria include King George III and Vincent van Gogh, although in the case of the former this was debunked (343). A definitive diagnosis of porphyria in the case of the artist remains elusive (344), and various origins of his symptoms and mental health state have been put forth, including schizoaffective disorder (345) and lead poisoning (346).

GIVLAARI targets aminolevulinate synthase 1 (*ALAS1*) mRNA and is composed of fully chemically modified 23mer and 21mer siRNA guide and passenger strands, respectively. The 3′-end of the passenger siRNA is linked to a triantennary N-acetylgalactosamine- (GalNAc-) containing ligand (Figure 18B). Except for the passenger terminus that is conjugated to the GalNAc ligand, the remaining termini are PS-modified at the last two bridging phosphates. The siRNA duplex contains 28 2′-*O*-Me modified nucleotides and 16 2′-F modified nucleotides, such that the modification chemistries in the guide siRNA are nearly balanced (12 2′-*O*-Me and 11 2′-F residues). The two analogs alternate along nearly the entire length of the guide; in the passenger strand the alternating mode is limited to the central 11mer (Figure 18B).

GalNAc conjugation chemistry requires no formulation and offers a delivery concept (82–88) that is entirely different from i.v. administration of LNP-encapsulated siRNA (Figure 20). GalNAc-siRNA conjugates allow targeted delivery to liver thanks to GalNAc sugars being recognized by the asialoglycoprotein receptor carbohydrate recognition domain (ASGPR-CRD) (347). ASGPR is predominantly expressed on the surface of hepatocytes but only exists in small quantities on extra-hepatic cells. This enables specific, receptor-mediated hepatocyte delivery of therapeutics for the treatment of hepatic afflictions while reducing risk of off-target effects (348). Galactose and GalNAc are sugars that ASGPR binds with high affinity, whereby the particular isomeric form, branching and galactose linkers, among others, influence ligand-receptor binding. Once docked to ASGPR, the receptor facilitates inter-

Figure 20. Platforms for delivery of functional siRNAs to liver: LNPs vs. GalNAc-siRNA conjugates.

Figure 21. (**A**) LNP multi-component formulation for efficient systemic delivery of the RNAi therapeutic ONPATTRO to hepatocytes. (**B**) LNP multi-component formulation for intramuscular administration of mRNA vaccines COMIRNATY and SPIKEVAX.

nalization of the conjugated siRNA by clathrin-mediated endocytosis.

GIVLAARI is administered subcutaneously once a month and exhibited a half-life of six hours, whereby metabolites were primarily eliminated in urine (48). Adverse events during clinical trials included nausea, injection site reactions, rash, increase in serum creatinine, and transaminase elevations. An immunogenic effect was observed in one patient (of 111) during placebo-controlled and open-label clinical studies (349).

OXLUMO and primary hyperoxaluria type 1

Primary hyperoxaluria 1 (PH1) is a rare genetic disorder that results in increased hepatic oxalate production. Debilitating and life-threatening clinical manifestations include kidney stones, kidney failure and systemic oxalosis. Novel therapeutic approaches aimed at lowering oxalate levels and minimizing renal damage and focused on different targets range from cell-, gene- and protein-based therapies to small molecule inhibitors and oxalate-degrading enzymes and bacteria (350). Substrate reduction therapy is a potentially successful strategy to treat inborn metabolic diseases. Thus, inhibiting the biosynthetic pathway to production of the main precursor of oxalate should in principle be therapeutically beneficial to PH1 patients.

RNAi offers an attractive approach for addressing an unmet need to treat PH1 with high efficacy and sufficient durability. Lumasiran is an siRNA that targets the mRNA of the hydroxyacid oxidase 1 (*HAO1*) gene that encodes glycolate oxidase (GO), thereby precluding the conversion of glycolate to glyoxylate, the main precursor of oxalate (350). This siRNA was approved by the US FDA in 2020 as OXLUMO for treatment of PH1, to lower urinary and plasma oxalate levels in pediatric and adult patients (351). GO lies upstream from alanine-glyoxylate aminotransferase (AGT) that normally metabolizes glyoxylate to glycine in liver peroxisomes. AGT deficiency due to genetic mutations in PH1 patients means that glyoxylate is not efficiently converted to glycine. Rather, glycine is oxidized to oxalate by cytosolic lactate dehydrogenase (LDH), causing urinary oxalate excretion to spike. As a consequence of the poor solubility of oxalate, it can crystallize in the form of calcium oxalate and aggregate into kidney stones or cause inflammation and nephrocalcinosis (350). With OXLUMO silencing *HAO1* mRNA, glyoxylate buildup is minimized and glycolate instead excreted in urine without resulting in kidney damage or toxic effects.

Like GIVLAARI, OXLUMO features fully modified 23mer and 21mer siRNA guide and passenger strands, respectively (Figure 18C). The 3′-end of the latter is linked to the triantennary GalNAc-containing ligand. Also, except for that passenger terminus, the three remaining termini are PS-modified at the last two bridging phosphates. In a double-blind phase 3 lumasiran trial, 39 PH1 patients aged 6 and older were randomly assigned in a 2:1 ratio to receive either the drug or placebo subcutaneously for a period of six months; afterwards all patients would receive lumasiran for a period of up to 54 months (352). It was found that the reduction in the 24-hour urinary ox-

alate excretion was 53.5% greater for patients on lumasiran compared to those receiving placebo during the six-month trial. Patients on lumasiran had normal or near-normal urinary oxalate levels at six months. Lumasiran treatment also resulted in substantially reduced plasma oxalate levels, thereby providing support for its mechanism of action. Patients in the lumasiran group showed elevated levels of plasma and urinary glycolate which is expected on the basis of the inhibition of GO enzyme production by the drug. In a separate case study of a teenage PH1 patient, lumasiran was found to consistently and rapidly reduce plasma oxalate and urinary excretion to normal or almost normal levels for 18 months. This patient did not develop new kidney stones and required no further urological interventions (353).

LEQVIO: the first 'millions of people' global RNAi therapeutic?

Inclisiran is an siRNA targeting proprotein convertase subtilisin-kexin type 9 (*PCSK9*) mRNA for the treatment of heterozygous familial hypercholesterolemia (HeFH) or clinical atherosclerotic cardiovascular disease (ASCVD) to lower low-density lipoprotein cholesterol (LDL-C). Hypercholesterolemia is characterized by elevated levels of LDL-C that carries a risk of premature ASCVD. In two phase 3 trials, inclisiran was found to significantly lower LDL-C in adults compared to those who received placebo with an acceptable safety profile (354,355). Inclisiran (300 mg dose) or matching placebo were given by subcutaneous injection on days 1, 90, 270 and 450, whereby the two primary endpoints were the % change from baseline in the LDL-C level on day 510 and the % change from baseline in the LDL-C level between days 90 and 540. The minor common side effects include injection site reactions such as pain, redness and swelling. The twice-yearly dosing regimen constitutes a major advantage of inclisiran compared to a monoclonal antibody against PCSK9 protein that also reduces LDL-C but needs to be administered every two to four weeks. Inclisiran was given approval under the brand name LEQVIO in the EU (52) and the US (53) in 2021 and 2022, respectively (Figure 3).

Like GIVLAARI, LEQVIO features 2′-F and 2′-*O*-Me modification chemistry with pairs of PS moieties at the 5′- and 3′-ends of the 23mer guide strand and at the 5′-end of the 21mer passenger strand. The latter consists mainly of 2′-*O*-Me nucleotides (just two 2′-F nucleotides in the 5′-half and a central 2′-deoxynucleotide; Figure 18D). The 3′-end of the passenger is tethered to the triantennary GalNAc conjugate. Phase 3 trials of the drug were completed by The Medicines Company (354,355) and Novartis subsequently acquired The Medicines Company and inclisiran in 2019. Compared to the majority of currently approved nucleic acid therapeutics that are used in the treatment of rare genetic disorders, LEQVIO targets both elevated LDL-C (in patients with the disease HeFH) and ASCVD due to elevated LDL-C, a condition that affects millions of patients worldwide. Thus, the drug will likely become the first 'millions-of-people' global RNAi therapeutic.

AMVUTTRA, a second-generation siRNA therapeutic for hATTR-mediated amyloidosis

AMVUTTRA® (vutrisiran) is a transthyretin-directed siRNA indicated for the treatment of the polyneuropathy of hereditary transthyretin-mediated amyloidosis in adults. AMVUTTRA has the same sequence as the failed investigational drug revusiran but with different chemistry to provide extended metabolic stability of the drug (revusiran clinical development was voluntarily stopped in 2016). AMVUTTRA uses GalNAc-conjugation for efficient delivery into hepatocytes and further follows the design of GIVLAARI and OXLUMO for having enhanced metabolic stability (ESC chemistry with additional terminal PS modification, Figure 18E). AMVUTTRA received FDA approval in June of 2022. It is the fifth siRNA-based drug reaching approval status in five years (Figure 3). Compared to the first-generation ONPATTRO, it offers the benefit of infrequent dosing, i.e. 25 mg administered by subcutaneous injection once every three months, without the need for IV premedications to reduce infusion-related reactions.

DELIVERY PLATFORMS

Lipid nanoparticles

The first two siRNA therapeutics to receive market approval, ONPATTRO and GIVLAARI, use entirely different delivery systems, LNP carrier versus triantennary carbohydrate conjugate to target ASGPR, respectively (Figure 20). Both approaches serve to deliver the siRNA duplex to the cytoplasm of hepatocytes in vivo. The development of efficient delivery systems is key to the success of oligonucleotide therapeutics and remains a very active area of research. Several excellent reviews of the oligonucleotide delivery field have been published in recent years and the interested reader may turn to these for more in-depth discussions of the various challenges and strategies being pursued to address them (356–360) including oral delivery (361).

Briefly, a first hurdle to overcome is getting the oligo to the particular tissue of therapeutic interest. The obstacles tissues have erected that need to be scaled include the vascular endothelial barrier, the reticuloendothelial system, renal excretion and its effects both on pharmacokinetics and biodistribution, as well as the blood-brain barrier (356). Receptor-mediated targeting may allow cell-specific delivery and internalization of the oligos. Examples of receptor families are integrins, G protein-coupled receptors, receptor tyrosine kinases, Toll-like receptors, scavenger receptor, folate receptor, and, as mentioned before, ASGPR. But after reaching cell surface and internalization by endocytosis (362), an oligonucleotide remains separated from the cytosol and thus its ultimate target if it cannot escape the endosome (363–365). Therefore, understanding the intracellular trafficking machinery and breaching the endosomal barrier critically affect the design and clinical success of oligonucleotide therapeutics (356). There are many other delivery approaches besides the aforementioned LNPs and GalNAc conjugates for targeting ASGPR, but because they proved successful first in the clinic, we will limit the discussion to these two in this review and perspective article.

LNPs represent important delivery systems for siRNA therapeutics (366) and the particular lipids and lipoids used in the multi-component formulation of the carrier for ONPATTRO are shown in Figure 21A. The second generation ionizable amino-lipid heptatriaconta-6,9,28,31-tetraen-19-yl-4-(dimethylamino) butanoate (DLin-MC3-DMA) afforded increased potency compared to first generation benchmark LNPs. In the positively charged state this lipid interacts with negatively charged lipids, thereby disrupting the bilayer membrane and allowing release of the siRNA from the endosome into the cytoplasm (367). Another key component is the PEG lipid mPEG$_{2000}$-C$_{14}$ glyceride that is associated with the surface of the LNP and influences the diameter of the particle in a concentration-dependent manner. PEG lipids can dissociate from the LNP and bind to lipoprotein particles in plasma which facilitates interactions between the unshielded LNP and target cells and thus enables uptake (49). Two additional components of the LNP are 1,2-distearoyl-*sn*-glycero-3-phosphocholine (DSPC) and cholesterol (Figure 21A). It was recently shown that DSPC-cholesterol resides in the outer layers when the LNP is empty, i.e. not containing the siRNA. However, once siRNAs are loaded into the system, DSPC-cholesterol becomes internalized together with siRNA, thus suggesting that they act as helper lipids and are key to stable encapsulation of the RNA cargo (368).

The mechanistic model of LNP-mediated delivery of ONPATTRO into hepatocytes entails the following steps (49). (i) PEG lipids are released from the particle surface. (ii) Endogenous apolipoprotein E (ApoE) is recruited to the LNP surface. (iii) ApoE promotes trafficking of LNPs through fenestrated endothelium and subsequent binding to lipoprotein receptors on the surface of hepatocytes. (iv) Internalization of LNPs via endocytosis. (v) The low pH in the endosome results in protonation of DLin-MC3-DMA. (vi) Interactions between positively charged DLin-MC3-DMA and negatively charged endogenous lipids destabilize the endosomal membrane. (vii) siRNA is released into the cytoplasm of hepatocytes and loaded into Ago2-RISC.

Asialoglycoprotein receptor and GalNAc conjugates

Chemical modification of oligonucleotides affects their physical-chemical properties and we discussed the effects of PS modification on pairing stability, nuclease resistance, protein binding, cellular uptake and pharmacokinetics and pharmacodynamics. Moreover, uptake and biodistribution of single-stranded ASOs and double-stranded siRNAs used alone versus in the presence of a carrier, e.g. LNPs, are obviously quite different and siRNAs face bigger hurdles with respect to delivery (316). Conjugation of a chemically modified oligonucleotide to a ligand potentially offers a strategy to overcome the challenges facing delivery of a polyanion of molecular weight >10 kDa across a cell membrane.

In pioneering work dating back >30 years, Letsinger and colleagues reported the synthesis, properties and activity of cholesteryl-conjugated oligos targeted against several HIV proteins in cell culture (369). The cholesterol moiety was tethered to the 3′-end of the oligos and significantly increased their antiviral potencies. The hydrophobic cholesterol conjugation was also shown to improve interactions

between siRNA and plasma lipoproteins, uptake and tissue distribution (370). Cholesterol promotes enhanced association of oligos with low-density or high-density lipoproteins (LDL or HDL, respectively).

Although hepatic targeting is most commonly pursued with cholesterol-conjugated siRNAs, delivery of siRNA to muscle and other extrahepatic tissues has also been demonstrated with cholesterol conjugation chemistry (360). A comprehensive study compared fifteen different lipid-conjugation chemistries with regards to siRNA tissue distribution and efficacy (371). In general, the hydrophobicity of the conjugate correlated with the degree of clearance and the distribution between liver and kidney. One notable finding was that several of the conjugates afforded accumulation of siRNA in extra-hepatic tissues such as muscle, lung, heart and adrenal glands. Moreover, cholesterol was inferior to several of the tested conjugates in promoting siRNA distribution to extra-hepatic tissues. This suggests that the chemical nature of the lipid conjugate plays an important role in enabling and maximizing siRNA delivery to organs other than liver. Current efforts directed at the development and clinical use of siRNA-bioconjugates have recently been reviewed (372). The bioconjugation platform for siRNA delivery is rapidly expanding and besides the abovementioned lipids, conjugates tethered to RNA termini include peptides, receptor ligands, aptamers, antibodies, and CpG oligos.

The triantennary GalNAc conjugate tethered to the 3′-terminus of the GIVLAARI siRNA passenger strand enables efficient ASGPR-mediated delivery of the therapeutic to hepatocytes. ASGPR is abundantly expressed in hepatocytes and congregates on the cell surface in coated pits. The receptor can form a trefoil composed of ASGPR1 and ASGPR2 subunits (called H1 and H2, respectively, in the human system), whereby the former features a carbohydrate recognition domain (CRD; Figure 22). Crystal structures of H1-CRD alone (373) and bound to either lactose or a bicyclic bridged ketal that efficiently binds to ASGPR (347) were determined. In addition, the crystal structure of a mannose binding protein mutant in complex with GalNAc provided insight into the preferential binding of ASGPR-CRD to this sugar compared with galactose (374) (Figure 22).

The carbohydrate binding site is shallow and exposed to solvent and this may explain why multiple subunits are needed to confer sufficient binding affinity and selectivity for the GalNAc sugar (375). Manoharan and coworkers designed modified siRNAs with trivalent GalNAc conjugates tethered to the 3′-end of the passenger strand. Careful optimization of the chemistry connecting the terminus of the passenger to the linker, the linker chemistry, and the spacers in the triantennary portion of the conjugate resulted in the current 'L96' design (82–88) (Figure 22). Thus, the 3′-terminal phosphate is attached to a prolinol sugar and a C_{12}-spacer connects via amide moieties prolinol sugar on one side and trivalent spacer and GalNAc sugars on the other. In the L96 conjugate, the spacers also contain two amide groups that interrupt the carbon chain and provide some polarity and conformational rigidity.

The GalNAc conjugation chemistry for ASGPR-mediated hepatic delivery and successfully applied in the case of GIVLAARI to treat acute hepatic porphyria is now

also being tested with other siRNAs and ASOs currently in the clinic. A recent review listed no fewer than 9 siRNAs and 12 ASOs with GalNAc conjugates in preclinical, phase 1 or phase 2 trials (360).

THE APTAMER APPROACH

Nucleic acid aptamers are single-stranded, folded RNA or DNA oligonucleotides that bind molecular targets (small molecules, proteins or nucleic acids) with high specificity and affinity. Aptamers against diverse targets can be identified from oligonucleotide libraries of sufficient sequence complexity by a process called 'systematic evolution of ligands by exponential enrichment' (SELEX (141,142)). They hold great potential in therapeutics as highly specific modulators of gene function as well as in diagnostics (376–380). As in the case of ASOs and siRNAs, native RNA and DNA aptamers are unsuitable for applications in biological systems because of rapid degradation *in vitro* and *in vivo*. They also have poor pharmacokinetic properties as putative therapeutics *in vivo*. Importantly, searching only sequence space often yields aptamers that are limited in specificity and particularly in affinity. Beyond sequence space, it is therefore necessary to explore the chemical and structure space to identify more mature functional aptamers.

MACUGEN (pegaptanib) was the first RNA-based therapeutic approved by the US FDA (2004, Figures 1 and 3) and is the only aptamer among oligonucleotide drugs that have reached the market to date. The 27-nucleotide aptamer targets VEGF for the treatment of wet age-related macular degeneration (AMD (381)). It is composed entirely of 2′-F and 2′-*O*-Me modified nucleotides except for two residues (382) (Figure 23A). Vascular endothelial growth factor (VEGF) is a prominent drug target and extensive studies confirmed a role for VEGF in ocular neovascular diseases and demonstrated that $VEGF_{165}$ is the isoform largely responsible for pathological ocular neovascularization (143). Although both $VEGF_{165}$ and $VEGF_{121}$ are effective mitogens for human umbilical vein endothelial cells, pretreatment of cells with active ingredient inhibited proliferative responses only to $VEGF_{165}$ (383). These findings are consistent with photo-crosslinking experiments that demonstrated that binding of pegaptanib to VEGF involves a close contact with Cys-137 of $VEGF_{165}$ (382). This residue is contained within the 55-amino-acid heparin-binding domain (HBD) of VEGF (Figure 23B) which is not present in $VEGF_{121}$ (384).

Exploration of sequence space using SELEX resulted in the initial anti-VEGF RNA aptamer. Subsequent trial-and-error exploration of the 'chemical space' to optimize the RNA sequence resulted in the high-affinity pegaptanib aptamer with a K_d of 49 pM (385). One limitation of the incorporation of 2′-F modified nucleotides was that only the pyrimidines were commercially available at the time. Hence the use of the 2′-*O*-Me modification chemistry for purine residues (Figure 23A). Another important modification concerns PEGylation at the 5′-end that confers drug-like properties to the aptamer for uptake and biodistribution (386); MACUGEN was administered by intravitreal injection. In principle, a certain amount of chemical modification can be built into the selection process, as in the case of
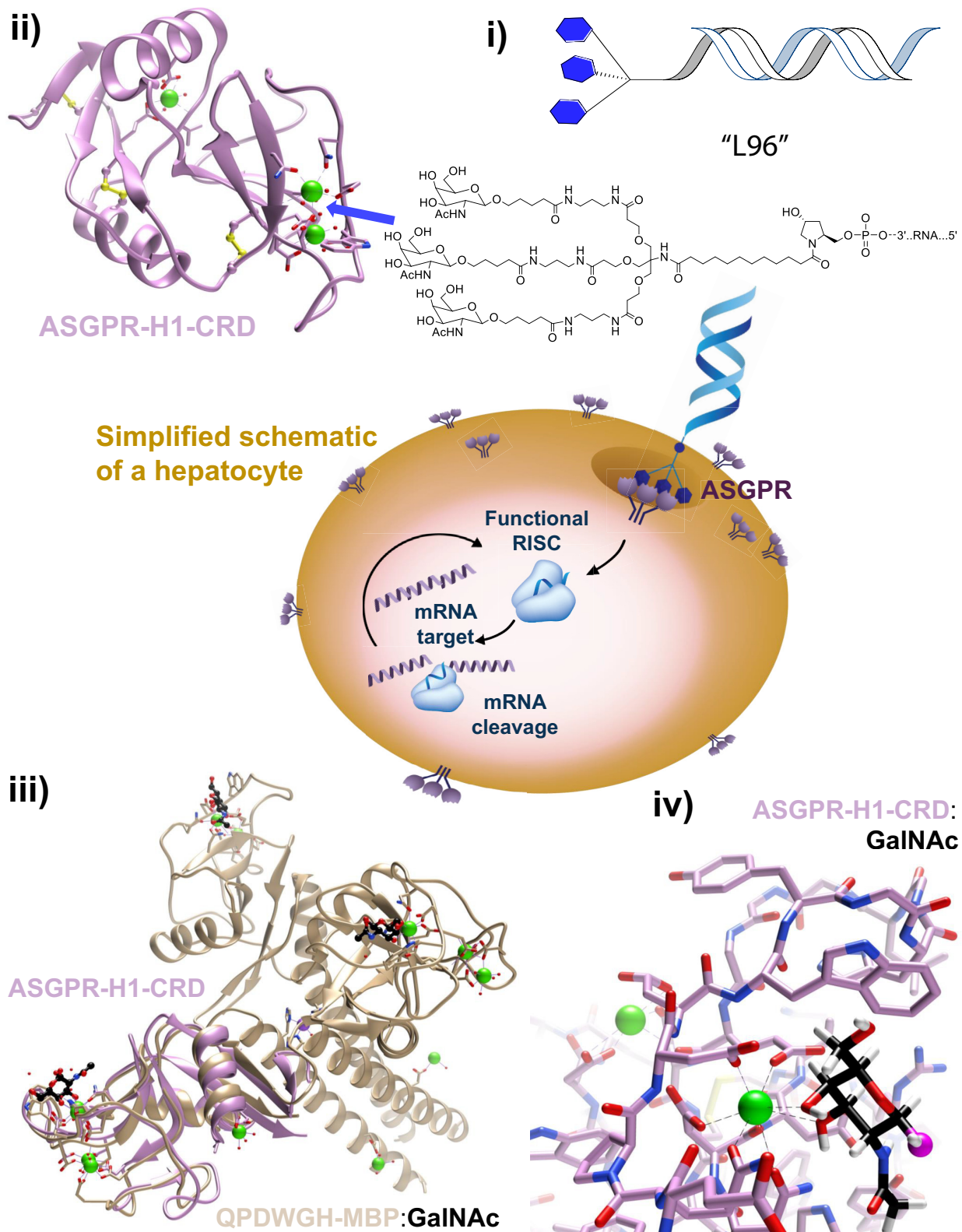
Figure 22. GalNAc conjugates for optimal hepatic delivery. The cartoon in the center shows siRNA–GalNAc conjugate binding and internalization by ASGPR, RISC loading and formation of functional RISC, mRNA target recognition and catalytic cleavage, and initiation of a new cycle. Panels around the simplified schematic of a hepatocyte depict, from the upper right and moving in a counterclockwise fashion: (i) The triantennary GalNAc conjugate L96. (ii) The crystal structure of ASGPR-H1-CRD (PDB ID 1DV8 (342)); Ca^{2+} ions are green, three disulfide bridges are highlighted in yellow, and the blue arrow points to the GalNAc binding site. (iii) The crystal structure of mannose binding protein (MBP) QPDWGH mutant bound to GalNAC (PDB ID 1BCH (343)); GalNAc carbon atoms are black and the ASGPR-H1-CRD is superimposed on one of the MBP-CRDs; note the central coiled-coil stalk that stabilizes the trimer. (iv) A model of GalNAc bound to ASGPR-H1-CRD based on the structure of the complex with lactose (PDB ID 5JPV (323)); the GalNAc oxygen attached to the L96 spacer is highlighted in magenta.
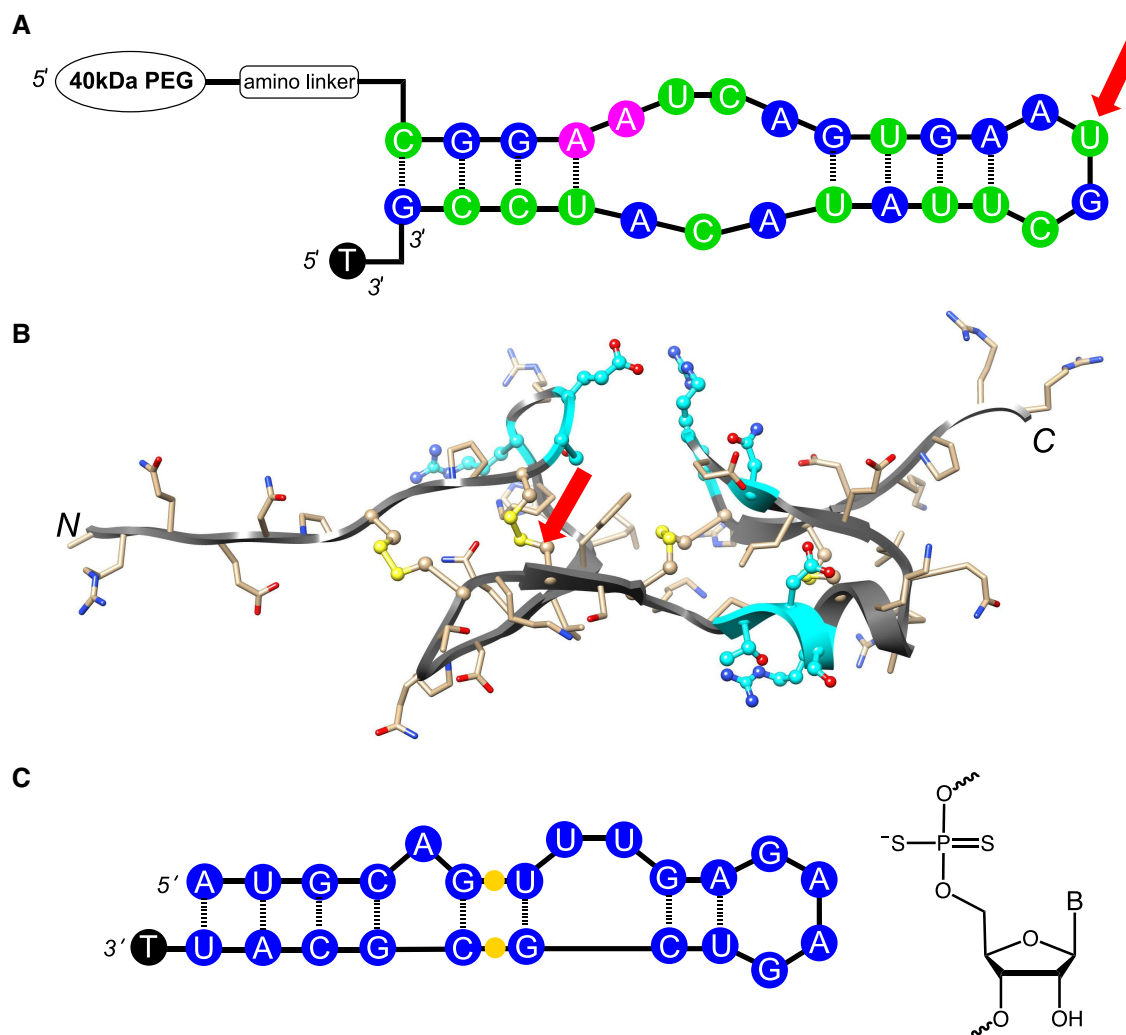
Figure 23. Aptamers that target VEGF. (**A**) Secondary structure and chemical modification of MACUGEN for treatment of wet age-related macular degeneration (AMD). Ribo-, 2′-deoxyribo-, 2′-O-Me- and 2′-F-nucleotides are depicted as circles colored in pink, black, blue and green, respectively. (**B**) NMR solution structure of the VEGF heparin binding domain (HBD) comprising Ala-111 to Arg-165 (PDB ID 1KMX (372)). The backbone is traced with a ribbon colored in gray, and disulfide bridges as well as side chains that show the largest chemical shifts upon aptamer binding (373) are depicted in ball-and-stick mode and are colored in yellow and cyan, respectively. Red arrows point to residues U14 and Cys-137 that could be photo-crosslinked in the RNA aptamer-VEGF$_{165}$ complex (355). (**C**) Secondary structure of an all-2′-O-Me modified VEGF aptamer (361). Incorporation of a PS2 modification (yellow sphere; structure shown on the right) at either site boosts the K_d 1000-fold to ca. 1 pM (368). Both aptamers bind exclusively to the VEGF-HBD.

a procedure to identify all-2′-O-Me RNA aptamers against VEGF (387) (Figure 23C). Such aptamers bound VEGF with equilibrium dissociation constants of 1–4 nM and were reasonably stable to degradation in serum. However, these affinities are significantly worse than the pM value for MACUGEN. Because pM binding affinities are highly desirable for increased potency in a therapeutic use this difference is noteworthy. For comparison, LUCENTIS® (ranibizumab), a monoclonal antibody-based therapeutic for wet AMD has a VEGF binding affinity of 140 pM. Antibody-based approaches have become the most prescribed therapies for AMD treatment (388) and have all but replaced MACUGEN (389).

Many approaches have been utilized to try and improve aptamer affinity including chemical modification (390–394). Thus, selection of aptamers against interleukin-6 (IL-6) from a library of DNA molecules containing 40 random

positions and 5-(N-benzylcarboxamide)-2′-deoxyuridine (BndU) or 5-[N-(1-naphthylmethyl)carboxamide]-2′-deoxyuridine (NapdU) replacing dT furnished candidates of improved binding (10-fold; relative to DNA) and inhibition (20-fold), but overall modest affinity ($K_d = 0.2$ nM) and potency (IC$_{50} = 0.2$ nM) (367). Further post-SELEX modification placing 2′-O-Me at certain sites improved the affinity minimally. Moreover, this selection process approach to enhance the hydrophobic contributions to the aptamer-protein target interface is laborious, expensive, and limited to modifications tolerated by the polymerases employed.

We demonstrated that a single phosphorodiothiate (PS2) modification can boost the affinity of RNA aptamers against VEGF and thrombin 1000-fold and tighten the binding affinity to 1–2 pM (394,395) (Figure 23C). Comparison of crystal structures for complexes between throm-

bin and the native and PS2-modified RNA aptamers and subsequent calculations identified three components that underlie the remarkable change in binding affinity enabled by a single PS2 modification. (i) A hydrophobic patch (phenylalanine, Phe) at the floor of a slight depression on the surface of the protein target. (ii) Local flexing of the RNA backbone that moves the PS2 moiety significantly closer to the edge of the phenyl ring compared to the native phosphate-Phe pair. (iii) An electric field generated by pairs of lysines and arginines that surround the hydrophobic patch and result in polarization of the sulfur that interacts with Phe.

One disadvantage of the VEGF system in regard to optimization of aptamer affinity and selectivity is that, unlike for other aptamers including the anti-thrombin RNA (394,396–398), the 3D structures of $VEGF_{165}$ and those of the native and chemically modified anti-VEGF RNA aptamers are not known. Thus, structural information regarding the components of the complex is limited to the NMR solution structure of the VEGF-HBD (399). Moreover, it was demonstrated by NMR that the secondary structures of the aptamer are maintained between the complexes with $VEGF_{165}$ and VEGF-HBD (55 residues) (400).

A recent exciting development is SELEX with adapted polymerases and xeno nucleic acids (XNAs) (401). Aptamers based on 2′-F-arabinonucleic acid (FANA), (3′→2′)-*L*-α-threofuranosyl nucleic acid (TNA) and other XNAs (402–404) are highly resistant to degradation and offer the prospect of expanded function and fold space. About a dozen aptamer therapeutic candidates are currently being evaluated in clinical trials (379,405). It is to be hoped that MACUGEN will not remain the only clinically approved aptamer for long.

A HEPATITIS B VACCINE OLIGONUCLEOTIDE ADJUVANT: CpG 1018 AND HEPLISAV-B®

HEPLISAV-B is a recombinant vaccine that prevents hepatitis B liver infection caused by hepatitis B virus (HBV) (406). It is composed of a 0.5 mL aqueous mixture of 20 μg of hepatitis B surface antigen (HBsAg) derived from Hansenula polymorpha with 3 mg of CpG 1018, an oligonucleotide adjuvant Toll-like receptor 9 (TLR9) agonist. The vaccine received US FDA approval in 2017 for use in adults ≥ 18 years. HEPLISAV-B is given by intramuscular injection in a 2-dose regimen spaced one month apart. CpG 1018 is a 22mer oligo-2′-deoxynucleotide phosphorothioate (PS-DNA) of sequence 5′-ps-d(TG AC TG T<u>G</u> <u>AA</u>**CGTTCG** AG AT GA)-3′ with two CpG steps (boldface) and a palindromic section (underlined) (407). The mechanism of action of this adjuvant oligo is quite different from those presented thus far and including ASOs, SSOs, siRNAs and aptamers (Figure 3).

The presence of the CpG motif is central to its mode of action and underlies the adjuvant's role as a TLR9 agonist. In eukaryotic DNAs CpG dinucleotides are present at lower frequency than in the prokaryotic DNA sequences. Moreover, the frequency of methylation at CpG sites is higher in eukaryotic DNA than in the DNA of microbes (408–410). Differential CpG-methylation affords a molecular basis for TLR9 to distinguish self from non-self DNA

in the host's defense immune response to microbial infections (166) and thereby potential therapeutic applications of (unmethylated) agonistic CpG-containing oligonucleotides (155,410). Thus, CpG 1018 was used in combination immunotherapy with rituximab to treat patients with non-Hodgkin lymphoma (411). Conversely, ASOs have $5^{Me}C$ rather than C, primarily to avoid any immune-stimulation when present along with G, but also to increase the binding affinity to the target RNA by 0.5°C/mod. The structural basis for a CpG-containing oligo to act as agonist (or antagonist in the methylated form) is depicted in Figure 24 (412).

The following are the principal actions of CpG 1018 in combination with HBsAg in the HEPLISAV-B vaccine against HBV infection: (i) Activation of plasmacytoid dendritic cells (pDCs) for secretion of interferons (IFNs) and cytokines (413). (ii) Conversion of pDCs into efficient antigen-presenting cells such that they present processed HBsAg peptides to CD4+ T cells. (iii) Promotion of T cell differentiation to functional helper T cells via pDC-derived IFNs and cytokines. Multiple signals to B cells specific for intact HBsAg are then provided by the antigen-specific helper T cells, resulting in the generation of antibody responses that afford protective immunity to HBV.

CpG 1018 exerts its biological actions locally at the injection site and draining lymph nodes. These stimulatory actions decline quite rapidly, such that biomarkers of 1018 activity return to baseline values within a week. At the doses that CpG 1018 is administered in HEPLISAV-B, the adjuvant is cleared from circulation within a couple of hours. Hence the oligonucleotide does not reach levels that would result in systemic TLR9-mediated immune stimulation. Therefore, it is the long-lived antibody responses and T and B cell memory that make up the durable effects of HEPLISAV-B immunization. Once these responses that are highly specific for the HBs antigen itself are generated, the continuing presence of either antigen or CpG 1018 adjuvant is no longer needed.

COMIRNATY AND SPIKEVAX: mRNA VACCINES

With many thousands of prescription drug products approved for marketing in the US alone, and small molecule compounds constituting the largest share among them, oligonucleotide therapeutics occupy niches. But SSOs and siRNAs have enabled breakthrough treatments for rare genetic disorders that have proven difficult targets for small molecules. In fact, both ASOs and siRNAs are in development or approved for at least several rare disorders, giving these patients options to participate in clinical research and access to treatment choices for the first time.

The traditional competition between antibody- and oligo-based therapeutics looks to increasingly become a synergistic partnership if mRNA vaccines live up to their immense promise. Thus, the ever-expanding RNA therapeutic toolbox includes molecules that range from those controlling gene expression (ASO, SSO, siRNA), regulation (antagomirs), proinflammatory effects (ssRNA and dsRNA) and recognizing proteins and receptors (aptamers) to RNA immunotherapeutics, such as mRNA vaccines that encode antigens of interest as well as
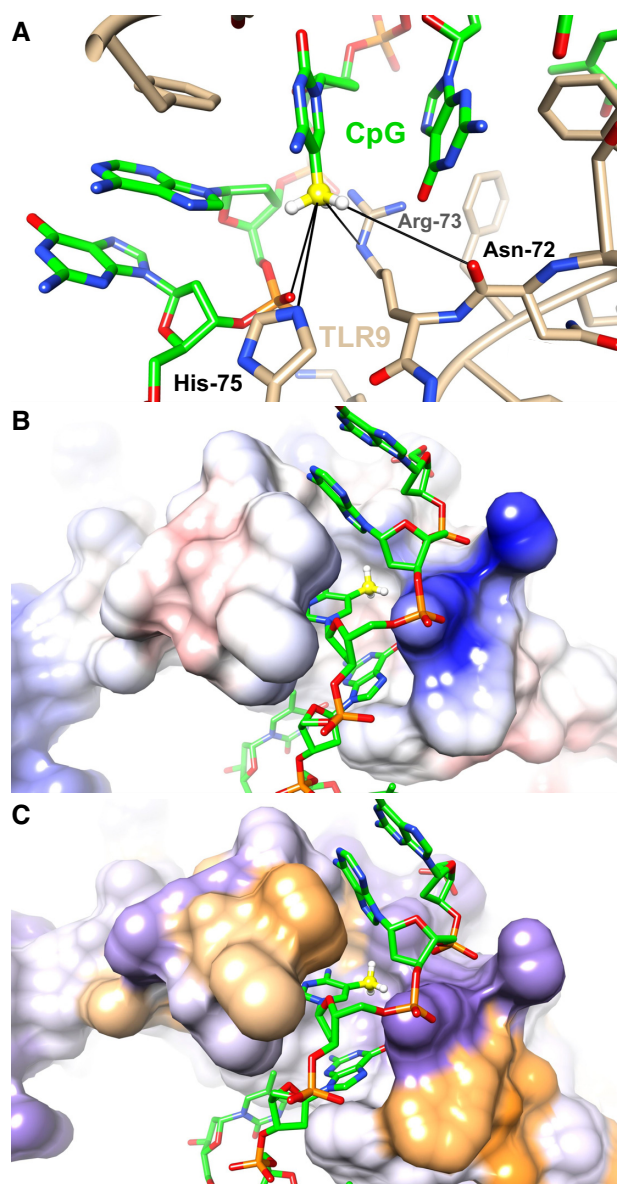
Figure 24. Structural basis of CpG recognition by TLR9 in the crystal structure of the DNA-receptor complex (PDB ID 3wpe (412)). (**A**) Close-up view of the interaction between the CpG step and TLR9. The C5-methyl of cytosine (carbon highlighted in yellow) is not present in the crystal structure. It was added to show contacts with neighboring polar moieties (thin solid lines) that reduce the affinity of an antagonist, i.e. an ^mCpG-containing oligo, by ca. threefold relative to the corresponding CpG-containing agonist oligo. Views of the DNA-TLR9 complex with the molecular surface of the receptor colored according to (**B**) Coulombic potential (blue, positively polarized, and red, negatively polarized) and (**C**) hydrophobicity potential (orange, most hydrophobic and purple, least hydrophobic).

self-amplifying RNAs (414–418). Provided the proteins encoded by mRNA vaccines elicit a robust neutralizing antibody response, the traditional antibody vs. oligo therapeutic '100m dash' is being transformed into a '400m relay', with RNA doing the early legwork and antibodies carrying the baton over the finishing line. Thus, early evidence in the development of a SARS-CoV-2 mRNA vaccine looked promising and the program received fast

track designation by the US FDA on 12 May 2020 (https://www.businesswire.com/news/home/20200512005277/en/). As well a preliminary account of a phase 1, dose-escalation, open-label trial with mRNA-1273 that included 45 healthy adults reported vaccine-induced anti-SARS-CoV-2 immune responses in all participants and an absence of trial-limiting safety concerns (419). A timeline of COVID-19 vaccine news and updates from the early days to the FDA-authorized emergency use of the Moderna SPIKEVAX® and Pfizer-BioNTech COMIRNATY® COVID-19 vaccines in children down to 6 months of age can be found here: https://www.fda.gov/emergency-preparedness-and-response/coronavirus-disease-2019-covid-19/covid-19-vaccines#authorized-vaccines.

The two FDA-approved mRNA COVID-19 vaccines, Moderna's SPIKEVAX and Pfizer-BioNTech's COMIRNATY are generally effective (420) and safe (421). Chemical modification, i.e. the use of N1-methyl-pseudouridine in place of U (422,423) (Figure 2A), reduces the intrinsic immune stimulation potential of exogenous mRNAs. Moreover, refined delivery strategies, LNP technology in the case of both the Moderna and Pfizer-BioNTech vaccines (Figure 21B), are crucial and indispensable instruments in the development and clinical implementation of mRNA vaccines (424–427). Stay tuned – the future of RNA therapeutics is finally here!

CONCLUSIONS AND FUTURE OUTLOOK

This article was written to celebrate a milestone in the 30-odd years nucleic acid chemistry, modification and drug discovery saga, the approval of the first 18 nucleic acid-based therapeutics (Figure 3, Table 1). Those following the evolution of the blueprint to turn oligos into drugs from the very first hours will remember the ups and downs the field experienced over the years and countless occasions that led doubters to predict the premature end of the pursuit to create ASO therapeutics. Enter RNAi and more apparent challenges to protect double-stranded siRNA against nuclease attacks and facilitate uptake and tissue-specific delivery. Chemical modification played a crucial role in overcoming these, and just five backbone chemistries make up the oligo drugs that were brought to market since 1998. That three of them - 2′-F, 2′-*O*-Me and PS - were the first nucleoside and nucleotide modifications explored by chemists in the 1960s is quite astonishing.

The current success and positive outlook for oligonucleotide therapeutics with dozens of candidates in late-stage clinical trials should not prevent one from looking beyond the apparent magic of the 2′-F, 2′-*O*-Me, 2′-*O*-MOE, PS and PMO modifications. Although it seems unlikely that a silver bullet has been missed among the expanding universe of modifications that have been synthesized to date, many need to be looked at more closely and may pave the road to more potent therapeutics. In this review we discussed many modifications beyond the clinically successful ones pointed out above. For example, LNA and cEt-BNA modifications are being evaluated in various modalities and results will be forthcoming. It is also important to point out the commercial and business considerations from biotechnology firms which are evaluating such chemistries and lim-

iting their evaluation to selected few for various proprietary and economic reasons. Yet another mentioned chemistry, GNA, has entered clinical trials in an RNAi therapeutic as an efficient off-target mitigator (88,330).

Probably the most important breakthrough in the successful launch of two RNAi therapeutics concerns delivery using LNPs or conjugation chemistry for receptor-mediated uptake and tissue-specific targeting. LNPs validated the RNAi platform (ONPATTRO) and a new delivery platform. Further, the latter validated the mRNA vaccine platform. Regarding the conjugates, GalNAc-containing LEQVIO that lowers LDL-cholesterol (LDL-C) by targeting *PCSK9* mRNA for the treatment of HeFH or atherosclerotic cardiovascular disease (ASCVD) and received regulatory approval in 2021/22, represents a game changer. ASCVD is the greatest health burden worldwide with an estimated 22 million deaths/year expected by 2040 (428). In clinical studies, inclisiran siRNA provided durable, potent and consistent LDL-C lowering over 18 months with a safety profile similar to placebo. With maintenance dosing every 6 months, LEQVIO offers a potentially more convenient option compared to approved monoclonal antibody (mAb) options (REPATHA and PRALUENT) that are dosed every 2–4 weeks. Thus, RNAi treatment has become more similar to a 'flu shot' taken a couple of times per year, but in this case to prevent development or progression of ASCVD. Successful hepatic delivery by targeting ASGPR with GalNAc conjugation chemistry as applied with GIVLAARI, OXLUMO, LEQVIO and AMVUTTRA points the way to using other receptor/ligand pairs in order to enable future delivery of oligo therapeutics to various tissues (360).

Beyond the LNP and GalNAc platforms, new approaches are being assessed for delivery to extrahepatic tissues. A lipid-conjugated siRNA for CNS applications (429) and an antibody-conjugated siRNA for muscle delivery (430) have entered clinical studies. Additional ligands and delivery platforms are on the horizon. Future challenges and available opportunities for nucleic acid-based medicines have been recently addressed (431).

ACKNOWLEDGEMENTS

FUNDING

REFERENCES

1. Renstrom,A.G. (2003) Wilbur & Orville Wright: A reissue of a chronology: commemorating the hundredth anniversary of the birth of Orville Wright, August 19, 1871. In: *Monographs in Aerospace History, Number 32*. NASA Publication SP-2003-4532, Washington DC, pp. 1–127.
2. United Press International (1961) Soviet orbits man and recovers him; space pioneer reports: 'I feel well'; sent messages while circling earth. *New York Times*, Apr. 12 ed., p. 1.
3. Witkin,R. (1961) US hurls man 115 miles into space; Shepard works controls in capsule; reports by radio in 15-minute flight. *New York Times*, May 6 ed., p. 1.
4. Turing,A.M. (1937) On computable numbers, with an application to the Entscheidungsproblem. *Proc. Lond. Math. Soc.*, **S2-42**, 230–265.
5. Kampe,F. and Nguyen,T.M. (1988) Performance comparison of the CRAY-2 and CRAY X-MP on a class of seismic data processing algorithms. *Parallel Comput.*, **7**, 41–53.
6. Sanger,F. and Thompson,E.O.P. (1953) The amino-acid sequence in the glycyl chain of insulin. I. The identification of lower peptides from partial hydrolysates. *Biochem. J.*, **53**, 353–366.
7. Sanger,F. and Thompson,E.O.P. (1953) The amino-acid sequence in the glycyl chain of insulin. II. The investigation of peptides from enzymic hydrolysates. *Biochem. J.*, **53**, 366–374.
8. Collins,F.S., Green,E.D., Guttmacher,A.E. and Guyer,M.S. (2003) A vision for the future of genomics research. *Nature (London, U. K.)*, **422**, 835–847.
9. Roehr,B. (1998) Fomivirsen approved for CMV retinitis. *J. Int. Assoc. Physicians AIDS Care*, **4**, 14–16.
10. Grillone,L.R. and Lanz,R. (2001) Fomivirsen. *Drugs Today*, **37**, 245–255.
11. Sanghvi,Y.S. (2011) A status update of modified oligonucleotides for chemotherapeutics applications. *Curr. Protoc. Nucleic Acid Chem.*, **Chapter 4**, Unit 4.1.1–4.1.22.
12. Strunecka,A., Patocka,J. and Connett,P. (2004) Fluorine in medicine. *J. Appl. Biomed.*, **2**, 141–150.
13. Hagmann,W.K. (2008) The many roles for fluorine in medicinal chemistry. *J. Med. Chem.*, **51**, 4359–4369.
14. Guo,F., Li,Q. and Zhou,C. (2017) Synthesis and biological applications of fluoro-modified nucleic acids. *Org. Biomol. Chem.*, **15**, 9552–9565.
15. Merki,E., Graham,M.J., Mullick,A.E., Miller,E.R., Crooke,R.M., Pitas,R.E., Witztum,J.L. and Tsimikas,S. (2008) Antisense oligonucleotide directed to human apolipoprotein B-100 reduces lipoprotein(a) levels and oxidized phospholipids on human apolipoprotein B-100 particles in lipoprotein(a) transgenic mice. *Circulation*, **118**, 743–753.
16. El Harchaoui,K., Akdim,F., Stroes,E.S.G., Trip,M.D. and Kastelein,J.J.P. (2008) Current and future pharmacologic options for the management of patients unable to achieve low-density lipoprotein-cholesterol goals with statins. *Am. J. Cardiovasc. Drugs*, **8**, 233–242.
17. Watson,J.D. and Crick,F.H.C. (1953) Molecular structure of nucleic acids. A structure for deoxyribose nucleic acid. *Nature (London, U. K.)*, **171**, 737–738.
18. Rich,A. and Davies,D.R. (1956) A new two-stranded helical structure: poly(adenylic acid) and poly(uridylic acid). *J. Am. Chem. Soc.*, **78**, 3548–3549.
19. Varshavsky,A. (2006) Discovering the RNA double helix and hybridization. *Cell*, **127**, 1295–1297.
20. Rich,A. (1960) A hybrid helix containing both deoxyribose and ribose polynucleotides and its relation to the transfer of information

between the nucleic acids. *Proc. Natl. Acad. Sci. U.S.A.*, **46**, 1044–1053.

21. Stephenson,M.L. and Zamecnik,P.C. (1978) Inhibition of Rous sarcoma viral RNA translation by a specific oligodeoxyribonucleotide. *Proc. Natl. Acad. Sci. U.S.A.*, **75**, 285–288.

22. Zamecnik,P.C. and Stephenson,M.L. (1978) Inhibition of Rous sarcoma virus replication and cell transformation by a specific oligodeoxynucleotide. *Proc. Natl. Acad. Sci. U.S.A.*, **75**, 280–284.

23. Lehman,N. (2015) The RNA world: 4,000,000,050 years old. *Life (Basel)*, **5**, 1583–1586.

24. Rich,A. (1962) On the problems of evolution and biochemical information transfer. In: *Horizons in Biochemistry*. pp. 103–126.

25. Michelson,A.M. and Todd,A.R. (1955) Nucleotides. XXXII. Synthesis of a dithymidine dinucleotide containing a 3′,5′-internucleotidic linkage. *J. Chem. Soc.*, 2632–2638.

26. Khorana,H.G., Tener,G.M., Moffatt,J.G. and Pol,E.H. (1956) A new approach to the synthesis of polynucleotides. *Chem. Ind. (Chichester, U. K.)*, 1523.

27. Smith,M., Rammler,D.H., Goldberg,I.H. and Khorana,H.G. (1962) Studies on polynucleotides. XIV. Specific synthesis of the C3″-C5″ interribonucleotide linkage. Syntheses of uridylyl-(3″→5″)-uridine and uridylyl-(3″→5″)-adenosine. *J. Am. Chem. Soc.*, **84**, 430–440.

28. Schaller,H., Weimann,G., Lerch,B. and Khorana,H.G. (1963) Studies on polynucleotides. XXIV. The stepwise synthesis of specific deoxyribopolynucleotides. Protected derivatives of deoxyribonucleoside-3″ phosphates. *J. Am. Chem. Soc.*, **85**, 3821–3827.

29. Letsinger,R.L. and Kornet,M.J. (1963) Popcorn polymer as a support In multistep syntheses. *J. Am. Chem. Soc.*, **85**, 3045–3046.

30. Letsinger,R.L., Kornet,M.J., Mahadevan,V. and Jerina,D.M. (1964) Reactions on polymer supports. *J. Am. Chem. Soc.*, **86**, 5163–5165.

31. Letsinger,R.L. and Mahadevan,V. (1965) Nucleotide chemistry. II. Oligonucleotide synthesis on a polymer support. *J. Am. Chem. Soc.*, **87**, 3526–3527.

32. Söll,D., Ohtsuka,E., Jones,D.S., Lohrmann,R., Hayatsu,H., Nishimura,S. and Khorana,H.G. (1965) Studies on polynucleotides, XLIX. Stimulation of the binding of aminoacyl-sRNA's to ribosomes by ribotrinucleotides and a survey of codon assignments for 20 amino acids. *Proc. Natl. Acad. Sci. U.S.A.*, **54**, 1378–1385.

33. Eckstein,F. (1966) Nucleoside phosphorothioates. *J. Am. Chem. Soc.*, **88**, 4292–4294.

34. Letsinger,R.L. and Ogilvie,K.K. (1969) Nucleotide chemistry. XIII. Synthesis of oligothymidylates via phosphotriester intermediates. *J. Am. Chem. Soc.*, **91**, 3350–3355.

35. Letsinger,R.L., Ogilvie,K.K. and Miller,P.S. (1969) Nucleotide chemistry. XV. Developments in syntheses of oligodeoxyribonucleotides and their organic derivatives. *J. Am. Chem. Soc.*, **91**, 3360–3365.

36. Agarwal,K.L., Buchi,H., Caruthers,M.H., Gupta,N., Khorana,H.G., Kleppe,K., Kumar,A., Ohtsuka,E., Rajbhandary,U.L., Van,D.S.J.H. *et al.* (1970) Total synthesis of the gene for an alanine transfer ribonucleic acid from yeast. *Nature*, **227**, 27–34.

37. Letsinger,R.L., Finnan,J.L., Heavner,G.A. and Lunsford,W.B. (1975) Nucleotide chemistry. XX. Phosphite coupling procedure for generating internucleotide links. *J. Am. Chem. Soc.*, **97**, 3278–3279.

38. Letsinger,R.L. and Lunsford,W.B. (1976) Synthesis of thymidine oligonucleotides by phosphite triester intermediates. *J. Am. Chem. Soc.*, **98**, 3655–3661.

39. Brown,E.L., Belagaje,R., Ryan,M.J. and Khorana,H.G. (1979) Chemical synthesis and cloning of a tyrosine tRNA gene. *Methods Enzymol.*, **68**, 109–151.

40. Beaucage,S.L. and Caruthers,M.H. (1981) Deoxynucleoside phosphoramidites. A new class of key intermediates for deoxypolynucleotide synthesis. *Tetrahedron Lett.*, **22**, 1859–1862.

41. Matteucci,M.D. and Caruthers,M.H. (1981) Synthesis of deoxyoligonucleotides on a polymer support. *J. Am. Chem. Soc.*, **103**, 3185–3191.

42. McBride,L.J. and Caruthers,M.H. (1983) Nucleotide chemistry. X. An investigation of several deoxynucleoside phosphoramidites useful for synthesizing deoxyoligonucleotides. *Tetrahedron Lett.*, **24**, 245–248.

43. Ogilvie,K.K., Usman,N., Nicoghosian,K. and Cedergren,R.J. (1988) Total chemical synthesis of a 77-nucleotide-long RNA sequence having methionine-acceptance activity. *Proc. Natl. Acad. Sci. U.S.A.*, **85**, 5764–5768.

44. Ogilvie,K.K., Theriault,N. and Sadana,K.L. (1977) Synthesis of oligoribonucleotides. *J. Am. Chem. Soc.*, **99**, 7741–7743.

45. Stec,W.J., Zon,G. and Egan,W. (1984) Automated solid-phase synthesis, separation, and stereochemistry of phosphorothioate analogs of oligodeoxyribonucleotides. *J. Am. Chem. Soc.*, **106**, 6077.

46. Codington,J.F., Doerr,I., Van Praag,D., Bendich,A. and Fox,J.J. (1961) Pyrimidine nucleosides. XIV. Synthesis of 2′-deoxy-2′-fluorouridine. *J. Am. Chem. Soc.*, **83**, 5030–5031.

47. Furukawa,Y., Kobayashi,K., Kanai,Y. and Honjo,M. (1965) Synthesis of 2′-O-methyluridine, 2′-O-methylcytidine and their relating compounds. *Chem.*, **13**, 1273–1278.

48. Scott,L.J. (2020) Givosiran: first approval. *Drugs*, **80**, 335–339.

49. Akinc,A., Maier,M.A., Manoharan,M., Fitzgerald,K., Jayaraman,M., Barros,S., Ansell,S., Du,X., Hope,M.J., Madden,T.D. *et al.* (2019) The Onpattro story and the clinical translation of nanomedicines containing nucleic acid-based drugs. *Nat. Nanotechnol.*, **14**, 1084–1087.

50. Crooke,S.T., Witztum,J.L., Bennett,C.F. and Baker,B.F. (2018) RNA-targeted therapeutics. *Cell Metab.*, **27**, 714–739.

51. Shen,X. and Corey,D.R. (2018) Chemistry, mechanism and clinical status of antisense oligonucleotides and duplex RNAs. *Nucleic Acids Res.*, **46**, 1584–1600.

52. Lamb,Y.N. (2021) Inclisiran: first approval. *Drugs*, **81**, 389–395.

53. Migliorati,J.M., Jin,J. and Zhong,X.-B. (2022) siRNA drug Leqvio (inclisiran) to lower cholesterol. *Trends Pharmacol. Sci.*, **43**, 455–456.

54. Altmann,K.-H., Fabbro,D., Dean,N.M., Geiger,T., Monia,B.P., Mueller,M. and Nicklin,P. (1996) Second-generation antisense oligonucleotides: structure-activity relationships and the design of improved signal-transduction inhibitors. *Biochem. Soc. Trans.*, **24**, 630–637.

55. Altmann,K.-H., Dean,N.M., Fabbro,D., Freier,S.M., Geiger,T., Haener,R., Huesken,D., Martin,P., Monia,B.P., Muller,M. *et al.* (1996) Second generation of antisense oligonucleotides. From nuclease resistance to biological efficacy in animals. *Chimia*, **50**, 168–176.

56. Martin,P. (1995) New access to 2′-O-alkylated ribonucleosides and properties of 2′-O-alkylated oligoribonucleotides. *Helv. Chim. Acta*, **78**, 486–504.

57. Geary,R.S., Watanabe,T.A., Truong,L., Freier,S., Lesnik,E.A., Sioufi,N.B., Sasmor,H., Manoharan,M. and Levin,A.A. (2001) Pharmacokinetic properties of 2′-O-(2-methoxyethyl)-modified oligonucleotide analogs in rats. *J. Pharmacol. Exp. Ther.*, **296**, 890–897.

58. Crooke,S.T. (2004) Progress in antisense technology. *Annu. Rev. Med.*, **55**, 61–95.

59. Crooke,S.T. (2017) Molecular mechanisms of antisense oligonucleotides. *Nucleic Acid Ther.*, **27**, 70–77.

60. Finkel,R.S., Mercuri,E., Darras,B.T., Connolly,A.M., Kuntz,N.L., Kirschner,J., Chiriboga,C.A., Saito,K., Servais,L., Tizzano,E. *et al.* (2017) Nusinersen versus sham control in infantile-onset spinal muscular atrophy. *N. Engl. J. Med.*, **377**, 1723–1732.

61. Gales,L. (2019) Tegsedi (inotersen): an antisense oligonucleotide approved for the treatment of adult patients with hereditary transthyretin amyloidosis. *Pharmaceuticals*, **12**, 78.

62. Mathew,V. and Wang,A.K. (2019) Inotersen: new promise for the treatment of hereditary transthyretin amyloidosis. *Drug Des. Dev. Ther.*, **13**, 1515–1525.

63. Paik,J. and Duggan,S. (2019) Volanesorsen: first global approval. *Drugs*, **79**, 1349–1354.

64. Summerton,J.E. (2017) Invention and early history of morpholinos: from pipe dream to practical products. Morpholino oligomers. *Methods Mol. Biol.*, **1565**, 1–15.

65. Lim,K.R.Q., Maruyama,R. and Yokota,T. (2017) Eteplirsen in the treatment of Duchenne muscular dystrophy., *Drug Des. Dev. Ther.*, **11**, 533–545.

66. Heo,Y.-A. (2020) Golodirsen: first approval. *Drugs*, **80**, 329–333.

67. Manoharan,M. (2004) RNA interference and chemically modified small interfering RNAs. *Curr. Opin. Chem. Biol.*, **8**, 570–579.

68. Bumcrot,D., Manoharan,M., Koteliansky,V. and Sah,D.W.Y. (2006) RNAi therapeutics: a potential new class of pharmaceutical drugs. *Nat. Chem. Biol.*, **2**, 711–719.

69. Crooke,S.T. (ed). (2007) *Antisense Drug Technology: Principles, Strategies, and Applications*. 2nd edn., CRC Press, Boca Raton.

70. Deleavey,G.F. and Damha,M.J. (2012) Designing chemically modified oligonucleotides for targeted gene silencing. *Chem. Biol. (Oxford, U. K.)*, **19**, 937–954.

71. Egli,M. and Herdewijn,P. (eds). (2012) *Chemistry and Biology of Artificial Nucleic Acids*. Wiley-VCH, Weinheim, Germany.

72. Wada,S., Obika,S., Shibata,M.-A., Yamamoto,T., Nakatani,M., Yamaoka,T., Torigoe,H. and Harada-Shiba,M. (2012) Development of a 2′,4′-BNA/LNA-based siRNA for dyslipidemia and assessment of the effects of its chemical modifications in vivo. *Mol. Ther. Nucleic Acids*, **1**, e45.

73. Koch,T. (2013) LNA antisense: a review. *Curr. Phys. Chem.*, **3**, 55–68.

74. Ni,S., Yao,H., Wang,L., Lu,J., Jiang,F., Lu,A. and Zhang,G. (2017) Chemical modifications of nucleic acid aptamers for therapeutic purposes. *Int. J. Mol. Sci.*, **18**, 1683.

75. Egli,M. and Manoharan,M. (2019) Re-engineering RNA molecules into therapeutic agents. *Acc. Chem. Res.*, **52**, 1036–1047.

76. Freier,S.M. and Altmann,K.-H. (1997) The ups and downs of nucleic acid duplex stability: structure-stability studies on chemically-modified DNA:RNA duplexes. *Nucleic Acids Res.*, **25**, 4429–4443.

77. Lebedeva,I. and Stein,C.A. (2001) Antisense oligonucleotides: promise and reality. *Annu. Rev. Pharmacol. Toxicol.*, **41**, 403–419.

78. Yamasaki,K., Akutsu,Y., Yamasaki,T., Miyagishi,M. and Kubota,T. (2020) Enhanced affinity of racemic phosphorothioate DNA with transcription factor SATB1 arising from diastereomer-specific hydrogen bonds and hydrophobic contacts. *Nucleic Acids Res.*, **48**, 4551–4561.

79. Hyjek-Skladanowska,M., Vickers,T.A., Napiorkowska,A., Anderson,B.A., Tanowitz,M., Crooke,S.T., Liang,X.-H., Seth,P.P. and Nowotny,M. (2020) Origins of the increased affinity of phosphorothioate-modified therapeutic nucleic acids for proteins. *J. Am. Chem. Soc.*, **142**, 7456–7468.

80. Iwamoto,N., Butler,D.C.D., Svrzikapa,N., Mohapatra,S., Zlatev,I., Sah,D.W.Y., Meena, Standley,S.M., Lu,G., Apponi,L.H. *et al.* (2017) Control of phosphorothioate stereochemistry substantially increases the efficacy of antisense oligonucleotides. *Nat. Biotechnol.*, **35**, 845–851.

81. Knouse,K.W., Degruyter,J.N., Schmidt,M.A., Zheng,B., Vantourout,J.C., Kingston,C., Mercer,S.E., McDonald,I.M., Olson,R.E., Zhu,Y. *et al.* (2018) Unlocking P(V): reagents for chiral phosphorothioate synthesis. *Science*, **361**, 1234–1238.

82. Nair,J.K., Willoughby,J.L.S., Chan,A., Charisse,K., Alam,M.R., Wang,Q., Hoekstra,M., Kandasamy,P., Kel'in,A.V., Milstein,S. *et al.* (2014) Multivalent N-acetylgalactosamine-conjugated siRNA localizes in hepatocytes and elicits robust RNAi-mediated gene silencing. *J. Am. Chem. Soc.*, **136**, 16958–16961.

83. Matsuda,S., Keiser,K., Nair,J.K., Charisse,K., Manoharan,R.M., Kretschmer,P., Peng,C.G., Kel'in,A.V., Kandasamy,P., Willoughby,J.L.S. *et al.* (2015) siRNA conjugates carrying sequentially assembled trivalent N-acetylgalactosamine linked through nucleosides elicit robust gene silencing in vivo in hepatocytes. *ACS Chem. Biol.*, **10**, 1181–1187.

84. Rajeev,K.G., Nair,J.K., Jayaraman,M., Charisse,K., Taneja,N., O'Shea,J., Willoughby,J.L.S., Yucius,K., Nguyen,T., Shulga-Morskaya,S. *et al.* (2015) Hepatocyte-specific delivery of siRNAs conjugated to novel non-nucleosidic trivalent N-acetylgalactosamine elicits robust gene silencing in vivo. *ChemBioChem*, **16**, 903–908.

85. Nair,J.K., Attarwala,H., Sehgal,A., Wang,Q., Aluri,K., Zhang,X., Gao,M., Liu,J., Indrakanti,R., Schofield,S. *et al.* (2017) Impact of enhanced metabolic stability on pharmacokinetics and pharmacodynamics of GalNAc-siRNA conjugates. *Nucleic Acids Res.*, **45**, 10969–10977.

86. Willoughby,J.L.S., Chan,A., Sehgal,A., Butler,J.S., Nair,J.K., Racie,T., Shulga-Morskaya,S., Nguyen,T., Qian,K., Yucius,K. *et al.* (2018) Evaluation of GalNAc-siRNA conjugate activity in pre-clinical animal models with reduced asialoglycoprotein receptor expression. *Mol. Ther.*, **26**, 105–114.

87. Foster,D.J., Brown,C.R., Shaikh,S., Trapp,C., Schlegel,M.K., Qian,K., Sehgal,A., Rajeev,K.G., Jadhav,V., Manoharan,M. *et al.* (2018) Advanced siRNA designs further improve in vivo performance of GalNAc-siRNA conjugates. *Mol. Ther.*, **26**, 708–717.

88. Janas,M.M., Schlegel,M.K., Harbison,C.E., Yilmaz,V.O., Jiang,Y., Parmar,R., Zlatev,I., Castoreno,A., Xu,H., Shulga-Morskaya,S. *et al.* (2018) Selection of GalNAc-conjugated siRNAs with limited off-target-driven rat hepatotoxicity. *Nat. Commun.*, **9**, 723.

89. Liebow,A., Li,X., Racie,T., Hettinger,J., Bettencourt,B.R., Najafian,N., Haslett,P., Fitzgerald,K., Holmes,R.P., Erbe,D. *et al.* (2017) An investigational RNAi therapeutic targeting glycolate oxidase reduces oxalate production in models of primary hyperoxaluria. *J. Am. Soc. Nephrol.*, **28**, 494–503.

90. Roberts,T.C., Langer,R. and Wood,M.J.A. (2020) Advances in oligonucleotide drug delivery. *Nat. Rev. Drug Discov.*, **19**, 673–694.

91. Hammond,S.M., Aartsma-Rus,A., Alves,S., Borgos,S.E., Buijsen,R.A.M., Collin,R.W.J., Covello,G., Denti,M.A., Desviat,L.R., Echevarría,L. *et al.* (2021) Delivery of oligonucleotide-based therapeutics: challenges and opportunities. *EMBO Mol. Med.*, **13**, E13243.

92. Yakovchuk,P., Protozanova,E. and Frank-Kamenetskii,M.D. (2006) Base-stacking and base-pairing contributions into thermal stability of the DNA double helix. *Nucleic Acids Res.*, **34**, 564–574.

93. Egli,M. (2009) On stacking. In: Comba,P. (ed). *Structure and Function*. Springer Publishers, Heidelberg, Germany, pp. 177-196.

94. Feng,B., Sosa,R.P., Martensson,A.K.F., Jiang,K., Tong,A., Dorfman,K.D., Takahashi,M., Lincoln,P., Bustamante,C.J., Westerlund,F. *et al.* (2019) Hydrophobic catalysis and a potential biological role of DNA unstacking induced by environment effects. *Proc. Natl. Acad. Sci. U.S.A.*, **116**, 17169–17174.

95. Rohs,R., Jin,X., West,S.M., Joshi,R., Honig,B. and Mann,R.S. (2010) Origins of specificity in protein-DNA recognition. *Annu. Rev. Biochem.*, **79**, 233–269.

96. Hermann,T. and Patel,D.J. (1999) Stitching together RNA tertiary architectures. *J. Mol. Biol.*, **294**, 829–849.

97. Denisov,V.P. and Halle,B. (2000) Sequence-specific binding of counterions to B-DNA. *Proc. Natl. Acad. Sci. U.S.A.*, **97**, 629–633.

98. Ferre-D'Amare,A.R. and Doudna,J.A. (1999) RNA folds: insights from recent crystal structures. *Annu. Rev. Biophys. Biomol. Struct.*, **28**, 57–73.

99. Egli,M. and Minasov,G. (2000), Recent advances in RNA crystallography. In: Krupp,G. and Gaur,R. (eds). *Ribozymes, Biochemistry and Biotechnology*. Eaton Publishing, Natick, MA, pp. 315–349.

100. Hendrix,D.K., Brenner,S.E. and Holbrook,S.R. (2005) RNA structural motifs: building blocks of a modular biomolecule. *Q. Rev. Biophys.*, **38**, 221–243.

101. Klostermeier,D. and Hammann,C. (eds). In: *RNA Structure and Folding*. De Gruyter, Berlin, Boston.

102. Mortimer,S.A., Kidwell,M.A. and Doudna,J.A. (2014) Insights into RNA structure and function from genome-wide studies. *Nat. Rev. Genet.*, **15**, 469–479.

103. Yusupova,G. and Yusupov,M. (2014) High-resolution structure of the eukaryotic 80S ribosome. *Annu. Rev. Biochem.*, **83**, 467–486.

104. Egli,M. (2022) DNA and RNA structure. In: Blackburn,G.M., Egli,M., Gait,M.J. and Watts,J.K. (eds). *Nucleic Acids in Chemistry and Biology*. 4th edn., R. Soc. Chem., Cambridge, UK, pp. 20–95.

105. Ha,S.C., Lowenhaupt,K., Rich,A., Kim,Y.-G. and Kim,K.K. (2005) Crystal structure of a junction between B-DNA and Z-DNA reveals two extruded bases. *Nature (London, U. K.)*, **437**, 1183–1186.

106. Krall,J., Nichols,P.J., Henen,M.A., Vicens,Q. and Vögeli,B. (2023) Formation and stabilization of Z-DNA and Z-RNA. *Molecules*, **28**, 843.

107. Gueron,M., Demaret,J.P. and Filoche,M. (2000) A unified theory of the B-Z transition of DNA in high and low concentrations of multivalent ions. *Biophys. J.*, **78**, 1070–1083.

108. Saenger,W., Hunter,W.N. and Kennard,O. (1986) DNA conformation is determined by economics in the hydration of phosphate groups. *Nature*, **324**, 385–388.

109. Thibaudeau,C. and Chattopadhyaya,J. (1999) In: *Stereoelectronic Effects in Nucleosides and Nucleotides and their Structural Implications*. Uppsala University Press, Uppsala, Sweden.

110. Rich,A. (2003) The double helix: a tale of two puckers. *Nat. Struct. Biol.*, **10**, 247–249.

111. Egli,M. (2018) Sugar pucker and nucleic acid structure. In: Zhang,S. (ed.) *The Excitement of Discovery: Selected Papers of Alexander Rich. A Tribute to Alexander Rich*. Series in Struct. Biol., World Scientific Publishers, Vol. **11**, pp. 309–315.

112. Egli,M., Portmann,S. and Usman,N. (1996) RNA hydration: a detailed look. *Biochemistry*, **35**, 8489–8494.

113. Fohrer,J., Hennig,M. and Carlomagno,T. (2006) Influence of the 2′-hydroxyl group conformation on the stability of A-form helices in RNA. *J. Mol. Biol.*, **356**, 280–287.

114. Soyfer,V.N. and Potaman,V.N. (1996) In: *Triple-Helical Nucleic Acids*. Springer Publishers, NY.

115. Campbell,N., Collie,G.W. and Neidle,S. (2012) Crystallography of DNA and RNA G-quadruplex nucleic acids and their ligand complexes. *Curr. Protoc. Nucleic Acid Chem.*, **Chapter 17**, Unit 17.16.

116. Egli,M. (2004) Nucleic acid crystallography: current progress. *Curr. Opin. Chem. Biol.*, **8**, 580–591.

117. Egli,M. and Pallan,P.S. (2010) The many twists and turns of DNA: template, telomere, tool, and target. *Curr. Opin. Struct. Biol.*, **20**, 262–275.

118. Ponce-Salvatierra,A., Wawrzyniak-Turek,K., Steuerwald,U., Hoebartner,C. and Pena,V. (2016) Crystal structure of a DNA catalyst. *Nature (London, U. K.)*, **529**, 231–234.

119. Bujold,K.E., Lacroix,A. and Sleiman,H.F. (2018) DNA nanostructures at the interface with biology. *Chem.*, **4**, 495–521.

120. Tamura,M. and Holbrook,S.R. (2002) Sequence and structural conservation in RNA ribose zippers. *J. Mol. Biol.*, **320**, 455–474.

121. Safaee,N., Noronha,A.M., Rodionov,D., Kozlov,G., Wilds,C.J., Sheldrick,G.M. and Gehring,K. (2013) Structure of the parallel duplex of poly(A) RNA: evaluation of a 50 year-old prediction. *Angew. Chem., Int. Ed.*, **52**, 10370–10373.

122. Su,L., Chen,L., Egli,M., Berger,J.M. and Rich,A. (1999) Minor groove RNA triplex in the crystal structure of a ribosomal frameshifting viral pseudoknot. *Nat. Struct. Biol.*, **6**, 285–292.

123. Emilsson,G.M., Nakamura,S., Roth,A. and Breaker,R.R. (2003) Ribozyme speed limits. *RNA*, **9**, 907–918.

124. Boccaletto,P., Machnicka,M.A., Purta,E., Piatkowski,P., Baginski,B., Wirecki,T.K., De Crecy-Lagard,V., Ross,R., Limbach,P.A., Kotter,A. *et al.* (2018) MODOMICS: a database of RNA modification pathways. 2017 update. *Nucleic Acids Res.*, **46**, D303–D307.

125. Wagner,M., Steinbacher,J., Kraus,T.F.J., Michalakis,S., Hackner,B., Pfaffeneder,T., Perera,A., Mueller,M., Giese,A., Kretzschmar,H.A. *et al.* (2015) Age-dependent levels of 5-methyl-, 5-hydroxymethyl-, and 5-formylcytosine in human and mouse brain tissues. *Angew. Chem., Int. Ed.*, **54**, 12511–12514.

126. Tong,T., Chen,S., Wang,L., Tang,Y., Ryu,J.Y., Jiang,S., Wu,X., Chen,C., Luo,J., Deng,Z. *et al.* (2018) Occurrence, evolution, and functions of DNA phosphorothioate epigenetics in bacteria. *Proc. Natl. Acad. Sci. U.S.A.*, **115**, E2988–E2996.

127. Wang,L., Jiang,S., Deng,Z., Dedon,P.C. and Chen,S. (2019) DNA phosphorothioate modification-A new multi-functional epigenetic system In bacteria. *FEMS Microbiol. Rev.*, **43**, 109–122.

128. Wang,L., Chen,S., Vergin,K.L., Giovannoni,S.J., Chan,S.W., Demott,M.S., Taghizadeh,K., Cordero,O.X., Cutler,M., Timberlake,S. *et al.* (2011) DNA phosphorothioation is widespread and quantized in bacterial genomes. *Proc. Natl. Acad. Sci. U.S.A.*, **108**, 2963.

129. Wang,L., Chen,S., Xu,T., Taghizadeh,K., Wishnok,J.S., Zhou,X., You,D., Deng,Z. and Dedon,P.C. (2007) Phosphorothioation of DNA in bacteria by dnd genes. *Nat. Chem. Biol.*, **3**, 709–710.

130. Xiong,L., Liu,S., Chen,S., Xiao,Y., Zhu,B., Gao,Y., Zhang,Y., Chen,B., Luo,J., Deng,Z. *et al.* (2019) A new type of DNA phosphorothioation-based antiviral system in archaea. *Nat. Commun.*, **10**, 1688.

131. Kaiser,S., Byrne,S.R., Ammann,G., Asadi Atoi,P., Borland,K., Brecheisen,R., DeMott,M.S., Gehrke,T., Hagelskamp,F., Heiss,M. *et al.* (2021) Strategies to avoid artifacts in mass spectrometry-based epitranscriptome analyses. *Angew. Chem., Int. Ed.*, **60**, 23885–23893.

132. Manoharan,M. (1999) 2′-Carbohydrate modifications in antisense oligonucleotide therapy: importance of conformation, configuration and conjugation. *Biochim. Biophys. Acta, Gene Struct. Expression*, **1489**, 117–130.

133. Egli,M., Minasov,G., Tereshko,V., Pallan,P.S., Teplova,M., Inamati,G.B., Lesnik,E.A., Owens,S.R., Ross,B.S., Prakash,T.P. *et al.* (2005) Probing the influence of stereoelectronic effects on the biophysical properties of oligonucleotides: comprehensive analysis of the RNA affinity, nuclease resistance, and crystal structure of ten 2′-O-ribonucleic acid modifications. *Biochemistry*, **44**, 9045–9057.

134. Uhlmann,E. and Peyman,A. (1990) Antisense oligonucleotides: a new therapeutic principle. *Chem. Rev.*, **90**, 543–584.

135. Matveeva,O., Nechipurenko,Y., Rossi,L., Moore,B., Saetrom,P., Ogurtsov,A.Y., Atkins,J.F. and Shabalina,S.A. (2007) Comparison of approaches for rational siRNA design leading to a new efficient and transparent method. *Nucleic Acids Res.*, **35**, e63.

136. Patzel,V. (2007) In silico selection of active siRNA. *Drug Discov. Today*, **12**, 139–148.

137. Sipes,T.B. and Freier,S.M. (2008) Prediction of antisense oligonucleotide efficacy using aggregate motifs. *J. Bioinf. Comput. Biol.*, **6**, 919–932.

138. Monia,B.P., Johnston,J.F., Geiger,T., Muller,M. and Fabbro,D. (1996) Antitumor activity of a phosphorothioate antisense oligodeoxynucleotide targeted against C-raf kinase. *Nat. Med. (N. Y.)*, **2**, 668–675.

139. Hodgson,J. (2020) The pandemic pipeline. *Nat. Biotechnol.*, **38**, 523–532.

140. Rigl,C.T., Lloyd,D.H., Tsou,D.S., Gryaznov,S.M. and Wilson,W.D. (1997) Structural RNA mimetics: N3′ → P5′ phosphoramidate DNA analogs of HIV-1 RRE and TAR RNA form A-type helixes that bind specifically to rev and tat-related peptides. *Biochemistry*, **36**, 650–659.

141. Ellington,A.D. and Szostak,J.W. (1990) In vitro selection of RNA molecules that bind specific ligands. *Nature*, **346**, 818–822.

142. Tuerk,C. and Gold,L. (1990) Systematic evolution of ligands by exponential enrichment: RNA ligands to bacteriophage T4 DNA polymerase. *Science*, **249**, 505–510.

143. Ng,E.W.M., Shima,D.T., Calias,P., Cunningham,E.T. Jr, Guyer,D.R. and Adamis,A.P. (2006) Pegaptanib, a targeted anti-VEGF aptamer for ocular vascular disease. *Nat. Rev. Drug Discov.*, **5**, 123–132.

144. Jarvis,T.C., Alby,L.J., Beaudry,A.A., Wincott,F.E., Beigelman,L., McSwiggen,J.A., Usman,N. and Stinchcomb,D.T. (1996) Inhibition of vascular smooth muscle cell proliferation by ribozymes that cleave C-myb mRNA. *RNA*, **2**, 419–428.

145. Weng,D.E. and Usman,N. (2001) Angiozyme: a novel angiogenesis inhibitor. *Curr. Oncol. Rep.*, **3**, 141–146.

146. Baker,B.F., Khalili,H., Wei,N. and Morrow,J.R. (1997) Cleavage of the 5′-cap structure of mRNA by a europium(III) macrocyclic complex with pendant alcohol groups. *J. Am. Chem. Soc.*, **119**, 8749–8755.

147. Morrow,J.R. and Iranzo,O. (2004) Synthetic metallonucleases for RNA cleavage. *Curr. Opin. Chem. Biol.*, **8**, 192–200.

148. Murtola,M., Wenska,M. and Stroemberg,R. (2010) PNAzymes that are artificial RNA restriction enzymes. *J. Am. Chem. Soc.*, **132**, 8984–8990.

149. Bennett,C.F. and Swayze,E.E. (2010) RNA targeting therapeutics: molecular mechanisms of antisense oligonucleotides as a therapeutic platform. *Annu. Rev. Pharmacol. Toxicol.*, **50**, 259–293.

150. Rich,A. (2006) Discovery of the hybrid helix and the first DNA-RNA hybridization. *J. Biol. Chem.*, **281**, 7693–7696.

151. Pontius,B.W. and Berg,P. (1990) Renaturation of complementary DNA strands mediated by purified mammalian heterogeneous nuclear ribonucleoprotein A1 protein: implications for a mechanism for rapid molecular assembly. *Proc. Natl. Acad. Sci. U.S.A.*, **87**, 8403–8407.

152. Skabkin,M.A., Evdokimova,V., Thomas,A.A.M. and Ovchinnikov,L.P. (2001) The major messenger ribonucleoprotein particle protein P50 (YB-1) promotes nucleic acid strand annealing. *J. Biol. Chem.*, **276**, 44841–44847.

153. Crooke,S.T., Wang,S., Vickers,T.A., Shen,W. and Liang,X.-H. (2017) Cellular uptake and trafficking of antisense oligonucleotides. *Nat. Biotechnol.*, **35**, 230–237.

154. Scoles,D.R., Minikel,E.V. and Pulst,S.M. (2019) Antisense oligonucleotides: a primer. *Neurol Genet.*, **5**, E323.

155. Marques,J.T. and Williams,B.R.G. (2005) Activation of the mammalian immune system by siRNAs. *Nat. Biotechnol.*, **23**, 1399–1405.

156. Krieg,A.M. (2006) Therapeutic potential of toll-like receptor 9 activation. *Nat. Rev. Drug Discov.*, **5**, 471–484.

157. Sheehan,J.P. and Phan,T.M. (2001) Phosphorothioate oligonucleotides inhibit the intrinsic tenase complex by an allosteric mechanism. *Biochemistry*, **40**, 4980–4989.

158. Senn,J.J., Burel,S. and Henry,S.P. (2005) Non-CpG-containing antisense 2′-methoxyethyl oligonucleotides activate a proinflammatory response independent of toll-like receptor 9 or myeloid differentiation factor 88. *J. Pharmacol. Exp. Ther.*, **314**, 972–979.

159. Kleinman,M.E., Yamada,K., Takeda,A., Chandrasekaran,V., Nozaki,M., Baffi,J.Z., Albuquerque,R.J.C., Yamasaki,S., Itaya,M., Pan,Y. *et al.* (2008) Sequence- and target-independent angiogenesis suppression by siRNA via TLR3. *Nature*, **452**, 591–597.

160. Henry,S.P., Giclas,P.C., Leeds,J., Pangburn,M., Auletta,C., Levin,A.A. and Kornbrust,D.J. (1997) Activation of the alternative pathway of complement by a phosphorothioate oligonucleotide: potential mechanism of action. *J. Pharmacol. Exp. Ther.*, **281**, 810–816.

161. Lima,W.F. and Crooke,S.T. (1997) Binding affinity and specificity of Escherichia coli RNase H1: impact on the kinetics of catalysis of antisense oligonucleotide-RNA hybrids. *Biochemistry*, **36**, 390–398.

162. Nowotny,M., Gaidamakov,S.A., Crouch,R.J. and Yang,W. (2005) Crystal structures of RNase H bound to an RNA/DNA hybrid: substrate specificity and metal-dependent catalysis. *Cell*, **121**, 1005–1016.

163. Nowotny,M., Gaidamakov,S.A., Ghirlando,R., Cerritelli,S.M., Crouch,R.J. and Yang,W. (2007) Structure of human RNase H1 complexed with an RNA/DNA hybrid: insight into HIV reverse transcription. *Mol. Cell*, **28**, 264–276.

164. Campbell,M.A. and Wengel,J. (2011) Locked vs. unlocked nucleic acids (LNA vs. UNA): contrasting structures work towards common therapeutic goals. *Chem. Soc. Rev.*, **40**, 5680–5689.

165. Swayze,E.E., Siwkowski,A.M., Wancewicz,E.V., Migawa,M.T., Wyrzykiewicz,T.K., Hung,G., Monia,B.P. and Bennett,C.F. (2007) Antisense oligonucleotides containing locked nucleic acid improve potency but cause significant hepatotoxicity in animals. *Nucleic Acids Res.*, **35**, 687–700.

166. Kasuya,T., Hori,S.-I., Watanabe,A., Nakajima,M., Gahara,Y., Rokushima,M., Yanagimoto,T. and Kugimiya,A. (2016) Ribonuclease H1-dependent hepatotoxicity caused by locked nucleic acid-modified gapmer antisense oligonucleotides. *Sci. Rep.*, **6**, 30377.

167. Haaima,G., Lohse,A., Buchardt,O. and Nielsen,P.E. (1996) Peptide nucleic acids (PNAs) containing thymine monomers derived from chiral amino acids: hybridization and solubility properties of D-lysine PNA. *Angew. Chem. Int. Ed. Engl.*, **35**, 1939–1941.

168. McMahon,B.M., Mays,D., Lipsky,J., Stewart,J.A., Fauq,A. and Richelson,E. (2002) Pharmacokinetics and tissue distribution of a peptide nucleic acid after intravenous administration. *Antisense Nucleic Acid Drug Dev.*, **12**, 65–70.

169. Iversen,P.L. (2008) Morpholinos. In: Crooke,S.T. (ed.) *Antisense Drug Technology: Principles, Strategies, and Applications.* CRC Press, Boca Raton, FL, pp. 565–582.

170. Miller,C.M., Blank,E.E., Egger,A.W., Kellar,B.M., Harris,E.N., Donner,A.J., Ostergaard,M.E. and Seth,P.P. (2016) Stabilin-1 and Stabilin-2 are specific receptors for the cellular internalization of phosphorothioate-modified antisense oligonucleotides (ASOs) in the liver. *Nucleic Acids Res.*, **44**, 2782–2794.

171. De,C.E. and Li,G. (2016) Approved antiviral drugs over the past 50 years. *Clin. Microbiol. Rev.*, **29**, 695–747.

172. Sully,E.K. and Geller,B.L. (2016) Antisense antimicrobial therapeutics. *Curr. Opin. Microbiol.*, **33**, 47–55.

173. Geary,R.S., Henry,S.P. and Grillone,L.R. (2002) Fomivirsen: clinical pharmacology and potential drug interactions. *Clin. Pharmacokinet.*, **41**, 255–260.

174. Perry,C.M. and Balfour,J.A.B. (1999) Fomivirsen. *Drugs*, **57**, 375–380.

175. De Smet,M.D., Meenken,C. and Van Den Horn,G.J. (1999) Fomivirsen - a phosphorothioate oligonucleotide for the treatment of CMV retinitis. *Ocul. Immunol. Inflammation*, **7**, 189–198.

176. Wallace,R.W. (1999) Does antisense make sense? *Drug Discov. Today*, **4**, 4–5.

177. Lipinski,C.A. (2004) Lead- and drug-like compounds: the rule-of-five revolution. *Drug Discov. Today Technol.*, **1**, 337–341.

178. Brown,D.A., Kang,S.H., Gryaznov,S.M., Dedionisio,L., Heidenreich,O., Sullivan,S., Xu,X. and Nerenberg,M.I. (1994) Effect of phosphorothioate modification of oligodeoxynucleotides on specific protein binding. *J. Biol. Chem.*, **269**, 26801–26805.

179. Bennett,C.F., Butler,M., Cook,P.D., Geary,R.S., Levin,A.A., Mehta,R., Teng,C.L., Desmukh,H., Tillman,L. and Hardee,G. (2000) Antisense oligonucleotide-based therapeutics. In: Templeton,N.S. and Lasic,D.D. (eds). *Gene Therapy: Therapeutic Mechanisms and Strategy*. Marcel Dekker, Inc, NY, pp. 305–332.

180. Phillips,J.A., Craig,S.J., Bayley,D., Christian,R.A., Geary,R. and Nicklin,P.L. (1997) Pharmacokinetics, metabolism, and elimination of a 20-mer phosphorothioate oligodeoxynucleotide (CGP 69846A) after intravenous and subcutaneous administration. *Biochem. Pharmacol.*, **54**, 657–668.

181. Geary,R.S., Leeds,J.M., Fitchett,J., Burckin,T., Truong,L., Spainhour,C., Creek,M. and Levin,A.A. (1997) Pharmacokinetics and metabolism in mice of a phosphorothioate oligonucleotide antisense inhibitor of C-raf-1 kinase expression. *Drug Metab. Dispos.*, **25**, 1272–1281.

182. Yu,R.Z., Geary,R.S., Leeds,J.M., Watanabe,T., Moore,M., Fitchett,J., Matson,J., Burckin,T., Templin,M.V. and Levin,A.A. (2001) Comparison of pharmacokinetics and tissue disposition of an antisense phosphorothioate oligonucleotide targeting human Ha-ras mRNA in mouse and monkey. *J. Pharm. Sci.*, **90**, 182–193.

183. Nicklin,P.L., Craig,S.J. and Phillips,J.A. (1998) Pharmacokinetic properties of phosphorothioates in animals — absorption, distribution, metabolism and elimination. In: Crooke,S.T. (ed). *Antisense Research and Application*. Springer, Berlin, Heidelberg, pp. 141–168.

184. Stein,C.A., Subasinghe,C., Shinozuka,K. and Cohen,J.S. (1988) Physicochemical properties of phosphorothioate oligodeoxynucleotides. *Nucleic Acids Res.*, **16**, 3209–3221.

185. Brautigam,C.A. and Steitz,T.A. (1998) Structural principles for the inhibition of the 3′-5′ exonuclease activity of *Escherichia coli* DNA polymerase I by phosphorothioates. *J. Mol. Biol.*, **277**, 363–377.

186. Koziolkiewicz,M., Wojcik,M., Kobylanska,A., Karwowski,B., Rebowska,B., Guga,P. and Stec,W.J. (1997) Stability of stereoregular oligo(nucleoside phosphorothioate)s in human plasma: diastereoselectivity of plasma 3′-exonuclease. *Antisense Nucleic Acid Drug Dev.*, **7**, 43–48.

187. Eckstein,F. (1985) Nucleoside phosphorothioates. *Annu. Rev. Biochem.*, **54**, 367–402.

188. Levin,A.A. (1999) A review of issues in the pharmacokinetics and toxicology of phosphorothioate antisense oligonucleotides. *Biochim. Biophys. Acta, Gene Struct. Expression*, **1489**, 69–84.

189. Krieg,A.M., Yi,A.-K., Matson,S., Waldschmidt,T.J., Bishop,G.A., Teasdale,R., Koretzky,G.A. and Klinman,D.M. (1995) CpG motifs in bacterial DNA trigger direct B-cell activation. *Nature*, **374**, 546–549.

190. Moore,R.D. and Chaisson,R.E. (1999) Natural history of HIV infection In the era of combination antiretroviral therapy. *AIDS*, **13**, 1933–1942.

191. Altona,C. and Sundaralingam,M. (1972) Conformational analysis of the sugar ring in nucleosides and nucleotides. New description using the concept of pseudorotation. *J. Amer. Chem. Soc.*, **94**, 8205–8212.

192. Sun,G., Voigt,J.H., Marquez,V.E. and Nicklaus,M.C. (2005) PROSIT, an online service to calculate pseudorotational parameters of nucleosides and nucleotides. *Nucleosides. Nucleotides. Nucleic. Acids.*, **24**, 1029–1032.

193. Uesugi,S., Miki,H., Ikehara,M., Iwahashi,H. and Kyogoku,Y. (1979) A linear relation between electronegativity of 2′-substituents and conformation of adenine nucleosides. *Tetrahedron Lett.*, **20**, 4073–4076.

194. Guschlbauer,W. and Jankowski,K. (1980) Nucleoside conformation is determined by the electronegativity of the sugar substituent. *Nucleic Acids Res.*, **8**, 1421–1433.

195. Ikehara,M. (1984) 2′-Substituted 2′-deoxypurinenucleotides their conformation and properties. *Heterocycles*, **21**, 75–90.

196. Bobst,A.M., Rottman,F. and Cerutti,P.A. (1969) Effect of the methylation of 2'-hydroxyl groups in polyadenylic acid on its structure in weakly acidic and neutral solutions and on its capability to form ordered complexes with polyuridylic acid. *J. Mol. Biol.*, **46**, 221–234.

197. Kawasaki,A.M., Casper,M.D., Freier,S.M., Lesnik,E.A., Zounes,M.C., Cummins,L.L., Gonzalez,C. and Cook,P.D. (1993) Uniformly modified 2'-deoxy-2'-fluoro-phosphorothioate oligonucleotides as nuclease-resistant antisense compounds with high affinity and specificity for RNA targets. *J. Med. Chem.*, **36**, 831–841.

198. Lubini,P., Zürcher,W. and Egli,M. (1994) Stabilizing effects of the RNA 2'-substituent: crystal structure of an oligodeoxynucleotide duplex containing 2'-O-methylated adenosines. *Chem. Biol.*, **1**, 39–45.

199. Egli,M., Tereshko,V., Teplova,M., Minasov,G., Joachimiak,A., Sanishvili,R., Weeks,C.M., Miller,R., Maier,M.A., An,H. *et al.* (2000) X-ray crystallographic analysis of the hydration of A- and B-form DNA at atomic resolution. *Biopolymers (Nucleic Acid Sciences)*, **48**, 234–252.

200. Tereshko,V., Gryaznov,S. and Egli,M. (1998) Consequences of replacing the DNA 3'-oxygen by an amino group: high-resolution crystal structure of a fully modified N3' → P5' phosphoramidate DNA dodecamer duplex. *J. Am. Chem. Soc.*, **120**, 269–283.

201. Egli,M., Usman,N., Zhang,S. and Rich,A. (1992) Crystal structure of an Okazaki fragment at 2-Å resolution. *Proc. Natl. Acad. Sci. U.S.A.*, **89**, 534–538.

202. Egli,M., Usman,N. and Rich,A. (1993) Conformational influence of the ribose 2'-hydroxyl group: crystal structures of DNA-RNA chimeric duplexes. *Biochemistry*, **32**, 3221–3237.

203. Ban,C., Ramakrishnan,B. and Sundaralingam,M. (1994) A single 2'-hydroxyl group converts B-DNA to A-DNA. Crystal structure of the DNA-RNA chimeric decamer duplex D(CCGGC)R(G)D(CCGG) with a novel intermolecular G-C base-paired quadruplet. *J. Mol. Biol.*, **236**, 275–285.

204. Egli,M. (1998) Towards the structure-based design of oligonucleotide therapeutics. *Adv. Enzyme. Regul.*, **38**, 181–203.

205. Fedoroff,O.Y., Salazar,M. and Reid,B.R. (1993) Structure of a DNA:RNA hybrid duplex. Why RNase H does not cleave pure RNA. *J. Mol. Biol.*, **233**, 509–523.

206. Pallan,P.S., Prakash,T.P., Li,F., Eoff,R.L., Manoharan,M. and Egli,M. (2009) A conformational transition in the structure of a 2'-thiomethyl-modified DNA visualized at high resolution. *Chem. Commun.*, **45**, 2017–2019.

207. Eoff,R.L., McGrath,C.E., Maddukuri,L., Salamanca-Pinzon,S.G., Marquez,V.E., Marnett,L.J., Guengerich,F.P. and Egli,M. (2010) Selective modulation of DNA polymerase activity by fixed-conformation nucleoside analogues. *Angew. Chem., Int. Ed.*, **49**, 7481–7485.

208. Ketkar,A., Zafar,M.K., Banerjee,S., Marquez,V.E., Egli,M. and Eoff,R.L. (2012) Differential furanose selection in the active sites of archaeal DNA polymerases probed by fixed-conformation nucleotide analogues. *Biochemistry*, **51**, 9234–9244.

209. Su,Y., Egli,M. and Guengerich,F.P. (2016) Mechanism of ribonucleotide incorporation by human DNA polymerase eta. *J. Biol. Chem.*, **291**, 3747–3756.

210. Su,Y., Ghodke,P.P., Egli,M., Li,L., Wang,Y. and Guengerich,F.P. (2019) Human DNA polymerase eta has reverse transcriptase activity in cellular environments. *J. Biol. Chem.*, **294**, 6073–6081.

211. Su,Y., Egli,M. and Guengerich,F.P. (2017) Human DNA polymerase eta accommodates RNA for strand extension. *J. Biol. Chem.*, **292**, 18044–18051.

212. Ohtani,N., Yanagawa,H., Tomita,M. and Itaya,M. (2004) Cleavage of double-stranded RNA by RNase HI from a thermoacidophilic archaeon, Sulfolobus tokodaii 7. *Nucleic Acids Res.*, **32**, 5809–5819.

213. Mikkola,S., Lonnberg,T. and Lonnberg,H. (2018) Phosphodiester models for cleavage of nucleic acids. *Beilstein J. Org. Chem.*, **14**, 803–837.

214. Song,J.-J., Smith,S.K., Hannon,G.J. and Joshua-Tor,L. (2004) Crystal structure of Argonaute and its implications for RISC slicer activity. *Science*, **305**, 1434–1437.

215. Parker,J.S., Roe,S.M. and Barford,D. (2005) Structural insights into mRNA recognition from a PIWI domain-siRNA guide complex. *Nature*, **434**, 663–666.

216. Ma,J.-B., Yuan,Y.-R., Meister,G., Pei,Y., Tuschl,T. and Patel,D.J. (2005) Structural basis for 5'-end-specific recognition of guide RNA by the *A. fulgidus* Piwi protein. *Nature*, **434**, 666–670.

217. Schirle,N.T., Sheu-Gruttadauria,J. and Macrae,I.J. (2014) Structural basis for microRNA targeting. *Science*, **346**, 608–613.

218. Pallan,P.S. and Egli,M. (2008) Insights into RNA/DNA hybrid recognition and processing by RNase H from the crystal structure of a non-specific enzyme-dsDNA complex. *Cell Cycle*, **7**, 2562–2569.

219. Pallan,P.S., Prakash,T.P., De Leon,A.R. and Egli,M. (2016) Limits of RNA 2'-OH mimicry by fluorine: crystal structure of Bacillus halodurans RNase H bound to a 2'-FRNA:DNA hybrid. *Biochemistry*, **55**, 5321–5325.

220. Lima,W.F., Nichols,J.G., Wu,H., Prakash,T.P., Migawa,M.T., Wyrzykiewicz,T.K., Bhat,B. and Crooke,S.T. (2004) Structural requirements at the catalytic site of the heteroduplex substrate for human RNase H1 catalysis. *J. Biol. Chem.*, **279**, 36317–36326.

221. Yazbeck,D.R., Min,K.-L. and Damha,M.J. (2002) Molecular requirements for degradation of a modified sense RNA strand by *Escherichia coli* ribonuclease H1. *Nucleic Acids Res.*, **30**, 3015–3025.

222. Walker,R.T. (1997) 4'-Thio-2'-deoxyribonucleosides, their chemistry and biological properties - a review. *Spec. Publ. - R. Soc. Chem.*, **198**, 203–237.

223. Lima,W.F., Rose,J.B., Nichols,J.G., Wu,H., Migawa,M.T., Wyrzykiewicz,T.K., Vasquez,G., Swayze,E.E. and Crooke,S.T. (2007) The positional influence of the helical geometry of the heteroduplex substrate on human RNase H1 catalysis. *Mol. Pharmacol.*, **71**, 73–82.

224. Kielpinski,L.J., Hagedorn,P.H., Lindow,M. and Vinther,J. (2017) RNase H sequence preferences influence antisense oligonucleotide efficiency. *Nucleic Acids Res.*, **45**, 12932–12944.

225. Damha,M.J., Wilds,C.J., Noronha,A., Brukner,I., Borkow,G., Arion,D. and Parniak,M.A. (1998) Hybrids of RNA and arabinonucleic acids (ANA and 2'F-ANA) are substrates of ribonuclease H. *J. Am. Chem. Soc.*, **120**, 12976–12977.

226. Berger,I., Tereshko,V., Ikeda,H., Marquez,V.E. and Egli,M. (1998) Crystal structures of B-DNA with incorporated 2'-deoxy-2'-fluoro-arabino-furanosyl thymines: implications of conformational preorganization for duplex stability. *Nucleic Acids Res.*, **26**, 2473–2480.

227. Trempe,J.-F., Wilds,C.J., Denisov,A.Y., Pon,R.T., Damha,M.J. and Gehring,K. (2001) NMR solution structure of an oligonucleotide hairpin with a 2'F-ANA/RNA stem: implications for RNase H specificity toward DNA/RNA hybrid duplexes. *J. Am. Chem. Soc.*, **123**, 4896–4903.

228. Denisov,A.Y., Noronha,A.M., Wilds,C.J., Trempe,J.-F., Pon,R.T., Gehring,K. and Damha,M.J. (2001) Solution structure of an arabinonucleic acid (ANA)/RNA duplex in a chimeric hairpin: comparison with 2'-fluoro-ANA/RNA and DNA/RNA hybrids. *Nucleic Acids Res.*, **29**, 4284–4293.

229. Li,F., Sarkhel,S., Wilds,C.J., Wawrzak,Z., Prakash,T.P., Manoharan,O.M. and Egli,M. (2006) 2'-Fluoroarabino- and arabinonucleic acid show different conformations, resulting in deviating RNA affinities and processing of their heteroduplexes with RNA by RNase H. *Biochemistry*, **45**, 4141–4152.

230. Denning,E.J. and Mackerell,A.D. (2012) Intrinsic contribution of the 2'-hydroxyl to RNA conformational heterogeneity. *J. Am. Chem. Soc.*, **134**, 2800–2806.

231. Tereshko,V., Portmann,S., Tay,E.C., Martin,P., Natt,F., Altmann,K.-H. and Egli,M. (1998) Correlating structure and stability of DNA duplexes with incorporated 2'-O-modified RNA analogs. *Biochemistry*, **37**, 10626–10634.

232. Teplova,M., Minasov,G., Tereshko,V., Inamati,G.B., Cook,P.D., Manoharan,M. and Egli,M. (1999) Crystal structure and improved antisense properties of 2'-O-(2-methoxyethyl)-RNA. *Nat. Struct. Biol.*, **6**, 535–539.

233. Griffey,R.H., Monia,B.P., Cummins,L.L., Freier,S., Greig,M.J., Guinosso,C.J., Lesnik,E., Manalili,S.M., Mohan,V. and Et,A. (1996) 2'-O-Aminopropyl ribonucleotides: a zwitterionic modification that enhances the exonuclease resistance and biological activity of antisense oligonucleotides. *J. Med. Chem.*, **39**, 5100–5109.

234. Teplova,M., Wallace,S.T., Tereshko,V., Minasov,G., Symons,A.M., Cook,P.D., Manoharan,M. and Egli,M. (1999) Structural origins of the exonuclease resistance of a zwitterionic RNA. *Proc. Natl. Acad. Sci. U.S.A.*, **96**, 14240–14245.

235. Prhavc,M., Prakash,T.P., Minasov,G., Cook,P.D., Egli,M. and Manoharan,M. (2003) 2′-O-(2-(2-(N,N-Dimethylamino)ethoxy)ethyl-modified oligonucleotides: symbiosis of charge interaction factors and stereoelectronic effects. *Org. Lett.*, **5**, 2017–2020.

236. Prakash,T.P., Pueschl,A.P., Lesnik,E., Mohan,V., Tereshko,V., Egli,M. and Manoharan,M. (2004) 2′-O-(2-(Guanidinium)ethyl)-modified oligonucleotides: stabilizing effect on duplex and triplex structures. *Org. Lett.*, **6**, 1971–1974.

237. Duell,P.B., Santos,R.D., Kirwan,B.-A., Witztum,J.L., Tsimikas,S. and Kastelein,J.J.P. (2016) Long-term Mipomersen treatment is associated with a reduction in cardiovascular events in patients with familial hypercholesterolemia. *J. Clin. Lipidol.*, **10**, 1011–1021.

238. Geary,R.S., Yu,R.Z., Watanabe,T., Henry,S.P., Hardee,G.E., Chappell,A., Matson,J., Sasmor,H., Cummins,L. and Levin,A.A. (2003) Pharmacokinetics of a tumor necrosis factor-α phosphorothioate 2′-O-(2-methoxyethyl) modified antisense oligonucleotide: comparison across species. *Drug Metab. Dispos.*, **31**, 1419–1428.

239. Yu,R.Z., Geary,R.S., Monteith,D.K., Matson,J., Truong,L., Fitchett,J. and Levin,A.A. (2004) Tissue disposition of 2′-O-(2-methoxy) ethyl modified antisense oligonucleotides in monkeys. *J. Pharm. Sci.*, **93**, 48–59.

240. Baek,M.-S., Yu,R.Z., Gaus,H., Grundy,J.S. and Geary,R.S. (2010) In vitro metabolic stabilities and metabolism of 2′-O-(methoxyethyl) partially modified phosphorothioate antisense oligonucleotides in preincubated rat or human whole liver homogenates. *Oligonucleotides*, **20**, 309–316.

241. Crooke,S.T., Baker,B.F., Kwoh,T.J., Cheng,W., Schulz,D.J., Xia,S., Salgado,N., Bui,H.-H., Hart,C.E., Burel,S.A. *et al.* (2016) Integrated safety assessment of 2′-O-methoxyethyl chimeric antisense oligonucleotides in nonhuman primates and healthy human volunteers. *Mol. Ther.*, **24**, 1771–1782.

242. Crooke,S.T., Baker,B.F., Witztum,J.L., Kwoh,T.J., Pham,N.C., Salgado,N., McEvoy,B.W., Cheng,W., Hughes,S.G., Bhanot,S. *et al.* (2017) The effects of 2′-O-methoxyethyl containing antisense oligonucleotides on platelets in human clinical trials. *Nucleic Acid Ther.*, **27**, 121–129.

243. Crooke,S.T., Baker,B.F., Pham,N.C., Hughes,S.G., Kwoh,T.J., Cai,D., Tsimikas,S., Geary,R.S. and Bhanot,S. (2018) The effects of 2′-O-methoxyethyl oligonucleotides on renal function In humans. *Nucleic Acid Ther.*, **28**, 10–22.

244. Rader,D.J. and Kastelein,J.J.P. (2014) Lomitapide and mipomersen: two first-in-class drugs for reducing low-density lipoprotein cholesterol in patients with homozygous familial hypercholesterolemia. *Circulation*, **129**, 1022–1032.

245. Won,J.I., Zhang,J., Tecson,K.M. and McCullough,P.A. (2017) Balancing low-density lipoprotein cholesterol reduction and hepatotoxicity with lomitapide mesylate and mipomersen in patients with homozygous familial hypercholesterolemia. *Rev. Cardiovasc. Med.*, **18**, 21–28.

246. Niemietz,C., Chandhok,G. and Schmidt,H. (2015) Therapeutic oligonucleotides targeting liver disease: TTR amyloidosis. *Molecules*, **20**, 17944–17975.

247. Bauman,J., Jearawiriyapaisarn,N. and Kole,R. (2009) Therapeutic potential of splice-switching oligonucleotides. *Oligonucleotides*, **19**, 1–13.

248. Salton,M. and Misteli,T. (2016) Small molecule modulators of pre-mRNA splicing in cancer therapy. *Trends Mol. Med.*, **22**, 28–37.

249. Zhao,X., Feng,Z., Ling,K.K.Y., Mollin,A., Sheedy,J., Yeh,S., Petruska,J., Narasimhan,J., Dakka,A., Welch,E.M. *et al.* (2016) Pharmacokinetics, pharmacodynamics, and efficacy of a small-molecule SMN2 splicing modifier in mouse models of spinal muscular atrophy. *Hum. Mol. Genet.*, **25**, 1885–1899.

250. Wang,J., Schultz,P.G. and Johnson,K.A. (2018) Mechanistic studies of a small-molecule modulator of SMN2 splicing. *Proc. Natl. Acad. Sci. U.S.A.*, **115**, E4604–E4612.

251. Cheung,A.K., Hurley,B., Kerrigan,R., Shu,L., Chin,D.N., Shen,Y., Obrien,G., Sung,M.J., Hou,Y., Axford,J. *et al.* (2018) Discovery of small molecule splicing modulators of survival motor neuron-2 (SMN2) for the treatment of spinal muscular atrophy (SMA). *J. Med. Chem.*, **61**, 11021–11036.

252. Seiler,M., Darman,R., Chan,B., Keaney,G., Thomas,M., Agrawal,A.A., Caleb,B., Csibi,A., Fekkes,P., Karr,C. *et al.* (2018) H3B-8800, An orally available small-molecule splicing modulator, induces lethality in spliceosome-mutant cancers. *Nat. Med.*, **24**, 497–504.

253. Zhang,J., Harvey,S.E. and Cheng,C. (2019) A high-throughput screen identifies small molecule modulators of alternative splicing by targeting RNA G-quadruplexes. *Nucleic Acids Res.*, **47**, 3667–3679.

254. Aird,D., Teng,T., Huang,C.-L., Pazolli,E., Banka,D., Cheung-Ong,K., Eifert,C., Furman,C., Wu,Z.J., Seiler,M. *et al.* (2019) Sensitivity to splicing modulation of BCL2 Family genes defines cancer therapeutic strategies for splicing modulators. *Nat. Commun.*, **10**, 137.

255. Butler,M., Hayes,C.S., Chappell,A., Murray,S.F., Yaksh,T.L. and Hua,X.Y. (2005) Spinal distribution and metabolism of 2′-O-(2-methoxyethyl)-modified oligonucleotides after intrathecal administration in rats. *Neuroscience*, **131**, 705–715.

256. Wurster,C.D. and Ludolph,A.C. (2018) Nusinersen for spinal muscular atrophy. *Ther. Adv. Neurol. Disord.*, **11**, 1–3.

257. Lunn,M.R. and Wang,C.H. (2008) Spinal muscular atrophy. *Lancet*, **371**, 2120–2133.

258. Singh,R.N. and Singh,N.N. (2018) Mechanism of splicing regulation of spinal muscular atrophy genes. *Adv Neurobiol*, **20**, 31–61.

259. De Vivo,D.C., Hwu,W.-L., Reyna,S.P., Farwell,W., Gheuens,S., Sun,P., Zhong,Z.J., Su,J., Schneider,E. and Bertini,E. (2017) Interim efficacy and safety results from the phase 2 NURTURE study evaluating nusinersen in presymptomatic infants with spinal muscular atrophy. *Neurology*, **88**, S46.003.

260. Mahajan,R. (2019) Onasemnogene Abeparvovec for spinal muscular atrophy: the costlier drug ever. *Int. J. Appl. Basic Med. Res.*, **9**, 127–128.

261. ICER (2019) Deflazacort, Eteplirsen, and Golodirsen for Duchenne muscular dystrophy: effectiveness and value. In: *Draft Evidence Report*. Institute For Clinical And Economic Review, pp. 1–112.

262. Moulton,H.M. and Moulton,J.D. (eds.) (2017) *Morpholino Oligomers*. Humana Press.

263. Bhadra,J., Pattanayak,S., Sinha,S., Bhadra,J. and Pattanayak,S. (2015) Synthesis of morpholino monomers, chlorophosphoramidate monomers, and solid-phase synthesis of short morpholino oligomers. *Curr. Protoc. Nucleic Acid Chem.*, **62**, 4.65.61–64.65.26.

264. Summerton,J. and Weller,D. (1997) Morpholino antisense oligomers: design, preparation, and properties. *Antisense Nucleic Acid Drug Dev.*, **7**, 187–195.

265. Pettersen,E.F., Goddard,T.D., Huang,C.C., Couch,G.S., Greenblatt,D.M., Meng,E.C. and Ferrin,T.E. (2004) UCSF chimera - a visualization system for exploratory research and analysis. *J. Comput. Chem.*, **25**, 1605–1612.

266. Case,D.A., Cheatham,T.E. III, Darden,T., Gohlke,H., Luo,R., Merz,K.M. Jr, Onufriev,A., Simmerling,C., Wang,B. and Woods,R.J. (2005) The AMBER biomolecular simulation programs. *J. Comput. Chem.*, **26**, 1668–1688.

267. Dhillon,S. (2020) Viltolarsen: first approval. *Drugs*, **80**, 1027–1031.

268. Shirley,M. (2021) Casimersen: first approval. *Drugs*, **81**, 875–879.

269. Aslesh,T., Maruyama,R. and Yokota,T. (2018) Skipping multiple exons to treat DMD promises and challenges. *Biomedicines*, **6**, 1.

270. Obika,S., Nanbu,D., Hari,Y., Morio,K.-I., In,Y., Ishida,T. and Imanishi,T. (1997) Synthesis of 2′-O,4′-C-methyleneuridine and -cytidine. Novel bicyclic nucleosides having a fixed C3′-endo sugar puckering. *Tetrahedron Lett.*, **38**, 8735–8738.

271. Koshkin,A.A., Singh,S.K., Nielsen,P., Rajwanshi,V.K., Kumar,R., Meldgaard,M., Olsen,C.E. and Wengel,J. (1998) LNA (Locked Nucleic Acids): synthesis of the adenine, cytosine, guanine, 5-methylcytosine, thymine and uracil bicyclonucleoside monomers, oligomerization, and unprecedented nucleic acid recognition. *Tetrahedron*, **54**, 3607–3630.

272. Seth,P.P. and Swayze,E.E.(2014) Unnatural nucleoside analogs for antisense therapy. In: Hanessian,S. (ed). *Natural Products In Medicinal Chemistry*. 1st edn., Wiley-VCH Verlag GmbH & Co., Germany, pp. 403–440.

273. Pallan,P.S., Allerson,C.R., Berdeja,A., Seth,P.P., Swayze,E.E., Prakash,T.P. and Egli,M. (2012) Structure and nuclease resistance of 2′,4′-constrained 2′-O-methoxyethyl (cMOE) and 2′-O-ethyl (cEt) modified DNAs. *Chem. Commun. (Cambridge, U. K.)*, **48**, 8195–8197.

274. Seth,P.P., Allerson,C.R., Berdeja,A., Siwkowski,A., Pallan,P.S., Gaus,H., Prakash,T.P., Watt,A.T., Egli,M. and Swayze,E.E. (2010)

An exocyclic methylene group acts as a bioisostere of the 2′-oxygen atom in LNA. *J. Am. Chem. Soc.*, **132**, 14942–14950.

275. Sorensen,M.D., Kvrno,L., Bryld,T., Hakansson,A.E., Verbeure,B., Gaubert,G., Herdewijn,P. and Wengel,J. (2002) alpha-L-Ribo-configured locked nucleic acid (alpha-L-LNA): synthesis and properties. *J. Am. Chem. Soc.*, **124**, 2164–2176.

276. Bondensgaard,K., Petersen,M., Singh,S.K., Rajwanshi,V.K., Kumar,R., Wengel,J. and Jacobsen,J.P. (2000) Structural studies of LNA:RNA duplexes by NMR: conformations and implications for RNase H activity. *Chemistry*, **6**, 2687–2695.

277. Egli,M., Lubini,P., Bolli,M., Dobler,M. and Leumann,C. (1993) Crystal structure of a parallel-stranded duplex of a deoxycytidylyl-(3′-5′)-deoxycytidine analog containing intranucleosidyl C(3′)-C(5′) ethylene bridges. *J. Am. Chem. Soc.*, **115**, 5855–5856.

278. Pallan,P.S., Ittig,D., Héroux,A., Wawrzak,Z., Leumann,C.J. and Egli,M. (2008) Crystal structure of tricyclo-DNA: an unusual compensatory change of two adjacent backbone torsion angles. *Chem. Comm.*, **44**, 883–885.

279. Murray,S., Ittig,D., Koller,E., Berdeja,A., Chappell,A., Prakash,T.P., Norrbom,M., Swayze,E.E., Leumann,C.J. and Seth,P.P. (2012) TricycloDNA-modified oligo-2′-deoxyribonucleotides reduce scavenger receptor B1 mRNA in hepatic and extra-hepatic tissues-a comparative study of oligonucleotide length, design and chemistry. *Nucleic Acids Res.*, **40**, 6135–6143.

280. Marquez,V.E. (2008) The properties of locked methanocarba nucleosides in biochemistry, biotechnology and medicinal chemistry. In: Herdewijn,P. (ed). *Modified Nucleosides in Biochemistry, Biotechnology and Medicine*. Wiley-VCH, Weinheim, Germany, pp. 305–341.

281. Jung,M.E., Dwight,T.A., Vigant,F., Ostergaard,M.E., Swayze,E.E. and Seth,P.P. (2014) Synthesis and duplex-stabilizing properties of fluorinated N-methanocarbothymidine analogs locked in the C-3′ endo conformation. *Angew. Chem., Int. Ed.*, **53**, 9893–9897.

282. Akabane-Nakata,M., Kumar,P., Das,R.S., Erande,N.D., Matsuda,S., Egli,M. and Manoharan,M. (2019) Synthesis and biophysical characterization of RNAs containing 2′-fluorinated Northern methanocarbacyclic nucleotides. *Org. Lett.*, **21**, 1963–1967.

283. Akabane-Nakata,M., Erande,N.D., Kumar,P., Degaonkar,R., Gilbert,J.A., Qin,J., Mendez,M., Woods,L.B., Jiang,Y., Janas,M.M. *et al.* (2021) siRNAs containing 2′-fluorinated Northern-methanocarbacyclic (2′-F-NMC) nucleotides: in vitro and in vivo RNAi activity and inability of mitochondrial polymerases to incorporate 2′-F-NMC NTPs. *Nucleic Acids Res.*, **49**, 2435–2449.

284. Koonin,E.V. (2017) Evolution of RNA- and DNA-guided antivirus defense systems in prokaryotes and eukaryotes: common ancestry vs convergence. *Biol. Direct*, **12**, 5.

285. Obbard,D.J., Gordon,K.H.J., Buck,A.H. and Jiggins,F.M. (2009) The evolution of RNAi as a defense against viruses and transposable elements. *Philos. Trans. R. Soc., B*, **364**, 99–115.

286. Sabin,L.R., Delas,M.J. and Hannon,G.J. (2013) Dogma derailed: the many influences of RNA on the genome. *Mol. Cell*, **49**, 783–794.

287. Koonin,E.V. (2014) The origins of cellular life. *Antonie Van Leeuwenhoek*, **106**, 27–41.

288. Ryazansky,S., Kulbachinskiy,A. and Aravin,A.A. (2018) The expanded universe of prokaryotic argonaute proteins. *mBio*, **9**, e01935-18.

289. Shabalina,S.A. and Koonin,E.V. (2008) Origins and evolution of eukaryotic RNA interference. *Trends Ecol. Evol.*, **23**, 578–587.

290. Yamaguchi,S., Naganuma,M., Nishizawa,T., Kusakizako,T., Tomari,Y., Nishimasu,H. and Nureki,O. (2022) Structure of the dicer-2–R2D2 heterodimer bound to a small RNA duplex. *Nature*, **607**, 393–398.

291. Bernstein,E., Caudy,A.A., Hammond,S.M. and Hannon,G.J. (2001) Role for a bidentate ribonuclease in the initiation step of RNA interference. *Nature*, **409**, 363–366.

292. Koonin,E.V., Dolja,V.V. and Krupovic,M. (2015) Origins and evolution of viruses of eukaryotes: the ultimate modularity. *Virology*, **479-480**, 2–25.

293. Fire,A., Xu,S., Montgomery,M.K., Kostas,S.A., Driver,S.E. and Mello,C.C. (1998) Potent and specific genetic interference by double-stranded RNA in Caenorhabditis elegans. *Nature*, **391**, 806–811.

294. Elbashir,S.M., Harborth,J., Lendeckel,W., Yalcin,A., Weber,K. and Tuschl,T. (2001) Duplexes of 21-nucleotide RNAs mediate RNA interference in cultured mammalian cells. *Nature*, **411**, 494–498.

295. Caplen,N.J., Parrish,S., Imani,F., Fire,A. and Morgan,R.A. (2001) Specific inhibition of gene expression by small double-stranded RNAs in invertebrate and vertebrate systems. *Proc. Natl. Acad. Sci. U.S.A.*, **98**, 9742–9747.

296. Setten,R.L., Rossi,J.J. and Han,S.-P. (2019) The current state and future directions of RNAi-based therapeutics. *Nat. Rev. Drug Discov.*, **18**, 421–446.

297. Lieberman,J. (2018) Tapping the RNA world for therapeutics. *Nat. Struct. Mol. Biol.*, **25**, 357–364.

298. Yu,A.-M., Jian,C., Yu,A.H. and Tu,M.-J. (2019) RNA therapy: are we using the right molecules? *Pharmacol. Ther.*, **196**, 91–104.

299. Alagia,A. and Eritja,R. (2016) siRNA and RNAi optimization. *Wiley Interdiscip. Rev. RNA*, **7**, 316–329.

300. Lima,W.F., Prakash,T.P., Murray,H.M., Kinberger,G.A., Li,W., Chappell,A.E., Li,C.S., Murray,S.F., Gaus,H., Seth,P.P *et al.* (2012) Single-stranded siRNAs activate RNAi in animals. *Cell*, **150**, 883–894.

301. Pendergraff,H.M., Debacker,A.J. and Watts,J.K. (2016) Single-stranded silencing RNAs: hit rate and chemical modification. *Nucleic Acid Ther.*, **26**, 216–222.

302. Shen,X., Kilikevicius,A., O'Reilly,D., Prakash,T.P., Damha,M.J., Rigo,F. and Corey,D.R. (2018) Activating frataxin expression by single-stranded siRNAs targeting the GAA repeat expansion. *Bioorg. Med. Chem. Lett.*, **28**, 2850–2855.

303. Elkayam,E., Kuhn,C.-D., Tocilj,A., Haase,A.D., Greene,E.M., Hannon,G.J. and Joshua-Tor,L. (2012) The structure of human argonaute-2 in complex with miR-20a. *Cell*, **150**, 100–110.

304. Wilson,R.C. and Doudna,J.A. (2013) Molecular mechanisms of RNA interference. *Annu. Rev. Biophys.*, **42**, 217–239.

305. Sheu-Gruttadauria,J. and MacRae,I.J. (2017) Structural foundations of RNA silencing by Argonaute. *J. Mol. Biol.*, **429**, 2619–2639.

306. Meister,G., Landthaler,M., Patkaniowska,A., Dorsett,Y., Teng,G. and Tuschi,T. (2004) Human Argonaute2 mediates RNA cleavage targeted by miRNAs and siRNAs. *Mol. Cell*, **15**, 185–197.

307. Liu,J., Carmell,M.A., Rivas,F.V., Marsden,C.G., Thomson,J.M., Song,J.-J., Hammond,S.M., Joshua-Tor,L. and Hannon,G.J. (2004) Argonaute2 is the catalytic engine of mammalian RNAi. *Science*, **305**, 1437–1441.

308. Sheu-Gruttadauria,J., Xiao,Y., Gebert,L.F. and MacRae,I.J. (2019) Beyond the seed: structural basis for supplementary microRNA targeting by human Argonaute2. *EMBO J.*, **38**, E101153.

309. Grimm,D., Streetz,K.L., Jopling,C.L., Storm,T.A., Pandey,K., Davis,C.R., Marion,P., Salazar,F. and Kay,M.A. (2006) Fatality In mice due to oversaturation of cellular microRNA/short hairpin RNA pathways. *Nature*, **441**, 537–541.

310. Sano,M., Sierant,M., Miyagishi,M., Nakanishi,M., Takagi,Y. and Sutou,S. (2008) Effect of asymmetric terminal structures of short RNA duplexes on the RNA interference activity and strand selection. *Nucleic Acids Res.*, **36**, 5812–5821.

311. Chang,C.I., Yoo,J.W., Hong,S.W., Lee,S.E., Kang,H.S., Sun,X., Rogoff,H.A., Ban,C., Kim,S., Li,C.J *et al.* (2009) Asymmetric shorter-duplex siRNA structures trigger efficient gene silencing with reduced nonspecific effects. *Mol. Ther.*, **17**, 725–732.

312. Sun,X., Rogoff,H.A. and Li,C.J. (2008) Asymmetric RNA duplexes mediate RNA interference in mammalian cells. *Nat. Biotechnol.*, **26**, 1379–1382.

313. Yuan,Z., Wu,X., Liu,C., Xu,G. and Wu,Z. (2012) Asymmetric siRNA: new strategy to improve specificity and reduce off-target gene expression. *Hum. Gene Ther.*, **23**, 521–532.

314. Manoharan,M., Akinc,A., Pandey,R.K., Qin,J., Hadwiger,P., John,M., Mills,K., Charisse,K., Maier,M.A., Nechev,L. *et al.* (2011) Unique gene-silencing and structural properties of 2′-fluoro-modified siRNAs. *Angew. Chem., Int. Ed.*, **50**, 2284–2288.

315. Patra,A., Paolillo,M., Charisse,K., Manoharan,M., Rozners,E. and Egli,M. (2012) 2′-Fluoro RNA shows increased Watson-Crick H-bonding strength and stacking relative to RNA: evidence from NMR and thermodynamic data. *Angew. Chem., Int. Ed.*, **51**, 11863–11866.

316. Dunitz,J.D. (2004) Organic fluorine: odd man out. *ChemBioChem*, **5**, 614–621.

317. Pallan,P.S., Greene,E.M., Jicman,P.A., Pandey,R.K., Manoharan,M., Rozners,E. and Egli,M. (2011) Unexpected origins of the enhanced pairing affinity of 2′-fluoro-modified RNA. *Nucleic Acids Res.*, **39**, 3482–3495.

318. Anzahaee,M.Y., Watts,J.K., Alla,N.R., Nicholson,A.W. and Damha,M.J. (2011) Energetically important C-H···F-C pseudo-hydrogen bonding in water: evidence and application to rational design of oligonucleotides with high binding affinity. *J. Am. Chem. Soc.*, **133**, 728–731.

319. Egli,M. (2012) The steric hypothesis for DNA replication and fluorine hydrogen bonding revisited in light of structural data. *Acc. Chem. Res.*, **45**, 1237–1246.

320. Arnold,J.J., Sharma,S.D., Feng,J.Y., Ray,A.S., Smidansky,E.D., Kireeva,M.L., Cho,A., Perry,J., Vela,J.E., Park,Y. *et al.* (2012) Sensitivity of mitochondrial transcription and resistance of RNA polymerase II dependent nuclear transcription to antiviral ribonucleosides. *PLoS Pathog.*, **8**, E1003030.

321. Janas,M.M., Zlatev,I., Liu,J., Jiang,Y., Barros,S.A., Sutherland,J.E., Davis,W.P., Liu,J., Brown,C.R., Liu,X. *et al.* (2019) Safety evaluation of 2′-deoxy-2′-fluoro nucleotides in GalNAc-siRNA conjugates. *Nucleic Acids Res.*, **47**, 3306–3320.

322. Allerson,C.R., Sioufi,N., Jarres,R., Prakash,T.P., Naik,N., Berdeja,A., Wanders,L., Griffey,R.H., Swayze,E.E. and Bhat,B. (2005) Fully 2′-modified oligonucleotide duplexes with improved in vitro potency and stability compared to unmodified small interfering RNA. *J. Med. Chem.*, **48**, 901–904.

323. Schirle,N.T., Kinberger,G.A., Murray,H.F., Lima,W.F., Prakash,T.P. and MacRae,I.J. (2016) Structural analysis of human argonaute-2 bound to a modified siRNA guide. *J. Am. Chem. Soc.*, **138**, 8694–8697.

324. Parmar,R.G., Brown,C.R., Matsuda,S., Willoughby,J.L.S., Theile,C.S., Charissé,K., Foster,D.J., Zlatev,I., Jadhav,V., Maier,M.A *et al.* (2018) Facile synthesis, geometry, and 2′-substituent-dependent in vivo activity of 5′-(E)- and 5′-(Z)-vinylphosphonate-modified siRNA conjugates. *J. Med. Chem.*, **61**, 734–744.

325. Fakhr,E., Zare,F. and Teimoori-Toolabi,L. (2016) Precise and efficient siRNA design: a key point in competent gene silencing. *Cancer Gene Ther.*, **23**, 73–82.

326. Lewis,B.P., Burge,C.B. and Bartel,D.P. (2005) Conserved seed pairing, often flanked by adenosines, indicates that thousands of human genes are microRNA targets. *Cell*, **120**, 15–20.

327. Vickers,T.A., Lima,W.F., Wu,H., Nichols,J.G., Linsley,P.S. and Crooke,S.T. (2009) Off-target and a portion of target-specific siRNA mediated mRNA degradation is Ago2 'slicer' independent and can be mediated by Ago1. *Nucleic Acids Res.*, **37**, 6927–6941.

328. Schlegel,M.K., Foster,D.J., Kel'in,A.V., Zlatev,I., Bisbe,A., Jayaraman,M., Lackey,J.G., Rajeev,K.G., Charisse,K., Harp,J. *et al.* (2017) Chirality dependent potency enhancement and structural impact of glycol nucleic acid modification on siRNA. *J. Am. Chem. Soc.*, **139**, 8537–8546.

329. Schlegel,M.K., Matsuda,S., Brown,C.R., Harp,J.M., Barry,JosephD., Berman,D., Castoreno,A., Schofield,S., Szeto,J., Manoharan,M. *et al.* (2021) Overcoming GNA/RNA base-pairing limitations using isonucleotides improves the pharmacodynamic activity of ESC+ GalNAc-siRNAs. *Nucleic Acids Res.*, **49**, 10851–10867.

330. Schlegel,M.K., Janas,M.M., Jiang,Y., Barry,J.D., Davis,W., Agarwal,S., Berman,D., Brown,C.R., Castoreno,A., Leblanc,S. *et al.* (2022) From bench to bedside: improving the clinical safety of GalNAc–siRNA conjugates using seed-pairing destabilization. *Nucleic Acids Res.*, **50**, 6656–6670.

331. Kumar,P., Parmar,R.G., Brown,C.R., Willoughby,J.L.S., Foster,D.J., Babu,I.R., Schofield,S., Jadhav,V., Charisse,K., Nair,J.K *et al.* (2019) 5′-Morpholino modification of the sense strand of an siRNA makes it a more effective passenger. *Chem. Commun.*, **55**, 5139–5142.

332. Frank,F., Sonenberg,N. and Nagar,B. (2010) Structural basis for 5′-nucleotide base-specific recognition of guide RNA by human AGO2. *Nature*, **465**, 818–822.

333. Elkayam,E., Parmar,R., Brown,C.R., Willoughby,J.L., Theile,C.S., Manoharan,M. and Joshua-Tor,L. (2017) siRNA carrying an (E)-vinylphosphonate moiety at the 5′ end of the guide strand augments gene silencing by enhanced binding to human argonaute-2. *Nucleic Acids Res.*, **45**, 3528–3536.

334. Prakash,T.P., Lima,W.F., Murray,H.M., Li,W., Kinberger,G.A., Chappell,A.E., Gaus,H., Seth,P.P., Bhat,B., Crooke,S.T. *et al.* (2015) Identification of metabolically stable 5′-phosphate analogs that support single-stranded siRNA activity. *Nucleic Acids Res.*, **43**, 2993–3011.

335. Mutisya,D., Hardcastle,T., Cheruiyot,S.K., Pallan,P.S., Kennedy,S.D., Egli,M., Kelley,M.L., Van Brabant Smith,A. and Rozners,E. (2017) Amide linkages mimic phosphates in RNA interactions with proteins and are well tolerated in the guide strand of short interfering RNAs. *Nucleic Acids Res.*, **45**, 8142–8155.

336. Hardcastle,T., Novosjolova,I., Kotikam,V., Cheruiyot,S.K., Mutisya,D., Kennedy,S.D., Egli,M., Kelley,M.L., Van Brabant Smith,A. and Rozners,E. (2018) A single amide linkage in the passenger strand suppresses its activity and enhances guide strand targeting of siRNAs. *ACS Chem. Biol.*, **13**, 533–536.

337. Adams,D., Koike,H., Slama,M. and Coelho,T. (2019) Hereditary transthyretin amyloidosis: a model of medical progress for a fatal disease. *Nat. Rev. Neurol.*, **15**, 387–404.

338. Yin,W. and Rogge,M. (2019) Targeting RNA: a transformative therapeutic strategy. *Clin. Transl. Sci.*, **12**, 98–112.

339. Adams,D., Gonzalez-Duarte,A., O'Riordan,W.D., Yang,C.C., Ueda,M., Kristen,A.V., Tournev,I., Schmidt,H.H., Coelho,T., Berk,J.L. *et al.* (2018) Patisiran, an RNAi therapeutic, for hereditary transthyretin amyloidosis. *N. Engl. J. Med.*, **379**, 11–21.

340. Soutschek,J., Akinc,A., Bramlage,B., Charisse,K., Constien,R., Donoghue,M., Elbashir,S., Geick,A., Hadwiger,P., Harborth,J. *et al.* (2004) Therapeutic silencing of an endogenous gene by systemic administration of modified siRNAs. *Nature*, **432**, 173–178.

341. Zimmermann,T.S., Lee,A.C.H., Akinc,A., Bramlage,B., Bumcrot,D., Fedoruk,M.N., Harborth,J., Heyes,J.A., Jeffs,L.B., John,M. *et al.* (2006) RNAi-mediated gene silencing in non-human primates. *Nature*, **441**, 111–114.

342. Stein,P.E., Badminton,M.N. and Rees,D.C. (2017) Update review of the acute porphyrias. *Br. J. Haematol.*, **176**, 527–538.

343. Peters,T.J. and Wilkinson,D. (2010) King George III and porphyria: a clinical re-examination of the historical evidence. *Hist. Psychiatry*, **21**, 3–19.

344. Loftus,L.S. and Arnold,W.N. (1991) Vincent Van Gogh's illness: acute intermittent porphyria? *Br. Med. J. (Clin. Res. Ed.)*, **303**, 1589–1591.

345. Cooper,Y. and Agius,M. (2018) Does schizoaffective disorder explain the mental illnesses of Robert Schumann and Vincent Van Gogh? *Psychiatr. Danub.*, **30**, 559–562.

346. González Luque,F.J. and Montejo González,A.L. (1997) Implication of lead poisoning in psychopathology of Vincent Van Gogh. *Actas Luso Esp. Neurol. Psiquiatr. Cienc. Afines*, **25**, 309–326.

347. Sanhueza,C.A., Baksh,M.M., Thuma,B., Roy,M.D., Dutta,S., Preville,C., Chrunyk,B.A., Beaumont,K., Dullea,R., Ammirati,M. *et al.* (2017) Efficient liver targeting by polyvalent display of a compact ligand for the asialoglycoprotein receptor. *J. Am. Chem. Soc.*, **139**, 3528–3536.

348. D'Souza,A.A. and Devarajan,P.V. (2015) Asialoglycoprotein receptor mediated hepatocyte targeting - strategies and applications. *J. Controlled Release*, **203**, 126–139.

349. Balwani,M., Sardh,E., Ventura,P., Peiró,P.A., Rees,D.C., Stölzel,U., Bissell,D.M., Bonkovsky,H.L., Windyga,J., Anderson,K.E. *et al.* (2020) Phase 3 trial of RNAi therapeutic Givosiran for acute intermittent porphyria. *N. Engl. J. Med.*, **382**, 2289–2301.

350. Hulton,S.-A. (2021) Lumasiran: expanding the treatment options for patients with primary hyperoxaluria type 1. *Expert Opin. Orphan Drugs*, **9**, 189–198.

351. Scott,L.J. and Keam,S.J. (2021) Lumasiran: first approval. *Drugs*, **81**, 277–282.

352. Garrelfs,S.F., Frishberg,Y., Hulton,S.A., Koren,M.J., O'Riordan,W.D., Cochat,P., Deschênes,G., Shasha-Lavsky,H., Saland,J.M., Van't Hoff,W.G. *et al.* (2021) Lumasiran, an RNAi therapeutic for primary hyperoxaluria type 1. *N. Engl. J. Med.*, **384**, 1216–1226.

353. Chiodini,B., Tram,N., Adams,B., Hennaut,E., Lolin,K. and Ismaili,K. (2022) Case report: sustained efficacy of Lumasiran at 18 months in primary hyperoxaluria type 1. *Front. Pediatr*, **9**, 791616.

354. Ray,K.K., Wright,R.S., Kallend,D., Koenig,W., Leiter,L.A., Raal,F.J., Bisch,J.A., Richardson,T., Jaros,M., Wijngaard,P.L.J. *et al.* (2020) Two phase 3 trials of inclisiran in patients with elevated LDL cholesterol. *N. Engl. J. Med.*, **382**, 1507–1519.

355. Raal,F.J., Kallend,D., Ray,K.K., Turner,T., Koenig,W., Wright,R.S., Wijngaard,P.L.J., Curcio,D., Jaros,M.J., Leiter,L.A. *et al.* (2020) Inclisiran for the treatment of heterozygous familial hypercholesterolemia. *N. Engl. J. Med.*, **382**, 1520–1530.

356. Juliano,R.L. (2016) The delivery of therapeutic oligonucleotides. *Nucleic Acids Res.*, **44**, 6518–6548.

357. Godfrey,C., Desviat,L.R., Smedsrød,B., Piétri-Rouxel,F., Denti,M.A., Disterer,P., Lorain,S., Nogales-Gadea,G., Sardone,V., Anwar,R. *et al.* (2017) Delivery is key: lessons learnt from developing splice-switching antisense therapies. *EMBO Mol. Med.*, **9**, 545–557.

358. Benizri,S., Gissot,A., Martin,A., Vialet,B., Grinstaff,M.W. and Barthelemy,P. (2019) Bioconjugated oligonucleotides: recent developments and therapeutic applications. *Bioconjugate Chem.*, **30**, 366–383.

359. Smith,C.I.E. and Zain,R. (2019) Therapeutic oligonucleotides: state of the art. *Annu. Rev. Pharmacol. Toxicol.*, **59**, 605–630.

360. Seth,P.P., Tanowitz,M. and Bennett,C.F. (2019) Selective tissue targeting of synthetic nucleic acid drugs. *J. Clin. Invest.*, **129**, 915–925.

361. O'Driscoll,C.M., Bernkop-Schnürch,A., Friedl,J.D., Préat,V. and Jannin,V. (2019) Oral delivery of non-viral nucleic acid-based therapeutics - do we have the guts for this? *Eur. J. Pharm. Sci.*, **133**, 190–204.

362. Doherty,G.J. and McMahon,H.T. (2009) Mechanisms of endocytosis. *Annu. Rev. Biochem.*, **78**, 857–902.

363. Varkouhi,A.K., Scholte,M., Storm,G. and Haisma,H.J. (2011) Endosomal escape pathways for delivery of biologicals. *J. Controlled Release*, **151**, 220–228.

364. Juliano,R.L., Ming,X. and Nakagawa,O. (2012) Cellular uptake and intracellular trafficking of antisense and siRNA oligonucleotides. *Bioconjugate Chem.*, **23**, 147–157.

365. Juliano,R.L. and Carver,K. (2015) Cellular uptake and intracellular trafficking of oligonucleotides. *Adv. Drug Delivery Rev.*, **87**, 35–45.

366. Leung,A.K.K., Tam,Y.Y.C. and Cullis,P.R. (2014) Lipid nanoparticles for short interfering RNA delivery. *Adv. Genet.*, **88**, 71–110.

367. Hafez,I.M., Maurer,N. and Cullis,P.R. (2001) On the mechanism whereby cationic lipids promote intracellular delivery of polynucleic acids. *Gene Ther.*, **8**, 1188–1196.

368. Kulkarni,J.A., Witzigmann,D., Leung,J., Tam,Y.Y.C. and Cullis,P.R. (2019) On the role of helper lipids in lipid nanoparticle formulations of siRNA. *Nanoscale*, **11**, 21733–21739.

369. Letsinger,R.L., Zhang,G., Sun,D.K., Ikeuchi,T. and Sarin,P.S. (1989) Cholesteryl-conjugated oligonucleotides: synthesis, properties, and activity as inhibitors of replication of human immunodeficiency virus in cell culture. *Proc. Natl. Acad. Sci. U.S.A.*, **86**, 6553–6556.

370. Wolfrum,C., Shi,S., Jayaprakash,K.N., Jayaraman,M., Wang,G., Pandey,R.K., Rajeev,K.G., Nakayama,T., Charisse,K., Ndungo,E.M. *et al.* (2007) Mechanisms and optimization of in vivo delivery of lipophilic siRNAs. *Nat. Biotechnol.*, **25**, 1149–1157.

371. Biscans,A., Coles,A., Haraszti,R., Echeverria,D., Hassler,M., Osborn,M. and Khvorova,A. (2018) Diverse lipid conjugates for functional extra-hepatic siRNA delivery in vivo. *Nucleic Acids Res.*, **47**, 1082–1096.

372. Chernikov,I.V., Vlassov,V.V. and Chernolovskaya,E.L. (2019) Current development of siRNA bioconjugates: from research to the clinic. *Front. Pharmacol.*, **10**, 444.

373. Meier,M., Bider,M.D., Malashkevich,V.N., Spiess,M. and Burkhard,P. (2000) Crystal structure of the carbohydrate recognition domain of the H1 subunit of the asialoglycoprotein receptor. *J. Mol. Biol.*, **300**, 857–865.

374. Kolatkar,A.R., Leung,A.K., Isecke,R., Brossmer,R., Drickamer,K. and Weis,W.I. (1998) Mechanism of N-acetylgalactosamine binding to a C-type animal lectin carbohydrate-recognition domain. *J. Biol. Chem.*, **273**, 19502–19508.

375. Mammen,M., Choi,S.-K. and Whitesides,G.M. (1998) Polyvalent interactions in biological systems: implications for design and use of multivalent ligands and inhibitors. *Angew. Chem. Int Ed Engl.*, **37**, 2754–2794.

376. Germer,K., Leonard,M. and Zhang,X. (2013) RNA aptamers and their therapeutic and diagnostic applications. *Int. J. Biochem. Mol. Biol.*, **4**, 27–40.

377. Sun,H., Zhu,X., Lu,P.Y., Rosato,R.R., Tan,W. and Zu,Y. (2014) Oligonucleotide aptamers: new tools for targeted cancer therapy. *Mol. Ther. Nucleic Acids*, **3**, E182.

378. Nimjee,S.M., White,R.R., Becker,R.C. and Sullenger,B.A. (2017) Aptamers as therapeutics. *Annu. Rev. Pharmacol. Toxicol.*, **57**, 61–79.

379. Zhou,J. and Rossi,J. (2017) Aptamers as targeted therapeutics: current potential and challenges. *Nat. Rev. Drug Discovery*, **16**, 181–202.

380. Al-Zamil,W.M. and Yassin,S.A. (2017) Recent developments in age-related macular degeneration: a review. *Clin. Interventions Aging*, **12**, 1313–1330.

381. Zhang,Y., Lai,B.S. and Juhas,M. (2019) Recent advances in aptamer discovery and applications. *Molecules*, **24**, 941.

382. Ruckman,J., Green,L.S., Beeson,J., Waugh,S., Gillette,W.L., Henninger,D.D., Claesson-Welsh,L. and Janjic,N. (1998) 2′-Fluoropyrimidine RNA-based aptamers to the 165-amino acid form of vascular endothelial growth factor (VEGF165). Inhibition of receptor binding and VEGF-induced vascular permeability through interactions requiring the exon 7-encoded domain. *J. Biol. Chem.*, **273**, 20556–20567.

383. Bell,C., Lynam,E., Landfair,D.J., Janjic,N. and Wiles,M.E. (1999) Oligonucleotide NX1838 inhibits VEGF165-mediated cellular responses in vitro. *In Vitro Cell. Dev. Biol. Anim.*, **35**, 533–542.

384. Ferrara,N. (2004) Vascular endothelial growth factor: basic science and clinical progress. *Endocr. Rev.*, **25**, 581–611.

385. Trujillo,C.A., Nery,A.A., Alves,J.M., Martins,A.H. and Ulrich,H. (2007) Development of the anti-VEGF aptamer to a therapeutic agent for clinical ophthalmology. *Clin. Ophthalmol.*, **1**, 393–402.

386. Boomer,R.M., Lewis,S.D., Healy,J.M., Kurz,M., Wilson,C. and McCauley,T.G. (2005) Conjugation to polyethylene glycol polymer promotes aptamer biodistribution to healthy and inflamed tissues. *Oligonucleotides*, **15**, 183–195.

387. Burmeister,P.E., Lewis,S.D., Silva,R.F., Preiss,J.R., Horwitz,L.R., Pendergrast,P.S., McCauley,T.G., Kurz,J.C., Epstein,D.M., Wilson,C. *et al.* (2005) Direct in vitro selection of a 2′-O-methyl aptamer to VEGF. *Chem. Biol.*, **12**, 25–33.

388. Klettner,A. and Roider,J. (2008) Comparison of Bevacizumab, Ranibizumab, and Pegaptanib in vitro: efficiency and possible additional pathways. *Invest. Ophthalmol. Vis. Sci.*, **49**, 4523–4527.

389. Tolentino,M.J. and Tolentino,M.S. (2014) The role of Pegaptanib in the treatment of exudative AMD and diabetic retinopathy. *Retinal Physician*, **11**, 34–40.

390. Kimoto,M., Yamashige,R., Matsunaga,K.-I., Yokoyama,S. and Hirao,I. (2013) Generation of high-affinity DNA aptamers using an expanded genetic alphabet. *Nat. Biotechnol.*, **31**, 453–457.

391. Fukaya,T., Abe,K., Savory,N., Tsukakoshi,K., Yoshida,W., Ferri,S., Sode,K. and Ikebukuro,K. (2015) Improvement of the VEGF binding ability of DNA aptamers through in silico maturation and multimerization strategy. *J. Biotechnol.*, **212**, 99–105.

392. Dolot,R., Lam,C.H., Sierant,M., Zhao,Q., Liu,F.-W., Nawrot,B., Egli,M. and Yang,X. (2018) Crystal structures of thrombin in complex with chemically modified thrombin DNA aptamers reveal the origins of enhanced affinity. *Nucleic Acids Res.*, **46**, 4819–4830.

393. Gupta,S., Hirota,M., Waugh,S.M., Murakami,I., Suzuki,T., Muraguchi,M., Shibamori,M., Ishikawa,Y., Jarvis,T.C., Carter,J.D. *et al.* (2014) Chemically modified DNA aptamers bind interleukin-6 with high affinity and inhibit signaling by blocking its interaction with interleukin-6 receptor. *J. Biol. Chem.*, **289**, 8706–8719.

394. Dinuka,A.N., Egli,M., Cox,N., Mercier,K., Jonas,N.C., Pallan,P.S., Mizurini,D.M., Sierant,M., Hibti,F.-E., Hassell,T. *et al.* (2016) Evoking picomolar binding in RNA by a single phosphorodithioate linkage. *Nucleic Acids Res.*, **44**, 8052–8064.

395. Egli,M. and Lybrand,T.P. (2019) Enhanced dispersion and polarization interactions achieved through dithiophosphate group incorporation yield a dramatic binding affinity increase for an RNA aptamer–thrombin complex. *J. Am. Chem. Soc.*, **141**, 4445–4452.

396. Convery,M.A., Rowsell,S., Stonehouse,N.J., Ellington,A.D., Hirao,I., Murray,J.B., Peabody,D.S., Phillips,S.E.V. and

Stockley,P.G. (1998) Crystal structure of an RNA aptamer-protein complex at 2.8 Å resolution. *Nat. Struct. Biol.*, **5**, 133–139.

397. Rowsell,S., Stonehouse,N.J., Convery,M.A., Adams,C.J., Ellington,A.D., Hirao,I., Peabody,D.S., Stockley,P.G. and Phillips,S.E.V. (1998) Crystal structures of a series of RNA aptamers complexed to the same protein target. *Nat. Struct. Biol.*, **5**, 970–975.

398. Long,S.B., Long,M.B., White,R.R. and Sullenger,B.A. (2008) Crystal structure of an RNA aptamer bound to thrombin. *RNA*, **14**, 2504–2512.

399. Stauffer,M.E., Skelton,N.J. and Fairbrother,W.J. (2002) Refinement of the solution structure of the heparin-binding domain of vascular endothelial growth factor using residual dipolar couplings. *J. Biomol. NMR*, **23**, 57–61.

400. Lee,J.-H., Canny,M.D., De Erkenez,A., Krilleke,D., Ng,Y.-S., Shima,D.T., Pardi,A. and Jucker,F. (2005) A therapeutic aptamer inhibits angiogenesis by specifically targeting the heparin binding domain of VEGF165. *Proc. Natl. Acad. Sci. U.S.A.*, **102**, 18902–18907.

401. Anosova,I., Kowal,E.A., Dunn,M.R., Chaput,J.C., Van Horn,W.D. and Egli,M. (2016) The structural diversity of artificial genetic polymers. *Nucleic Acids Res.*, **44**, 1007–1021.

402. Pinheiro,V.B., Taylor,A.I., Cozens,C., Abramov,M., Renders,M., Zhang,S., Chaput,J.C., Wengel,J., Peak-Chew,S.-Y., McLaughlin,S.H. *et al.* (2012) Synthetic genetic polymers capable of heredity and evolution. *Science*, **336**, 341–344.

403. Ferreira-Bravo,I.A., Cozens,C., Holliger,P. and Destefano,J.J. (2015) Selection of 2′-deoxy-2′-fluoroarabinonucleotide (FANA) aptamers that bind HIV-1 reverse transcriptase with picomolar affinity. *Nucleic Acids Res.*, **43**, 9587–9599.

404. Dunn,M.R., McCloskey,C.M., Buckley,P., Rhea,K. and Chaput,J.C. (2020) Generating biologically stable TNA aptamers that function with high affinity and thermal stability. *J. Am. Chem. Soc.*, **142**, 7721–7724.

405. Fu,Z. and Xiang,J. (2020) Aptamers, the nucleic acid antibodies, in cancer therapy. *Int. J. Mol. Sci.*, **21**, 2793.

406. Eng,N.F., Bhardwaj,N., Mulligan,R. and Diaz-Mitoma,F. (2013) The potential of 1018 ISS adjuvant In Hepatitis B vaccines. *Hum. Vaccin. Immunother.*, **9**, 1661–1672.

407. Campbell,J.D. (2017) Development of the CpG adjuvant 1018: a case study. *Methods Mol. Biol.*, **1494**, 15–27.

408. Razin,A. and Friedman,J. (1981) DNA methylation and its possible biological roles. *Prog. Nucleic Acid Res. Mol. Biol.*, **25**, 33–52.

409. Wagner,H. (1999) Bacterial CpG DNA activates immune cells to signal infectious danger. *Adv. Immunol.*, **73**, 329–368.

410. Chuang,Y.-C., Tseng,J.-C., Huang,L.-R., Huang,C.-M., Huang,C.-Y.F. and Chuang,T.-H. (2020) Adjuvant effect of toll-like receptor 9 activation on cancer immunotherapy using checkpoint blockade. *Front. Immunol.*, **11**, 1075.

411. Friedberg,J.W., Kim,H., McCauley,M., Hessel,E.M., Sims,P., Fisher,D.C., Nadler,L.M., Coffman,R.L. and Freedman,A.S. (2005) Combination immunotherapy with a CpG oligonucleotide (1018 ISS) and rituximab in patients with non-Hodgkin lymphoma: increased interferon-α/β–inducible gene expression, without significant toxicity. *Blood*, **105**, 489–495.

412. Ohto,U., Shibata,T., Tanji,H., Ishida,H., Krayukhina,E., Uchiyama,S., Miyake,K. and Shimizu,T. (2015) Structural basis of CpG and inhibitory DNA recognition by toll-like receptor 9. *Nature*, **520**, 702–705.

413. Fitzgerald-Bocarsly,P., Dai,J. and Singh,S. (2008) Plasmacytoid dendritic cells and type I IFN: 50 years of convergent history. *Cytokine Growth Factor Rev.*, **19**, 3–19.

414. Schlake,T., Thess,A., Fotin-Mleczek,M. and Kallen,K.-J. (2012) Developing mRNA-vaccine technologies. *RNA Biol.*, **9**, 1319–1330.

415. Pastor,F., Berraondo,P., Etxeberria,I., Frederick,J., Sahin,U., Gilboa,E. and Melero,I. (2018) An RNA toolbox for cancer immunotherapy. *Nat. Rev. Drug Discov.*, **17**, 751–767.

416. Pardi,N., Hogan,M.J., Porter,F.W. and Weissman,D. (2018) Messenger RNA vaccines - A new era in vaccinology. *Nat. Rev. Drug Discov.*, **17**, 261–279.

417. Zhang,C., Maruggi,G., Shan,H. and Li,J. (2019) Advances in mRNA vaccines for infectious diseases. *Front. Immunol.*, **10**, 594.

418. Espeseth,A.S., Cejas,P.J., Citron,M.P., Wang,D., Distefano,D.J., Callahan,C., Donnell,G.O., Galli,J.D., Swoyer,R., Touch,S. *et al.* (2020) Modified mRNA/lipid nanoparticle-based vaccines expressing respiratory syncytial virus F protein variants are immunogenic and protective in rodent models of RSV infection. *NPJ Vaccines*, **5**, 16.

419. Jackson,L.A., Anderson,E.J., Rouphael,N.G., Roberts,P.C., Makhene,M., Coler,R.N., McCullough,M.P., Chappell,J.D., Denison,M.R., Stevens,L.J. *et al.* (2020) An mRNA vaccine against SARS-Cov-2 — Preliminary report. *N. Engl. J. Med.*, **383**, 1920–1931.

420. Stuart,L.M. (2021) In gratitude for mRNA vaccines. *N. Engl. J. Med.*, **385**, 1436–1438.

421. Anand,P. and Stahel,V.P. (2021) The safety of Covid-19 mRNA vaccines: a review. *Patient Saf. Surg.*, **15**, 20.

422. Nance,K.D. and Meier,J.L. (2021) Modifications in an emergency: the role of N1-methylpseudouridine in COVID-19 vaccines. *ACS Cent. Sci.*, **7**, 748–756.

423. Morais,P., Adachi,H. and Yu,Y.-T. (2021) The critical contribution of pseudouridine to mRNA COVID-19 vaccines. *Front. Cell Dev. Biol.*, **9**, 789427.

424. Szabó,G.T., Mahiny,A.J. and Vlatkovic,I. (2022) COVID-19 mRNA vaccines: platforms and current developments. *Mol. Ther.*, **30**, 1850–1868.

425. Kim,S.C., Sekhon,S.S., Shin,W.-R., Ahn,G., Cho,B.-K., Ahn,J.-Y. and Kim,Y.-H. (2022) Modifications of mRNA vaccine structural elements for improving mRNA stability and translation efficiency. *Mol. Cell. Toxicol.*, **18**, 1–8.

426. Fang,E., Liu,X., Li,M., Zhang,Z., Song,L., Zhu,B., Wu,X., Liu,J., Zhao,D. and Li,Y. (2022) Advances In COVID-19 mRNA vaccine development. *Signal Transduction Targeted Ther.*, **7**, 94.

427. Elkhalifa,D., Rayan,M., Negmeldin,A.T., Elhissi,A. and Khalil,A. (2022) Chemically modified mRNA beyond COVID-19: potential preventive and therapeutic applications for targeting chronic diseases. *Biomed. Pharmacother.*, **145**, 112385.

428. Foreman,K.J., Dolgert,A., Fukutaki,K., Fullman,N., McGaughey,M., Pletcher,M.A., Smith,A.E., Tang,K., Yuan,C.-W., Brown,J.C. *et al.* (2018) Forecasting life expectancy, years of life lost, and all-cause and cause-specific mortality for 250 causes of death: reference and alternative scenarios for 2016-40 for 195 countries and territories. *Lancet*, **392**, 2052–2090.

429. Brown,K.M., Nair,J.K., Janas,M.M., Anglero-Rodriguez,Y.I., Dang,L.T.H., Peng,H., Theile,C.S., Castellanos-Rizaldos,E., Brown,C., Foster,D. *et al.* (2022) Expanding RNAi therapeutics to extrahepatic tissues with lipophilic conjugates. *Nat. Biotechnol.*, **40**, 1500–1508.

430. Levin,A.A. (2017) Targeting therapeutic oligonucleotides. *N. Engl. J. Med.*, **376**, 86–88.

431. Corey,D.R., Damha,M.J. and Manoharan,M. (2021) Challenges and opportunities for nucleic acid therapeutics. *Nucleic Acid Ther.*, **32**, 8–13.

<u>APPENDIX</u>

ODE TO OLIGOS *

A code based on strands that intertwine
A structure for Watson and Crick to define
Two nucleic acids, sugars and bases diverse
Yet pairing together and not adverse

Oligos proposed to target and pair
Antigene or antisense, a kind of repair
Thus limiting proteins that cause despair
Creating oligo drugs for future care

A challenge to get oligos across the bilayer
Before nucleases attack, an oligo's slayer
DNA and RNA fall prey to attack
Chemistry to the rescue, modifications fight back

Backbone and bases become targets of change
Two puckers with C2 in charge of exchange
Helping oligos to mount an attack
While keeping the cell healthy and intact

Thioates, methoxy and fluoro lead the pack
MOE, NMA and GNA provide a new knack
Some adding grease, G-clamp a charge
Kinetically favorable and distributed at large

Unwieldy and polar, Chris Lipinski aghast
Lipids deliver oligos past the barrier fast
GalNAc receptors render siRNA profuse
Hepatocytes entered, the message cut loose

Cholesterolemia, porphyria, ailments most profound
Fight hereditary amyloidosis the managers propound
Optimized guides and passengers designed
Faulty message and guide in Argonaute2 combined

From in vitro in dishes to in vivo in mice
Successful with patients in clinical phases thrice
Patisiran data compiled and submitted
The FDA affirming in 2018: ONPATTRO permitted!

* By M.E., on the occasion of M.M. receiving the Lifetime
  Achievement Award from the Oligonucleotide Therapeutics
  Society at the OTS Meeting in Munich, Germany, Oct. 2019.